University of Florence

International Doctorate in Structural Biology

Cycle XX (2005-2007)

Mass Spectrometry as a tool in Structural Biology

Ph.D. thesis of

Guido Mastrobuoni

Tutor **Coordinator**

Prof. Gloriano Moneti ***Prof. Claudio Luchinat***

1. INTRODUCTION

1.1. Mass spectrometry in structural biology

One of the principal and most intriguing intellectual challenges in the scientific research is understanding cellular functions at a molecular level. For almost two decades, most efforts from scientific community were addressed to sequencing all the genes from a variety of organisms, opening the so called "genome era". Consequently, the availability of the gene sequence for an increasing number of organisms (including human) provided the life sciences research community with a new wealth of opportunities for starting new researches. However it has become rapidly evident that genome sequence alone does not provide all the information required to understand the functions of a cell, but they are merely the starting point of this study.

Thus in the post-genomic era the main goal is the development of research methodologies and techniques able to assign a function to each hypothetical protein reported on the basis of genome sequencing.

One possible approach, which is commonly indicated as "expression proteomics", is by design "unfocussed" because it is used to display alterations in global protein expression between cells or tissues in different condition (e.g. "normal" or "pathological" condition) or after different treatments (e.g. before and after a drug administration). In this way disease-related or drug-affected proteins can be identified.

A complementary strategy, besides these "expression proteomics" is termed "structural proteomics" and concentrates on specific proteins to determine their structure including post-translational modifications. Its function and its role within biological pathways in the cell can be revealed, for example, by identifying its interaction partners. Another way to obtain information on protein function can be through the structure determination of all proteins from an organism, with a strategy commonly termed "structural biology".

In fact, it becomes clear that the function of a protein is closely related to its structure and that proteins with different sequences but similar three-dimensional structure can have the same function;[1,2] in particular, structural biology makes use of high resolution

[1] Bashford D., Chotia C. and Lesk AM. *J. Mol. Biol*. **1987,** *196*, 199-216

[2] Chotia C. and Lesk AM. *EMBO J*. **1986**, *5*, 823-826

techniques, such as nuclear magnetic resonance (NMR) and X-ray crystallography, and computational methods to determine three-dimensional structures.

The first phase of this approach consists in the individuation and characterization of families of structures, defined as "base", from which is possible to model and build the structures of remaining proteins belonging to the same family, on the basis of sequence homology and computational methods.[3,4] It has been estimated the existence of around 1000-1500 families of structures in nature;[5] however only 50-60% of them are represented by a deposited three-dimensional structure in database. A second phase is to find similarities between three-dimensional structures. This helps to make hypothesis (to be proved successively through appropriate assays) on the function of new gene products, considering that structures are generally more conserved than aminoacidic sequences also between evolutionary distant organisms. From the analysis of structures in Protein Data Bank it could be expected that half of the newly determined structures can be related to known structures, while the remaining ones will allow to identify new families not represented at the moment; these structures will contribute to understand characteristics and functionality of these proteins.

It must be mentioned that, despite these high resolution techniques provide high-quality data, they have their intrinsic limitations, such as high sample consumption, strict requirements on sample purity and low throughput; moreover the analytical condition is often far from the physiological ones, so that the resulting structures could not correspond to those actually present *in vivo*.

In this view it becomes critical the integration with other complementary techniques, that, even if unable to provide structural details at atomic resolution, disclose other different information on proteins and protein systems, allowing to overcome limitations that hamper other high-resolution structural methods.

The recent technical advancement in mass spectrometry instrumentation allows this technique to play a key role in protein structural biology, adding complementary information to better elucidate biological problems.

In fact the variety of information that can be given by mass spectrometry is noticeably wide; for example hydrogen/deuterium exchange and limited proteolysis protocols can

[3] Jones TA. e Thirup S. *EMBO J.* **1986,** *5*, 819-822
[4] Tramontano A. and Lesk AM. *Biotechnol.* **1993** *8*, 9-16
[5] Baker D., Sali A., *Science*. **2001**, *294*, 93-6.

provide properly structural information, although at low resolution, indicating the regions that are more flexible or exposed to the solvent.[6,7,8,9]

Moreover nowadays, advancement in ionization techniques, especially electrospray, allows exploration of heterogeneous and large protein assemblies and obtainment of information on their stoichiometry and strength of interaction.

Another kind of information can be simply the peptide sequence determination and/or the determination of its variation between protein isoforms, without the need of accurate sample purification; also, exploration of complexes between proteins and their ligands or drugs can be performed by mass spectrometry, opening new possibilities to determine stoichiometry and strength of their interaction.

In addition, the ability to analyze inhomogeneous samples and complex protein mixtures offers possibilities for less focused approaches; for example, in the "fishing for partners" strategy a whole subset of proteins that interact in physiological conditions is investigated, obtaining new insights on protein interaction networks, discovering new members of complex systems and gaining new clues on protein functions. Another example, in which ability to analyze complex mixtures is fundamental, concerns the molecular profiling approach, as a comprehensive understanding of cell and organisms systems in diseased as well as healthy state.[10]

This approach cannot be realistically determined by studying one gene or one protein at a time, owing to the complexity and interdependence of biological systems. Thus this approach gives a more comprehensive overview on alterations in protein expression between different cell states and highlights differences between closely related organisms, in order to perform functional classification based on statistical methods.[11,12]

Finally, the recent advances in data handling software, mass spectrometry instrumentation and histological sample preparation make possible to analyze proteins

---

[6] Fontana A., Fassino G., Vita C., Dalzoppo D., Zanai M. and Zambonin M. *Biochemistry* **1986,** *25*, 1847-1851

[7] Zappacosta F., Pessi A., Bianchi E., Ventrini S., Sollazzo M., Tramontano A., Marino G. and Pucci P. *Protein Sci.* **1996,** *5*, 802-813

[8] Woodward C., Simon I. and Tuchsen E *Mol. Cell Biochem.* **1982,** *48*, 135-160

[9] Robinson CV, Grob M, Eyles SJ, Ewbank JJ, Mayhew M, Hartl FU, Dobson CM e Radford SE *Nature* **1994,** *372*, 646-651

[10] Liotta L. and Petricoin E. *Nat Rev* Genet **2000,** *1*, 48-56

[11] Zhu Y., Wu R., Sangha N., Yoo C., Cho KR., Shedden KA., Katabuchi H., Lubman DM.. *Proteomics*. **2006,** *621,* 5846-56

[12] Ketterlinus R., Hsieh SY., Teng SH., Lee H., Pusch W. *Biotechniques*. **2005,** *Jun*; 37-4

directly on fresh tissue sample (Mass Spectrometry Imaging)[13]. This approach couples many of the above mentioned mass spectrometry potentialities, allowing a molecular view of the spatial distribution of all the detectable proteins present in the tissue. This opportunity allows classifying different tissues or regions of the same tissue on the basis of their molecular profile, obtained directly from a histological sample, and eventually proceeding with molecular characterization and identification of signals of interest. Moreover this approach is not limited to protein analysis, but it can be also applied to small molecules as drugs and lipids, giving new information on their delivery pathways complementing data obtained from other approaches.

1.2. Aims of the research project

In this PhD thesis I describe applications of mass spectrometry, and in particular of some advanced mass spectrometry techniques, to different biological problems are described, evaluating and highlight their potentialities in the field of structural biology.

The applications of mass spectrometry reported hereafter concern:

- the comparison of the medium molecular weight venom fraction of five species of common social wasps through spectra profiling by Matrix-Assisted Laser Desorption Ionization-Time of Flight mass spectrometry (MALDI-ToF MS) and characterization of discriminating molecules.

- the characterization of specific metallodrug/protein adducts, by combination of ElectroSpray Ionization Mass Spectrometry (ESI MS), high resolution Fourier Transform mass spectrometry and other biochemical and spectrometric techniques.

- the characterization and localization of allergenic proteins in Rosaceae fruits by High Resolution Mass Spectrometry (HRMS) and Imaging Mass Spectrometry (IMS).

[13] Caprioli RM., Farmer TB., Gile J. *Anal Chem*. **1997**, *69,* 4751-60.

2. COMPARISON OF THE MEDIUM MOLECULAR WEIGHT VENOM FRACTION OF FIVE SPECIES OF COMMON SOCIAL WASPS THROUGH SPECTRA PROFILING BY MATRIX-ASSISTED LASER DESORPTION IONIZATION-TIME OF FLIGHT MASS SPECTROMETRY AND CHARACTERIZATION OF DISCRIMINATING MOLECULES

2.1 Introduction

2.1.1. Social wasps venom

Hymenoptera (bees, wasps and ants) venoms are complex mixtures containing simple organic molecules, proteins, peptides, and other bioactive elements. In social Hymenoptera venom is used in colony defence and is injected into the enemy body through a true sting or a barbed tip. This secretion is the result of a long evolutionary process from the secretion of solitary species that use it to paralyze preys for the nutrition of their larvae.

In social wasps the venom secretion has a variety of functions ranging from alarm and sexual pheromone[14] to chemical weapon against enemies and antimicrobial agent.[15,16] In fact, one of the main threat to colony survival are bacteria and pathogenic organisms, which due to the abundance of organic matter in the nest, to the high concentration of individuals in a limited space and to the low genetic variability within colony members, may cause lethal epidemics. Venom components can be roughly divided into three main fractions: a low molecular fraction, mainly constituted by volatile compounds, a medium molecular weight fraction and a proteic fraction.[17]

---

[14] Landolt PJ., Jeanne RL., Reed HC. *In Pheromone Communication in Social Insects* Westview Press: Boulder, **1998**, 216.

[15] Schmidt JO. In *Insect Defenses*, New York Press: Albany, **1990,** 354.

[16] Schmidt JO., Blum MS., Overal WL. *Arch. Insect Biochem.* **1983,** *1*, 155.

[17] Hoffman DR. in *Monograph on Insect Allergy*, American Academy of Allergy, Asthma & Immunology: Milwaukee, **2004,** 37.

The proteic fraction of social wasp venom contains the main components responsible for allergenic reactions induced by wasp sting;[18] nevertheless, the diffusion of these large molecules into the tissues of stung victims is undoubtedly aided by a set of smaller molecules, including peptides.

Since hymenoptera venoms can trigger serious allergenic reactions in humans, up to anaphylactic shock and death, the study of venom proteins is of great interest.[19] Preventive treatment in these patients is made with a desensitizing immunotherapy based on the administration of increasing quantities of venom [Venom ImmunoTherapy, (VIT)].

Notwithstanding the presence of cross-reactivity between venoms of different species, it seems probable that VIT would be more efficient if carried out with actual venoms; this leads to the need of a full understanding of their chemical composition.

MALDI-ToF MS technique has been already used for characterizing the venoms of various organisms including arachnids, insects, jellyfish, snakes etc.[20,21] In some cases, this approach has been used for establishing the phylogenetic relationships between various species belonging to the same taxonomic group[22] or to highlight differences between individuals belonging to the same species. Regarding social *Vespidae*, MS techniques have been employed for the study and the characterization of the most important allergens in the venom of several species, although this was performed mainly on the basis of differences in their amino acid sequences.

2.2. Methods

2.2.1. Mass spectrometry

In the Matrix-Assisted Laser Desorption Ionization (MALDI),[23,24] gaseous ions are generated by laser irradiation (usually with nitrogen laser, 337 nm wavelength) of a solid mixture formed by a large excess of matrix material that is coprecipitated with the analyte onto a metal plate.

---

[18] King TP., Spangfort MD. *Int. Arch. Allergy Imm.* 2000, **123**, 99

[19] Golden DBK. *J. Allergy Clin. Immun.* 2005, **115**, 439.

[20] Nakajima T., Naoki H.m Corzo G., Li D., Escoubas P., Yamaji N., Nagai H., Yasuda A., Andrianstiferana M., Haupt J., Oshiro N. *J. Toxicol. Toxin. Rev.* 2003, **22**, 509.

[21] Pimenta AMC., De Lima ME. *J. Pept. Sci.* 2005, **11**, 670.

[22] Serrao Wermelinger L., Dutra DLS., Oliveira-Carvalho AL., Soares MR., Bloch C., Zingali RB. *Rapid Commun. Mass Spectrom.* 2005, **19**, 1703.

[23] Karas M., Hillenkamp F. *Anal. Chem.* **1988,** *60*, 2299–301

[24] Beavis RC. and Chait BT. *Rapid Commun Mass Spectrom*. **1989**, *3*, 436-9

The matrix is typically a small organic molecule with absorbance at the wavelength of the laser employed.

The precise nature of the ionization process in MALDI is still largely unknown and the signal intensities depend on a number of factors as incorporation of the analytes into crystals, their likelihood of capturing and/or retaining a proton during the desorption process, and a number of other factors including suppression effects in peptide mixtures. The so formed ions are then accelerated in the mass analyzer by applying a short pulse of potential to the metal plate.

Usually MALDI source is coupled to a Time-of-Flight analyzer, which essentially consists in a field-free region under high vacuum (10^{-7} mbar). In figure 1 is reported the combination of MALDI source and a ToF analyzer: as stated before, small ion packets are formed after laser irradiation; these ions are accelerated to a fixed amount of kinetic energy and travel down the flight tube. The small ions have a higher velocity and are recorded on a detector before the larger ones, producing the time-of-flight spectrum. At the end of the tube ions are detected usually by a micro-channel plate detector. The kinetic energy distribution in the direction of ion flight can be corrected by using a reflectron.[25] The reflectron uses an electrostatic field to reflect the ion beam toward the detector. The more energetic ions penetrate deeper into the reflectron, and take a slightly longer path to the detector. Less energetic ions of the same charge and mass only will penetrate a short distance into the reflectron and take a shorter path the detector. The detector is placed at the focal point where ions of different energies focused by the reflectron strike the detector at the same time. An additional advantage to the reflectron arrangement is that twice the flight path is achieved in a given length of instrument.

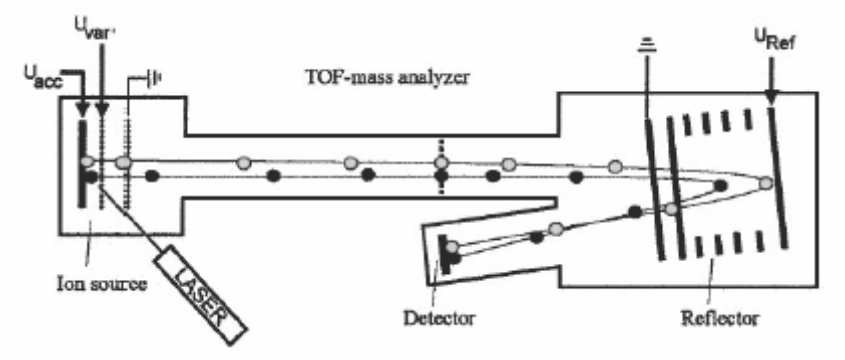

Figure 1. Scheme of MALDI-ToF mass spectrometer

[25] Mamyrin BA., Karataev VI., Shmikk DV., Zagulin VA. *Sov. Phys. JETP*, **1973**, *37*, 45

Moreover, the development of new MALDI-MS/MS technology,[26,27] brought to the diffusion of a new generation of MALDI-ToF/ToF instruments, able to give structural information on proteins and peptides in a rapid and easy manner, for example determining their sequence or post-translational modifications.

2.2.2. Experimental system

In order to reach a better characterization of the venoms of some common social wasps (family *Vespidae*), widespread in Europe and United States, and to highlight differences occurring amongst them, their reference spectra (profiling) were obtained by MALDI MS and analyzed through a statistical approach.

This study was carried out mainly to test the suitability of this approach for the comparison and classification of these secretions, to develop a quick and reliable analytical method for the quality control of venom preparations to be used in VIT and finally to collect data which could be used for the study of this species phylogeny. We also proceeded with the characterization of some of the molecules responsible for venom discrimination by statistical softwares; moreover the interest in the latter point was also given by the evidence that some of these substances which are also found on the insect cuticle and on the nest, have a strong antibiotic activity.

For the study three common species of European wasps (*Polistes dominulus, P. gallicus,* and *P. nimphus),* an American one (*P. exclamans*) and a species belonging to a different genus (*Vespa crabro*) were taken in consideration. Wasps were captured on nests or in flight in the surroundings of Florence (Central Italy) and in the country-side around Houston (Texas, U.S.A.).

2.2.3. Sample preparation

Venoms were obtained by dissection of single individuals by an entomologist. Two slightly different sample preparation methods were followed, in order to asses the influence of sample preparation on the resulting molecular profile. Group A was

[26] Medzihradszky KF., Campbell JM., Baldwin MA., Falick AM., Juhasz P., Vestal ML., Burlingame AL. *Anal. Chem*. **2000,** *72,* 552.
[27] Suckau D., Resemann A., Schurenberg M., Hufnagel P., Franzen J, Holle A. *Anal. Bioanal. Chem*. **2003,** *376,* 952.

constituted by 10 individuals of each of European *Polistes*, 9 of *Vespa crabro* and 7 of *P. exclamans*. Venom droplet obtained through squeezing the venom sacs were diluted in a water/methanol mixture and then filtrated in Centricon® vials (cut-off 3000 Da) in order to eliminate proteic fraction (Centricon approach). Group B was constituted by 20 individuals of *P. dominulus.* In this case the squeezed venom drops were subjected only to dilution and short centrifugationand, without any other processing (simple dilution approach).

The purification of two discriminating peptides found in *P. dominulus* venom and cuticle, was performed by RP-HPLC on whole body methanol extracts. The antimicrobial activity of these two peptides was tested against *E. coli* and *B. subtilis* strains.

2.3. Results

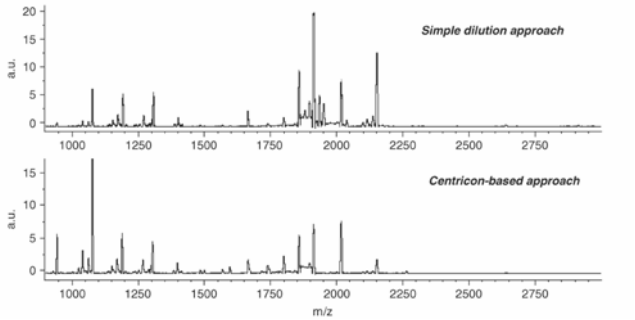

Figure 2. Average MALDI spectra of the *P. dominulus* venom samples obtained with the two sample preparation methods.

To evaluate the influence of sample preparation on the molecular mass profiles, the two sets of *P. dominulus* (from group A, N=10, group B, N=20) were compared.

The employed software (ClinPro Tool™, CPT) calculates average spectrum for each group and generates statistical models predicting how further samples are classified in the already analyzed groups.

Even if the average spectra obtained for the venom processed using the two different methods seemed almost superimposable (figure 2), the generated model discriminated correctly 97.5 % of the samples with 97.6 % for cross validation. For that reason all the samples from the other species were prepared with the same method (Centricon approach).

When comparing the spectra of the five different species (group A, N=46) (figure 3),

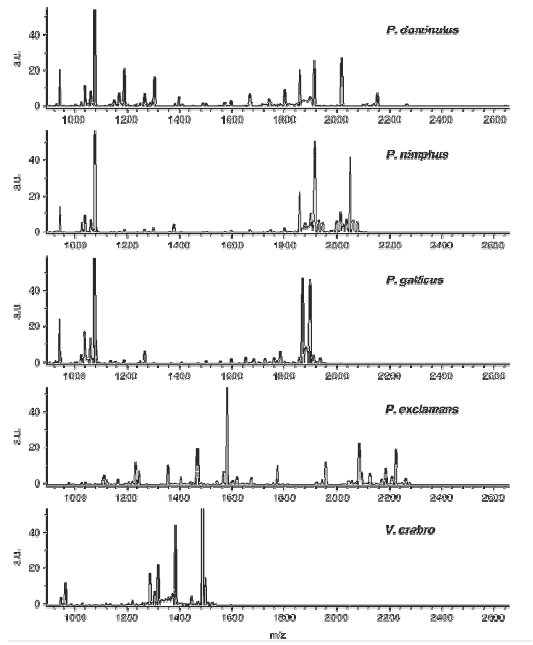

Figure 3. Average MALDI spectra of venoms from the five examined species, obtained with the Centricon-based approach.

the CPT software found 28 peaks suitable for model elaboration ; the produced model was able to discriminate correctly 98% (99.17 % with cross validation) of the samples in the right species.

Two of the discriminating peptides from *P. dominulus* were already known to be present on female cuticle and show antibacterial activity; for that reason they were the first to be subjected to further studies.

Their full primary structure was determined by tandem MS experiments on a MALDI-ToF/ToF and a linear ion trap mass spectrometers, and confirmed by Edman sequencing and high resolution mass spectrometry. The two peptides were named as Dominulin A and Dominulin B.

Once synthesized in laboratory, antibacteric activity of the two peptides was tested by Minimum Inhibition Concentration (MIC) determination, using the synthetic samples in bioassays on *B. subtilis* and *E. coli*. The MIC values on *B. subtilis* and *E. coli* were 2 µg/ml and 8 µg/ml, respectively, both for Dominulin A (MW=1854,08 Da) and for Dominulin B (MW=1909,12).

These two peptides are leucine-rich and show a high degree of identity, especially in the N-terminal part (Dominulin A: INWKKIAEVGGKILSSL-am; Dominulin B: INWKKIAEIGKQVLSAL-am). The MS/MS data also revealed the amidation of the C-terminal, a modification found in other peptides with antimicrobial activity from insects[28].

At present, the characterization of the proteic fraction of venoms is still in progress, as well as the chemical analyses aimed at the identification of other peaks contributing to the discrimination model. The peptidic nature of some peaks in the profile of other wasp species was confirmed, applying the same technique used for Dominulins.

[28] Rees JA., Moniatte M., Bulet P. *Insect Biochem. Mol. Biol*. **1997,** *27*, 413–422.

2.4. Publications

Dominulin A and B: Two New Antibacterial Peptides Identified on the Cuticle and in the Venom of the Social Paper Wasp *Polistes dominulus* Using MALDI-TOF, MALDI-TOF/TOF, and ESI-Ion Trap

Stefano Turillazzi, Guido Mastrobuoni, Francesca R. Dani, Gloriano Moneti, Giuseppe Pieraccini, and Giancarlo la Marca
Centro Interdipartimentale di Spettrometria di Massa, Università di Firenze, Firenze, Italy

Gianluca Bartolucci
Dipartimento di Scienze Farmaceutiche, Università di Firenze, Firenze, Italy

Brunella Perito, Duccio Lambardi, Vanni Cavallini, and Leonardo Dapporto
Dipartimento di Biologia Animale e Genetica, Università di Firenze, Firenze, Italy

Two new antibacterial peptides, denominated as Dominulin A and B, have been found on the cuticle and in the venom of females of the social paper wasp *Polistes dominulus*. The amino acidic sequence of the two peptides, determined by mass spectrometry, is INWKKIAE VGGKIL SSL for Dominulin A (MW = 1854 Da) and INWKKIAEIGKQVL SAL (MW = 1909 Da) for Dominulin B. Their presence on the cuticle was confirmed using MALDI-TOF by means of micro-extractions and direct analyses on body parts. The presence in the venom and the primary structure of the dominulins suggest their classification in the mastoparans, a class of peptides found in the venom of other *Aculeate hymenoptera*. Their antimicrobial action against Gram+ and Gram− bacteria fits in the range of the best natural antimicrobial peptides. Dominulins can represent an important defense of the colony of *Polistes dominulus* against microbial pathogens. (J Am Soc Mass Spectrom 2006, 17, 376–383) © 2006 American Society for Mass Spectrometry

Colonies of social insects (termites, ants, and many species of wasps and bees) may consist of thousands of insects, and are therefore potentially prone to infections by pathogenic microorganisms [1]; moreover their vulnerability to pathogens is often enhanced by the reduced genetic variability of their members [2]. The first defense of the colony against spreading of infectious diseases is represented by a set of hygienic behaviors (such as the elimination of corpses and organic wastes and the removal of infected insects from the nest), and by the use of fungicides and bactericides which may be produced by the colony members or be collected from plants [1]. As a further protection, the immune system of insects responds to microorganisms penetrating the body by releasing antimicrobial and antifungal peptides and proteins into the hemolymph [3–6]. Although the fat body is clearly the main source of the inducible antipathogenic peptides in insects [4], epidermis, including epithelial cells underlying cuticle, has also been demonstrated to produce antibacterial and antifungal peptides in response to local infections [7, 8, and quotations reported therein]. Additionally, some of these peptides have also been found to be constitutively expressed in the female reproductive apparatus of some dipterans [8 and quotations reported therein]. Many antimicrobial secretions of insect origin have been reported, and several have been studied in social insects, and in particular in the honeybees. In ants, the metapleural gland produces secretions with antiseptic and antifungal activity [9 and references therein]. In leaf cutter ants, these secretions protect the ants themselves and their clonal mutualistic fungus [2].

For social wasps, it is known that larval saliva contains antimicrobial agents [10, 11], while an old

Published online January 30, 2006

Address reprint requests to Professor S. Turillazzi, Centro Interdipartimentale di Spettrometria di, Massa dell'Universit di Firenze, Vle Pieraccini 6, 50100, Firenze, Italy. E-mail: turillazzi@dbag.unifi.it

1044-0305/06/$32.00
doi:10.1016/j.jasms.2005.11.017

Received September 22, 2005
Revised November 17, 2005
Accepted November 24, 2005

paper by Pavan [12] reports antimicrobial activity of body ethanol extracts of the hornet *Vespa crabro*. Venom antimicrobial activity has already been reported in ants [13–15], and social wasps [16–20]. In general, however, the antiseptic exocrine secretions described so far are generally of non-proteic nature [1, 21 and literature cited therein].

The chemistry of the most external layer of the insect cuticle, the epicuticle, is well known for several insect species. The epicuticle is covered by complex mixtures of lipids [22 and references reported therein], which defend insects against dehydration and probably also play some role against microorganisms [23, 24, 25]. However, to the best of our knowledge, antimicrobial peptides have never been reported on the epicuticle, neither for solitary nor for social insects. To demonstrate a possible antimicrobial activity of the compounds found in this epicuticular layer, we performed microbiological tests and report here about the presence of two new antibacteric peptides on the surface of the female cuticle in the social wasp *Polistes dominulus*. We found these molecules also in the venom and we named them Dominulin A and Dominulin B. Their sequences, determined by MALDI-TOF/TOF experiments and confirmed by biochemical methods, were compared with those of peptides already reported for the venom of other social wasps. Their origin and social function is discussed after a survey of their presence in other components of the colonies (larvae, pupae, nest paper), and in different body parts of female insect.

Materials and Methods

Chemicals

Methanol, acetonitrile, and *n*-pentane were of chromatography grade and purchased by Riedel de Haen (Sigma Aldrich Italia, Milan, Italy). Purified and deionized water was prepared using a Milli-Q system (Millipore, Bedford, MA). Formic acid and trifluoroacetic acid (TFA) was purchased from Fluka (Sigma Aldrich Italia). The α-cyano 4-hydroxycinnamic acid was obtained from Bruker Daltonics (Bremen, Germany). The matrix for MALDI-TOF experiments was a mixture of saturated solution of α-ciano 4-hydroxycinnamic acid in acetonitrile and 0.1% TFA in water (1:2, vol:vol). Unless stated otherwise, all other reagents were of analytical grade and used as supplied.

Biological Subjects

Studied species. *Polistes dominulus* is a common European species of paper wasp, which is now very common also in the United States, after it was accidentally imported almost 20 years ago. It has an annual colony cycle, unenveloped nests composed of a single comb, and colonies usually inhabited by up to 200 adults at the seasonal peak (usually in July) [26].

Collection of insects for analyses. Colonies of *Polistes dominulus* were collected in the countryside around Florence, Tuscany, Central Italy, during May and June 2002–2004. Colonies were stored in a freezer at −20 °C or reared for a while in the laboratory in glass cages (15 × 15 × 15 cm) with water, sugar, and fly maggots *ad libitum*. The external cuticular layer of single adult individuals were washed with solvents (methanol, *n*-pentane) to obtain extracts to be preliminarily tested for antimicrobial activity. Groups of females were used to collect large quantities of methanol extracts for RP-HPLC purification of the active substances. Single adult wasps, both male and female, eggs, larvae, pupae, and pieces of nest paper were used for the survey of particular peptides using MALDI-TOF.

To avoid transfer of substances between adult members of the colony, we also analyzed wasps (both males and females), previously artificially extracted from their operculated cells and allowed to complete their pupal development in plastic vials far from their nest. These analyses were performed three days after the emergence of the wasps from the artificial vials.

Microbiological Assays

We assayed microbial growth inhibition by the agar diffusion method and determination of minimal inhibitory concentration (MIC).

Agar diffusion tests. The agar diffusion test was performed with the *Bacillus subtilis* strain ATCC 6633 on Nutrient Agar (Oxoid, Basingstoke, UK) as previously described [11]. Penicillin G, used as standard, was spotted on a plate surface as 1 μl solution (12.5 μg/ml). Substances to be tested for antimicrobial activity were spotted on a plate surface as 5 μl solution. Pure solvents (in spots of 5 μl) were also tested in the same Petri dishes. Petri dishes were checked after one day of incubation at 37 °C. Antimicrobial activity was indicated by clear zones of growth inhibition on the plates. At the beginning we tested (8 trials) for their antimicrobial activity the extracts in methanol (2 ml) of a group of 10 female *P. dominulus* and the extract in pentane (2 ml) of another group of 10 females. Extracts had been dried in an air stream and then resuspended in 200 μl of the same solvent. Then, we tested with the same technique the methanol extracts (each of 250 μl) obtained from 10 single female *P. dominulus*. We used this test also to check the antibacterial activity of the peaks fractioned with RP-HPLC from methanol extracts of females.

Determination of minimal inhibitory concentration of synthetic peptides (MIC). The MIC was defined as the peptide minimal concentration that completely inhibited microbial growth by eye evaluation of turbidity. Bacteria used were *B. subtilis* ATCC 6633 as Gram+ and *Escherichia coli* JM109 as Gram− reference strains. They were grown in Nutrient Broth (Oxoid) and in PY Antibiotic Medium N. 3 (Oxoid) media, respectively.

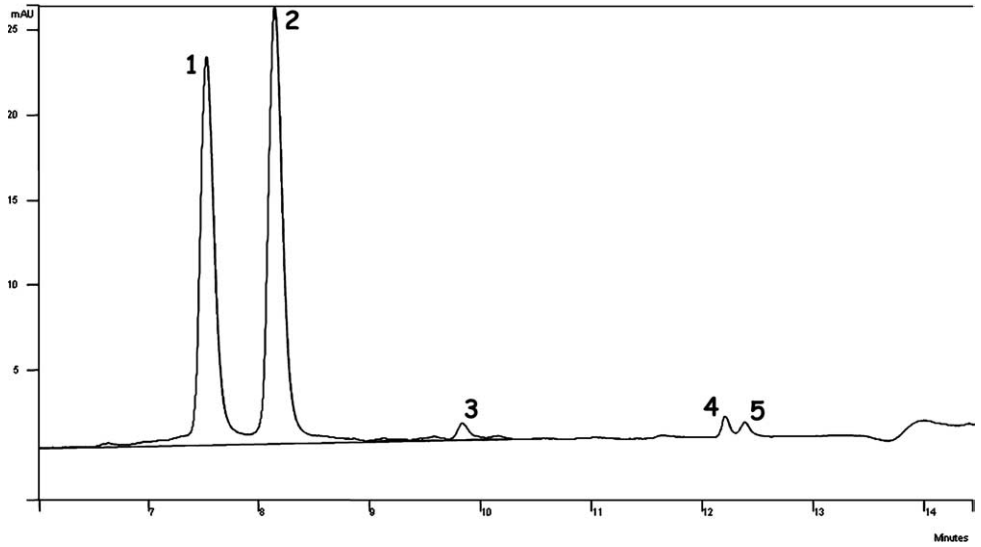

Figure 1. HPLC-UV analysis of methanol extract of the cuticle of female *P. dominulus* Peaks 1 and 2 correspond to Dominulin A and Dominulin B, respectively.

Overnight cultures were diluted in appropriate fresh medium; 50 μl of cell suspension containing 104 cells were inoculated in 900 μl of fresh medium and 50 μl of each peptide water solution (in a concentration range 0.1–100 μg/ml) in 12 ml glass tubes. Positive (50 μl of cells inoculated in 950 μl of medium) and negative (1000 μl of uninoculated medium) controls were prepared in each experiment. Cells were incubated at 37 °C with shaking at 110 rpm for 18 h. The experiments were done at least three times.

Chemical Analyses

Peptide fractionation. Five groups of 100 insects were placed in methanol for 5 min in five 50 ml plastic tubes. Insects were removed and after centrifugation (10,000 *g*, room-temperature, 5 min) the solvent was recovered, reunited in one single tube, and completely evaporated. Extracts were then resuspended in 4 ml of a solution of water and acetonitrile (80:20 vol/vol containing 0.5% formic acid). HPLC-UV analyses of the extract showed the presence of 5 peaks (Figure 1). The two most abundant peptides were separated in a Series 200 (Perkin-Elmer, Boston, MA) HPLC system including an autosampler, a quaternary pump, and an UV-VIS detector coupled with a fraction collector Biologic BioFrac (BioRad, Hercules, CA). The RP-HPLC column was a Luna C8, 150 Å × 4.6 mm, 5 μm (Phenomenex, Torrance, CA), operating at a flow rate of 0.75 ml/min. The absorbance was monitored at 254 nm. Deionized water and acetonitrile, both containing 0.5% formic acid, were used as the eluents; the elution gradient program started at 20% acetonitrile, then to 50% acetonitrile in 3 min, and to 80% acetonitrile in 15 min. The same column, elution gradient program, and wavelength were used in all HPLC separations cited in the following paragraphs. The collected fractions were lyophilized and resuspended in a solution of water and acetonitrile (80:20 vol/vol containing 0.5% formic acid) for MS analysis.

Mass spectrometry. The methanolic extract solution and the solutions of the two principal peptides, prepared as above described, were analyzed by ESI-TOF, ESI-IT and MALDI- TOF instruments.

The solution obtained from the evaporated extract of groups of individuals was injected in an HPLC 9012 (Varian Italia, Leinì, Turin, Italy); after the UV detector, the eluate was split in a 1:4 ratio and about 200 μl/min were directed to the ESI interface of a Mariner TOF mass spectrometer (Applied Biosystems, Foster City, CA). The spray tip and nozzle potentials were set to 3.8 kV and 120 V, respectively. The positive ion ESI mass spectra were recorded. For the two principal peptides, these were characterized by the presence of intense doubly and triply charged species, indicating a molecular weight of 1854.1 Da and 1909.1 Da for Dominulin A and B, respectively.

MALDI-TOF experiments were performed on an Ultraflex TOF-TOF instrument (Bruker) operating in reflector mode and positive polarity. The accelerating voltage was set to 25 kV, the IS 2 was set to 21.9 kV, and the delay time was 20 ns. Calibration was performed using the Bruker Peptide Calibration Standard.

A 1 μl volume of the peptide solution was mixed with the MALDI matrix (1:1, vol:vol), and the mixture was transferred on a stainless steel target; the droplet was allowed to evaporate before introducing the target into the mass spectrometer.

TOF-TOF mass spectra of the two principal ions (at *m/z* 1910,14 and 1855,11) were recorded using the LIFT device of the instrument. The isolation mass window was set to 1% of parent mass and the laser power boost to induce fragmentation was 80%.

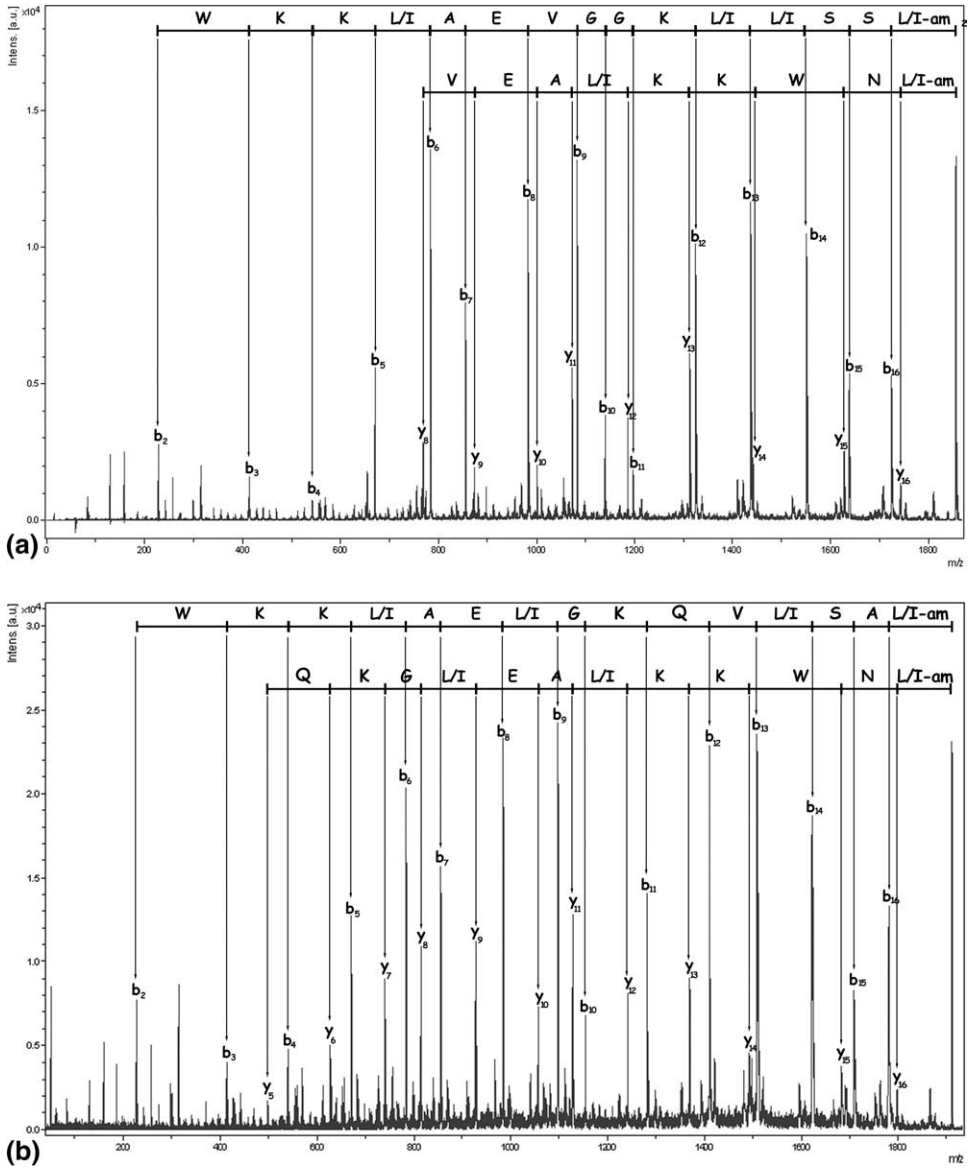

Figure 2. MALDI-TOF MSMS spectra of Dominulin A (**a**) and Dominulin B (**b**).

The sequence of each of the two peptides was deduced by interpreting the MS/MS spectra (Figure 2a and b, Table 1 a and b). A modification on the C-terminal peptide was suspected in both the sequences. The presence of a primary amide group, instead of a carboxylic group, was consistent with the experimental data obtained.

MS/MS spectra were also recorded in a LTQ mass spectrometer (Thermo, San Jose, CA). The solution of each peptide was introduced by flow injection mode (5 μl/min) in the ESI interface of LTQ. The ESI interface and mass spectrometer parameters were the following: I spray voltage 4.2 kV, capillary voltage 35 V, capillary temperature 250 °C, tube lens 180). The MS/MS spectrum was recorded by isolation and collision of the doubly charged ion of each peptide, using an isolation window of 2.0 Th, collision energy of 30% of the total RF energy.

Peptide sequencing. The full sequences derived from the interpretation of the MS/MS spectra of the two peptides were compared with the partial sequence obtained by Edman degradation, performed at C.E.I.N.G.E. Laboratory (University of Naples, Italy). This enabled the resolution of uncertainties about the presence of leucine and isoleucine, with the exception of the C-terminal that could have been either an amidate leucine or isoleucine, remained undetermined by Edman degradation. To determine the identity of C-terminal amino acid residue, the two peptides were hydrolyzed in a 1 M HCl solution (100 μl) for 24 h at 80 °C. The solution was evaporated, reconstituted in 100 μl of water and then processed using the EzFaast easy-fast amino acid sample testing kit (Phenomenex) for determination of amino acid composition through GCMS. A Hewlett Packard GC-MS system (Palo Alto, CA), composed by a GC 5890 series II coupled with a 5970A MSD operating in EI mode, was used. The ratio

Table 1. a) MALDI-TOF MSMS fragment ions of Dominulin A b) MALDI-TOF MSMS fragment ions of Dominulin B

a)

Dominulin A fragment ions			
b Series		y Series	
b_{16}	1724.91	y_{16}	1741.94
b_{15}	1637.84	y_{15}	1627.87
b_{14}	1550.84	y_{14}	1441.82
b_{13}	1437.73	y_{13}	1313.73
b_{12}	1324.65	y_{12}	1185.64
b_{11}	1196.59	y_{11}	1072.56
b_{10}	1139.52	y_{10}	1001.52
b_{9}	1082.55	y_{9}	872.48
b_{8}	983.48	y_{8}	773.41
b_{7}	854.44		
b_{6}	783.40		
b_{5}	670.32		
b_{4}	542.26		
b_{3}	414.12		
b_{2}	228.12		

b)

Dominulin B fragment ions			
b Series		y Series	
b_{16}	1779.92	y_{16}	1796.93
b_{15}	1708.88	y_{15}	1682.89
b_{14}	1621.85	y_{14}	1496.81
b_{13}	1508.77	y_{13}	1368.75
b_{12}	1409.70	y_{12}	1240.69
b_{11}	1281.64	y_{11}	1127.61
b_{10}	1153.58	y_{10}	1056.57
b_{9}	1096.56	y_{9}	927.53
b_{8}	983.48	y_{8}	814.45
b_{7}	854.44	y_{7}	757.43
b_{6}	783.40	y_{6}	629.37
b_{5}	670.32	y_{5}	501.31
b_{4}	542.26		
b_{3}	414.20		
b_{2}	228.12		

between leucine and isoleucine concentration allowed us to identify the C-terminal amino acid. The assignment was also confirmed by repeating this procedure on the peptides obtained by chemical synthesis (see below).

Peptide synthesis. The two main peptides were synthesized by an external laboratory according to the sequence determined as previously described. MALDI-TOF and TOF/TOF spectra of the two synthetic peptides were acquired and compared with those obtained from the natural ones. The purity of the synthetic peptides was determined by RP-HPLC-UV as better than 90%.

Survey of peptide presence in different colonial components and individual body parts with MALDI-TOF. Cuticle samples of female and male *Polistes dominulus* were analyzed by MALDI-TOF for the presence of peptides in different ways: (1) the whole body of a single individual was put in 500 μl of methanol for 1 min in a 1.5 ml Eppendorf vial. Water (175 μl) was added to the methanol extract and 5 μl of this solution was mixed with 5 μl of MALDI matrix. One μl of the mixture was dropped on an AnchorChip 600 target (Bruker); (2) a single drop of methanol (about 2 μl) was sprinkled on specific points of the insect body and recollected at once in the same micropipette tip. The drop was then mixed with the matrix directly on the MALDI stainless steel target; (3) anatomical pieces were mounted directly on a MALDI stainless steel target after soaking them with the matrix; (4) the venom apparatus was dissected out of the female abdomen and, by squeezing the venom sac, the venom was collected in a glass capillary and deposited directly on MALDI target where it was immediately mixed with the matrix. In all the procedures, drops of extracts and matrix were allowed to crystallize before introducing the target in the instrument. MALDI-TOF spectra were recorded as previously described.

Results

Preliminary agar diffusion tests performed with the extract of 10 females in methanol and pentane with *Bacillus subtilis* indicated good antimicrobial activity in methanol extract and a very low activity in pentane extract, compared to the activity of penicillin G, and a null activity of pure solvents. We thus decided to continue our screening with methanol extractions. A methanol extract of the whole body of a single *P. dominulus* wasp was active against *B. subtilis* in agar diffusion tests. Five μl of a 250 μl methanol extract of a single female wasp gave a growth inhibition zone of average diameter of 8.3 mm (N = 10, SD 1.0 mm) in comparison to a growth inhibition zone of 13.3 mm average diameter (N = 10, SD 1.2 mm) given by the penicillin G used as a positive control. In all the 10 tests, 5 μl spots of pure methanol were inactive against the bacterium. HPLC-UV analyses of methanol extract of the whole body of females *P. dominulus* resulted in the separation of 5 main peaks (Figure 1). Peaks 1 and 2 were collected and showed activity against *B. subtilis* in antibiogram agar diffusion tests. Peak numbers 3, 4, and 5, and control pure methanol spots gave only negative results.

HPLC-ESI-MS analyses gave a molecular weight for peaks 1 and 2 of 1854.08 Da and 1909.12 Da., as confirmed by MALDI-TOF analyses performed on the two separated peptides. TOF/TOF spectra put in evidence the peptidic nature of the two molecules (Table 1a and b). They are composed of 17 amino acids and their sequence is INWKKIAEVGGKILSSL for the 1854.11 Da peptide (which we named Dominulin A) and INWKKIAEIGKQVLSAL for the 1909.15 Da peptide (which we named Dominulin B). The sequence was confirmed by Edman degradation performed in an external laboratory; the C-terminal amino acid was determined as an amidated leucine. The spectra of the

Table 2. Presence of the two peptides Dominulin A and B in different samples from *P. dominulus* wasps as determined through MALDI analyses

		MeOH Micro-extraction of cuticle or of body parts		Entire body or nest paper MeOH extraction or secretion	
	Dominulin	Detected	Not detected	Detected	Not detected
Young female cuticle	A			10	0
	B			10	0
Old female cuticle	A	10	3	50	0
	B	10	3	48	2
Young males	A			0	8
	B			0	8
Old males	A			0	8
	B			1	8
Venom	A			16	15
	B			24	7
Dufour's gland	A	3	0		
	B	3	0		
Eggs	A	0	4		
	B	0	4		
Larvae	A	2	12	0	7
	B	1	13	0	7
Pupae	A			2	4
	B			2	4
Nest paper	A			7	4
	B			7	4

synthetic peptides were identical to those of the natural ones.

Antibacterial activity of the two peptides was tested by MIC determination using synthetic samples on *B. subtilis* and *E. coli*. The MIC values on *B. subtilis* and *E. coli* were 2 μg/ml and 8 μg/ml, respectively, both for Dominulin A and for Dominulin B.

The survey of the two peptides made with MALDI-TOF on different colonial components (adults, larvae, pupae, nest paper) of various colonies and on different parts of the cuticle and of the body of adult female *P. dominulus* gave the results reported in Table 2. From this, clearly only females produce the two peptides. Females isolated from the nest at the pupal stage presented the peptides when checked three days after emergence from artificial cells (10 out of 10 insects) while males lacked completely the dominulins (8 out of 8 insects) and only one older insect, which lived for a while together with females, presented some traces of the two molecules. On the other hand, clearly, females can apply the peptides on the nest surface as both the dominulins were present in the methanol extracts in 7 out of 11 different nests we analyzed. Pupae presented traces of the peptides only in the 2 specimens (out of 6) that were almost ready to emerge. Larvae (N = 21) presented Dominulin A and B on their cuticle in only 2 cases and 1 case, respectively, while eggs did not present any of the two peptides (4 out of 4 eggs) (see also Figure 3).

Laser shots on specific parts of the cuticle, the antennae and wings, and micro-sampling with methanol on other parts of the cuticle showed that the two peptides are present all over the body of the females (even if sometimes in the same individual they could be detected only in some parts of the cuticle and not in others). The quantities of Dominulin A and B on the cuticle of a single wasp, estimated through the comparison of HPLC-UV signals of wasp methanol extracts (N = 5) and synthetic dominulins, were respectively 7.14 (SD 2.26) μg and 5.4 (SD 1.99) μg per wasp.

Dominulins were present in the venom even if not in all specimens examined (16 out of 31 females had Dominulin A, while 24 out of 31 females had Dominulin B), and were present also in the Dufour's gland (an exocrine gland close to the sting apparatus) even though we could analyze only 3 specimens.

Discussion

Although anecdotal reports about the presence of antibiotic substances on the surface of some insects do exist, only a protein with antibacterial properties, the phenoloxidase, has been reported to be present on the cuticle of several insect species [4]. We found that antimicrobial peptides cover the cuticle of female *Polistes* wasps as a probable first protection against micro-organisms. The two peptides characterized so far (Dominulins A and B) are rich in leucine and show a high degree of identity, especially in the N-terminal part. The MS/MS data also revealed the amidation of the C-terminal, a modification found also in other peptides with antimicrobial activity from insects [27].

The molecular weights of dominulins are similar to those of apidaecins, inducible hemolymph peptides with antibiotic activities reported for several Hy-

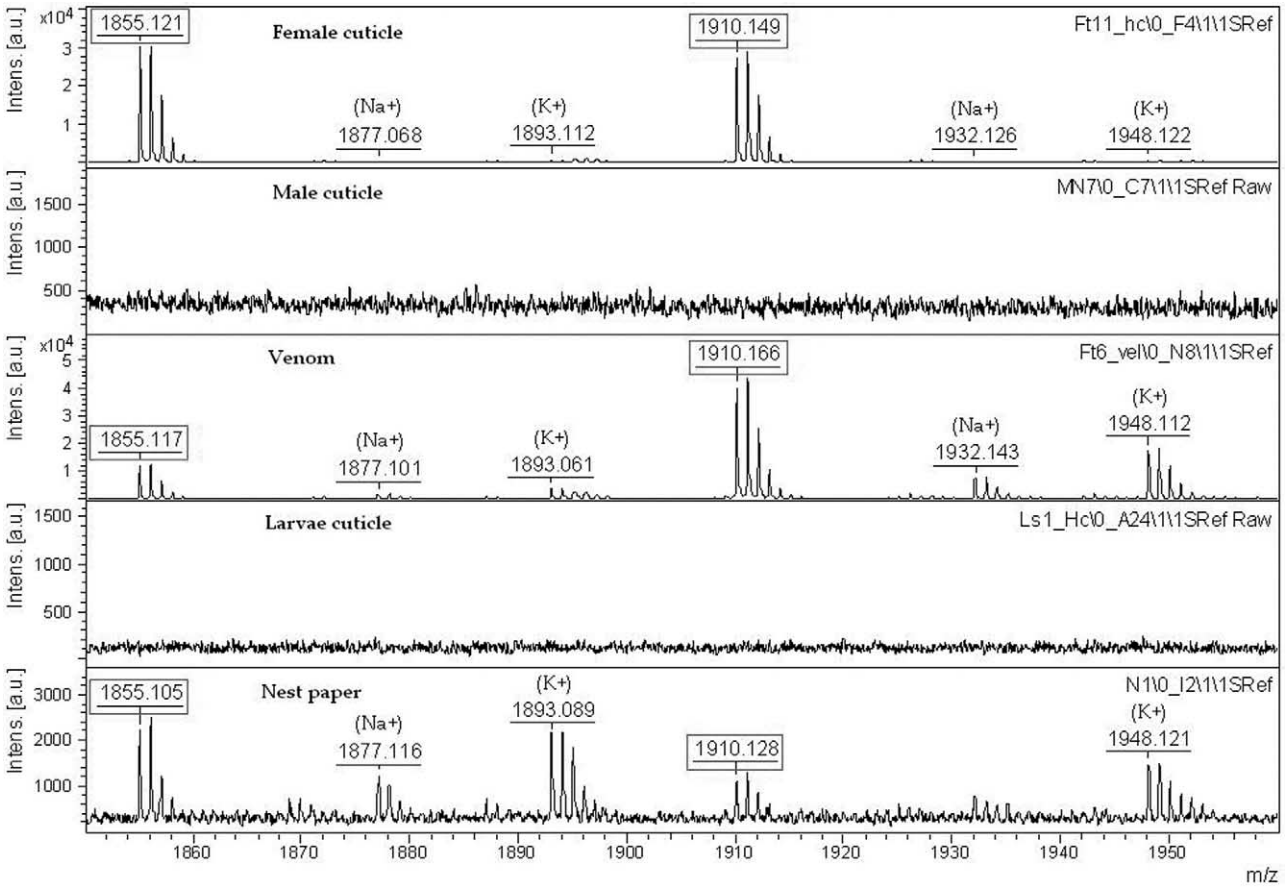

Figure 3. Examples of MALDI-TOF spectra in the range 1850–1960 *m/z* of methanol extracts of female and male adults, larvae, venom and nest paper of *Polistes dominulus.*

menopterans [28]. However both the amino acid composition and sequence of apidaecins strongly differ from dominulins.

Between a wide list of antimicrobial and cytolytic peptides reported for the venom of Arthropods [6], dominulins appear more similar to some peptides included in the class of mastoparans, hemolytic tetradecapeptides which have from 7 to 10 hydrophobic amino acid residues and from 2 to 4 lysine residues in their primary sequence. Mastoparans have been found in the venom of various solitary and social wasps [29]. The known mastoparans, which are more similar to the dominulins, are the so-called Mastoparan X from the venom of the vespine *Vespa xanthoptera* [30] (14 amino acids, having the same sequence of the first four residues from the N terminal of the dominulins), the peptide B from the venom of the Polistine wasp *Protonectarina sylveirae* [19] (14 amino acids, having the same sequence of the first four residues from the N terminal of the dominulins) and that from the venom of *Parapolybia indica* [31] (14 amino acids, having the same sequence of the first five residues from the N-terminal of the dominulins). However, the only mastoparans described so far from the venom of a *Polistes* (*P. jadwigae* from Japan), have only a sequence of four amino acids similar to that of Dominulin A (second to sixth from the N-terminal) and two more residues (in Positions 11 and 13) similar to those present in the sequence of Dominulin B [32] (see Table 3). Thus, even if longer than 14 amino acid residues, dominulins could be included in

Table 3. Comparison of AA sequence between Dominulins and other mastoparan peptides described from the venom sac of other social wasps

Peptide name	Social wasp	aa. Sequence	Reference
Dominulin A	*Polistes dominulus*	I N W K K I A E V G G K I L S S L	This paper
Dominulin B	*Polistes dominulus*	I N W K K I A E I G K Q V L S A L	This paper
Polistes mastoparan	*Polistes jadwigae*	V D W K K I G Q H I K S V L	[32]
Mastoparan X	*Vespa xanthoptera*	I N W K G I A A M A K K L L	[30]
Peptide B	*Protonectarina sylveirae*	I N W K A L L D A A K K V L	[19]
Venom sac peptide	*Parapolybia indica*	I N W K K M A A T A L K M I	[31]

the mastoparans and the venom could be the source of these peptides, which could be spread all over the cuticle by the frequent grooming movements of the female wasps. It is known that mastoparans injected with the venom can cause hemolysis in mammal cells and mast cell degranulation whilst another important biological activity of these substances is the activation of venom enzymes [29]. Here we observe that another important function of these peptides can be promoting the formation of a cuticular barrier against micro organisms. These substances, moreover, end up constituting a social protection against infections for the whole colony when they are applied to the nest surface. However, uncertainty about the source of these peptides remains, as they were systematically found on the cuticle but not always in the venom, where Dominulin B was more prominent than Dominulin A. This difference could have been caused by errors in the preparation procedure or by other unknown factors (including differential secretory activity of the two substances by the venom glands in different insects and at different ages).

Our microbiological tests have to be considered as preliminary as they were limited to only two bacteria species; however the dominulin MIC values are in the range of MICs (1–8 μg/ml) of the best natural antibacterial peptides against a wide number of bacteria [33], considering also the 90% purity of our synthetic peptides. For example, MIC values of dominulins on *B. subtilis* and *E. coli* were lower than those of Protonectin (an *Agelaia pallipes* venom peptide with antimicrobial activity) on the same bacteria [18]. At this time, we are enlarging the range of tests against other species of bacteria and fungi, including well known pathogens for insects and man, to verify the effective importance of these compounds in the colonial and individual protection of these wasps.

Acknowledgments

The authors thank S. Gorfer and C. Indorato (Dip. Biologia Animale e Genetica, University of Florence) for their help in microbiological tests, D. Mastroianni (Tecnogen SpA, Piana di Monte Verna, Caserta, Italy), F. De Angelis (Dip. di Chimica, Ingegneria Chimica e Materiali, University of L'Aquila), L. Calamai (Dip. di Scienza del Suolo e Nutrizione della Pianta, University of Firenze) for their help in chemical analyses. Two anonymous referees made important criticisms and suggestions for the improvement of the paper. The authors also thank Ente Cassa di Risparmio di Firenze for funding the acquisition of the Ultraflex and LTQ mass spectrometers. The research was also funded by Università di Firenze and by Anallergo Srl Firenze.

References

1. Schmid-Hempel, P. *Parasites in Social Insects*; Princeton University Press: Princeton, NJ, 1998; p 392
2. Bot, A. N. M.; Ortius-Lechner, D.; Finster, K.; Maile, R.; Boomsma, J. J. Variable Sensitivity of and Bacteria to Compounds Produced by the Metapleural Glands of Leaf-Cutting Ants. *Insect. Soc.* **2002,** *49,* 363–370.
3. Bulet, P.; Stockling, R. Insect Antimicrobial Peptides: Structures, Properties, and Gene Regulation. *Protein Pept. Lett.* **2005,** *12,* 3–11.
4. Gillespie, J. P.; Kanost, M. R.; Trenczek, T. Biological Mediators of Insect Immunity. *Annu. Rev. Entomol.* **1997,** *42,* 611–643.
5. Otvos, L. Antibacterial Peptides Isolated from Insects. *J. Pept. Sci.* **2000,** *6,* 497–511.
6. Kuhn-Nentwig, L. Antimicrobial and Cytolytic Peptides of Venomous Arthropods. *Cell. Mol. Life Sci.* **2003,** *60,* 2651–2668.
7. Brey, P.; Lee W. J.; Yamakawa, M.; Koizumi, Y.; Perrot, S.; Francois, M.; Ashida, M. Role of the Integument in Insect Immunity: Epicuticular Abrasion and Induction of Cecropin Synthesis in Cuticular Epithelial Cells. *Proc. Natl. Acad. Sci. U.S.A.* **1993,** *90,* 6275–6279.
8. Ferrandon, D.; Jung, A. C.; Criqui, M.-C.; Lemaitre, B.; Uttenweiler-Joseph, S.; Michaut, L.; Reichhart, J.-M.; Hoffmann, J. A. A Drosomycin-GFP Reporter Transgene Reveals a Local Immune Response in *Drosophila* that is not Dependent on the *Toll* Pathway. *EMBO J.* **1998,** *17,* 1217–1227.
9. Hölldobler, B.; Wilson, E. O. *The Ants*; Belknap Press of Harvard University Press: Cambridge, MA, 1990.
10. Gambino, P. Antibiotic Activity of Larval Saliva of *Vespula* Wasps. *J. Inv. Pathol.* **1993,** *61,* 110.
11. Turillazzi, S.; Perito, B.; Pazzagli, L.; Pantera, B.; Gorfer, S.; Tancredi. M.Antibacterial Activity of Larval Saliva of the European Paper Wasp *Polistes dominulus* (Hymenoptera, Vespidae). *Insect. Sociaux.* **2004,** *51,* 339–341
12. Pavan, M. Sugli antibiotici di origine animale. *Bollettino dell'Istituto Sieroterapico Milanese Serafino Belfanti* **1952**, *31*, 232–245.
13. Phisalix, M. *Animaux venimeux et venins*, *Vol. II.*; Masson et C.: Paris, 1922.
14. Storey, G. K.; Vandermeer, R. K.; Boucias, D. G.; McCoy, C. W. Effect of Fire Ant (*Solenopsis invicta*) Venom Alkaloids on the in Vitro Germination and Development of Selected Entomogenous Fungi. *J. Inv. Pathol.* **1991,** *58,* 88–95.
15. Orivel, J.; Redeker, V.; Le Caer, J. P.; Krier, F.; Revol-Junelles, A. M.; Longeon, A.; Chaffotte, A.; Dejean, A.; Rossier, J. Ponericins, New Antibacterial and Insecticidal Peptides from the Venom of the Ant *Pachycondyla goeldii*. *J. Biol. Chem.* **2001,** *276,* 17823–17829.
16. Schmidt, J. O.; Blum, M. S.; Overal, W. L. Hemolytic Activities of Stinging Insect venoms. *Arch. Insect. Biochem. Physiol.* **1983,** *1,* 1155–160.
17. Krishnakumari, V.; Nagaraj, R. Antimicrobial and Hemolytic Activities of Crabrolin, a 13-Residue from the Venom of the European Hornet, *Vespa crabro*, and its analogs. *J. Pept. Res.* **1997,** *50,* 88–93.
18. Mendes, M. A.; Monson. de Souza, B.; Ribeiro Marques, M.; Palma, M. S. Structural and biological characterization of two novel peptides from the venom of the neotropical social wasp *Agelaia pallipes pallipes*. *Toxicon* **2004,** *44,* 67–74.
19. Dohtsu, K; Okumura, K.; Hagiwara, K.; Palma, M. S.; Nakajima, T. Isolation and Sequence Analysis of Peptides from the Venom of *Protonectarina sylveirae* (Hymenoptera, Vespidae). *J. Nat. Toxins* **1993,** *1,* 271–276.
20. Park, N. G.; Yamato, Y.; Lee, S.; Sugihara, G. Interaction of Mastoparan-B from Venom of a Hornet in Taiwan with Phospholipid-Bilayers and Its Antimicrobial Activity. *Biopolymers* **1995,** *36,* 793–801.
21. Ayasse, M.; Paxton, R. Brood Protection in Social Insects. Hilker, M.; Meiners, T., Eds.; In Chemoecology of Insect Eggs and Egg Deposition; Blackwell: Berlin, 2002, pp 117–148.
22. Howard, R. W.; Blomquist, G. J. Ecological, Behavioral, and Biochemical Aspects of Insect Hydrocarbons. *Annu. Rev. Entomol.* **2005,** *50,* 371–393.
23. Blomquist, G.; Dillwith, J. W. Cuticular Lipids. In: *Comprehensive Insect Physiology, Biochemistry, and Pharmacology, Vol. III*; Kerkut, G.; Gilbert, L. I., Eds.; Pergamon Press: Oxford, 1985; pp 117–154.
24. Buckner, J. S. Cuticular Polar Lipids of Insects. In: *Insect lipids*; Stanley-Samuelson, D. W.; Nelson, D. R., Eds.; University of Nebraska Press: Lincoln and London, 1993; pp 271–316.
25. James, R. R.; Buckner, J. S. Freeman, T. P. Cuticular Lipids and Silverleaf Whitefly Stage Affect Conidial Germination of *Beauveria bassiana* and *Paecilomyces fumosoroseus*. *J. Inv. Pathol.* **2003,** *84,* 67–74.
26. Turillazzi, S.; West-Eberhard, M. J., Eds., *Natural History and Evolution of Paper Wasps*; Oxford University Press: Oxford, UK 1996.
27. Rees, J. A.; Moniatte, M.; Bulet, P. Novel Antibacterial Peptides Isolated from a European Bumblebee, *Bombus pascuorum* (Hymenoptera, Apoidea). *Insect Biochem. Mol. Biol.* **1997,** *27,* 413–422.
28. Casteels, P.; Ampe, C.; Jacobs, F.; Vaeck, M.; Tempst, P. Apidaecins: Antibacterial Peptides from Honeybees. *EMBO J.* **1989,** *8,* 2387–2391.
29. Mendes, M. A.; Monson. de Souza, B.; Palma, M. S. Structural and Biological Characterization of Three Novel Mastoparan Peptides from the Venom of the Neotropical Social Wasp *Protopolybia exigua* (Saussure). *Toxicon* **2005,** *45,* 101–106.
30. Hirai, Y.; Kuwada, M.; Yasuhara, T.; Yoshida, H.; Nakajima, T. A New Mast Cell degranulating Peptide Homologous to Mastoparan in the Venom of Japanese Hornet (*Vespa xanthoptera*). *Chem. Pharm. Bull.* **1979,** *27,* 1945–1946.
31. Toki, T.; Yasuhara, T.; Nakajima, T. Isolation and Sequential Analysis of Peptides on the Venom Sac of *Parapolybia indica*. *Eisei Dobutsu* **1988,** *39,* 105–111.
32. Hirai, Y.; Ueno, Y.; Yasuhara, T.; Yoshida, H.; Nakajima, T. A New Mast Cell Degranulating Peptide, Polistes Mastoparan, in the Venom of *Polistes jadwigae*. *J. Biomed. Res.* **1980,** *1,* 185–187.
33. Hancock, R.; Chapple, D. S. Peptide Antibiotics. *Antimicrob. Agents Chemother.* **1999,** *43,* 1317–1323.

JOURNAL OF MASS SPECTROMETRY
J. Mass Spectrom. 2007; **42**: 199–205
Published online 18 December 2006 in Wiley InterScience
(www.interscience.wiley.com) DOI: 10.1002/jms.1152

JMS

Comparison of the medium molecular weight venom fractions from five species of common social wasps by MALDI-TOF spectra profiling

Stefano Turillazzi,[1,2]* Claudia Bruschini,[1] Duccio Lambardi,[2] Simona Francese,[1] Igino Spadolini[3] and Guido Mastrobuoni[1]

[1] Centro Interdipartimentale di Spettrometria di Massa, Università degli Studi di Firenze, Italy
[2] Dipartimento di Biologia Animale e Genetica, Università degli Studi di Firenze, Italy
[3] Anallergo SpA, Firenze, Italy

Received 12 July 2006; Accepted 31 October 2006

The average spectral profiles and the exact mass weight (MW) of biomolecules present in the medium fraction (from 900 to 3000 Da) of the venom of five social wasps (three European and one North American *Polistes* and the European hornet *Vespa crabro*) were determined by matrix assisted laser desorption ionization time of flight (MALDI-TOF) MS. Data were obtained analyzing the venom of single specimens (N = 46) and elaborated with the ClinProTools 2.0 (CPT) software to search for differences among the five species examined. Interesting differences in the spectral profiles were found, allowing the discrimination of venoms belonging to the different species, and their possible use as a quality control method in venom immunotherapy (VIT) for allergic patients. Copyright © 2006 John Wiley & Sons, Ltd.

KEYWORDS: MALDI; ClinProTools; venom; immunotherapy; social wasps

INTRODUCTION

Venom of social Hymenoptera is a complex and multi-functional secretion that covers a wide range of defensive necessities of colonies, sometimes containing thousands of individuals. This secretion is dispensed by means of a sting apparatus derived from the transformation of abdominal sclerites; it is produced by tubular (and convoluted) glands and stored in a reservoir.[1] The secretion is a product of a long evolutionary process from solitary species that use it as a fluid to paralyze preys for the rearing of their larvae, to social species that use it mainly for defensive purposes. Social wasps in particular, use the venom as an alarm and sexual pheromone,[2] as an antimicrobial agent[3] and as a chemical weapon against invertebrate and vertebrate enemies.[4,5] The venom is constituted of a mixture of several substances, which can be roughly divided into three main fractions: a low molecular weight (MW) volatile fraction, a medium MW fraction and a proteic fraction.[6]

From the medical point of view, the venom of stinging Hymenoptera has a noteworthy importance, as it can induce strong allergic reactions, up to anaphylactic shock and death, in sensitive patients.[7] The allergic reaction is mainly caused by antigenic proteins, which in the social Vespidae are represented by three principal enzymes (phospholipase A, protease, and hyaluronidase) and a nonenzymatic protein[6,8] called *Antigen 5*; nevertheless, diffusion of these large molecules into the tissues of the victims is certainly facilitated by a set of smaller molecules, including peptides having MW not exceeding 3000 Da. Preventive treatment of allergic patients is made with a desensitizing immunotherapy based on the administration of increasing quantities of venom [Venom Immunotherapy, (VIT)]. A recent review on the argument, after observing that the estimated incidence of 40 fatal reactions each year in the United States of America is probably an underestimate, concludes that the efficacy of VIT (reported to be 95%) is greater than that of any other type of allergen immunotherapy.[7] Notwithstanding the fact that the venom of various species presents cross-reactivity, it seems obvious that VIT could have more efficacy if carried out with the actual venoms, resulting in a positive skin test or radioallergosorbent test (RAST) result. This leads to the necessity to fully understand the chemical composition of the venom of the most common stinging Hymenoptera species. However, owing to the remarkable complexity and the species-specificity of this secretion, information is limited at present mainly to the antigenic proteins and the main pharmacologically active substances of the most common species.[6] As a contribution to this research, we employed the matrix assisted laser desorption ionization-time of flight mass spectrometry (MALDI-TOF MS) technique to determine the reference spectra (profiling) of the venom of some common Vespids (family Vespidae). Peptide mapping and spectra profiling using MALDI-TOF MS analysis and other MS techniques have already been made for characterizing the venoms of

*Correspondence to: Stefano Turillazzi, Centro Interdipartimentale di Spettrometria di Massa (CISM), Università degli Studi di Firenze, Viale Pieraccini 6, 50139 Firenze, Italy.
E-mail: turillazzi@dbag.unifi.it

various organisms including arachnids, insects, jellyfish, snakes etc.[9,10] In some cases, this approach has been used for establishing the phylogenetic relationships between various species belonging to the same taxonomical group (see, e.g. Wermelinger *et al*. for snakes of the genus *Bothrops* and *Crotalus*[11]) or to highlight differences between individuals belonging to the same species (as Jabukowski *et al*. did for venomous fish-hunting *Conus* snails[12]). Regarding social Vespidae, MS techniques have been employed for the study and the characterization of the most important allergens of the venom of various species, although this was performed mainly on the basis of differences in their amino acid sequences (for a recent review see Kolarich *et al*.[13]).

The aims of our research were: (1) testing the suitability of the MALDI-TOF technique for the comparison of the venoms belonging to different species of social Vespids on the basis of their spectral profiles, (2) the collection of data that could be used for the study of the phylogeny of this group of insects and (3) the design of a quick and reliable analytical method for the quality control of venom preparations to be used in VIT. The MALDI technique requires very low amounts of substance and this allowed us to analyze, in a very short time, the venom of single individuals belonging to each examined species – this was important for treating the data with statistical tests controlling for intraspecies variations. In particular, we used ClinProTools 2.0 (CPT), a software until now used mainly in medical researches, primarily developed for proteomic analyses and for the individuation of disease markers in body fluids.[14,15] In this paper, we report the main preliminary results obtained from analyses of the venom fraction ranging from 900 to 3000 Da collected from three European and one North American paper wasps (genus *Polistes*) and from the European hornet *Vespa crabro*. These species can be considered to be within the most common Vespids in the Mediterranean regions and the United States. We chose four species belonging to the same genus (*Polistes*) and one to a relatively phylogenetically distant one (*Vespa*), as we expected different degrees of differentiation in the chemical profile of their venoms. The analysis of the volatile fraction of the venom for some *Polistes* species has been reported by Bruschini *et al*.,[16,17] whereas the comparative analysis of the higher MW proteic fraction is in progress.

EXPERIMENTAL

Species analyses

Polistes dominulus, *P. gallicus*, and *P. nimphus* are common paper wasps in the Mediterranean regions and belong to the subgenus *Polistes s.s*. The first one was introduced in the United States of America almost 20 years ago and here it became the dominant paper wasp species in the Eastern and Central States.[18] *P. exclamans* is a North American species belonging to the subgenus *Aphanilopterus*.[19,20] *V. crabro* is a hornet widespread in Europe, Asia, and North America, where it was introduced in the second half of the 19th century. For a review on social wasps biology, refer to Ross and Matthews.[21]

Wasps were captured from nests or in flight in the surroundings of Florence (Central Italy) and in the countryside around Houston (Texas, U.S.A.).

Chemicals

Methanol and acetonitrile were of chromatography grade and purchased from Riedel de Haen (Sigma Aldrich, Milan, Italy). Purified and deionized water was obtained using a Milli-Q system (Millipore, Bedford, MA, USA.). Formic acid and trifluoroacetic acid (TFA) were purchased from Fluka (Sigma Aldrich, Milan, Italy). Centricon filter unit's vials with nominal MW cutoff of 3000 Da were purchased from Millipore (Bedford, MA, USA.). α-Cyano-4-hydroxycinnamic acid (HCCA) was obtained from Sigma (Sigma Aldrich, Milan, Italy). The matrix for MALDI-TOF experiments was a mixture of a saturated solution of HCCA in acetonitrile and 0.1% TFA in water (1 : 2, v : v).

Venom collection and sample preparation

Wasps were killed at low temperature (−20 °C) and stored in a freezer. After dissection, the venom sacs were gently squeezed until the venom came out from the tip of the sting and was immediately collected in a thin glass capillary.

A. Preliminarily, we performed several analyses on the venom from single specimens of *P. dominulus* (around 0.3 µl for each specimen) directly deposited on an AnchorChip™ 400 target (Bruker) followed by matrix application (0.35 µl of matrix solution HCCA 5 g/l in 1 : 1 acetonitrile : water containing TFA 0.1%).
B. The venom obtained from single specimens of *P. dominulus* ($N = 20$) was diluted in 50 µl of 1 : 1 methanol : water containing TFA 0.1% and then centrifuged for 2 min at 4500 *g*. This dilution ratio was established after several dilution trials. We applied 1 µl of the supernatant on the MALDI plate, left it to dry and then applied 0.35 µl of matrix on the sample.
C. In order to enhance the peak signal intensity in the mass range considered, the venom obtained from single specimens of *P. dominulus* ($N = 10$), after dilution (as above), was filtered using a Centricon unit (with a filter cutting above 3 kDa) and then 1 µl of the filtrate was applied on the AnchorChip™ target as described above. This same procedure was used for preparation of venom samples obtained from single individuals of the other two European species, *P. gallicus* ($N = 10$), *P. nimphus* ($N = 10$) and of the North American *P. exclamans* ($N = 7$) and of the European hornet *V. crabro* ($N = 9$).

The AnchorChip™ target, prepared with all the sample sets (as described in A, B and C), was analyzed using an automatic procedure available on the MALDI mass spectrometer in order to standardize the results.

Mass spectrometry analyses

Spectra were acquired using a MALDI Ultraflex TOF/TOF (Bruker Daltonics, Bremen, Germany). The instrument was operated in positive ion reflector mode; the accelerating voltage and the Ion Source 2 were set to 25.0 and 21.9 kV, respectively, and the delay time was 20 ns; 300 shots were automatically accumulated for each spectrum.

External calibration was performed using the Bruker Standard Peptide Calibration kit.

We performed also an internal calibration using the Flex Analysis™ software by Bruker Daltonics, Bremen, Germany,

DOI: 10.1002/jms

as we had the exact mass of two peptides (1854 and 1909 Da) that we recently identified in the venom of *P. dominulus*.[3]

Data processing

The procedure used for data processing with CPT was suggested by the software manual and is similar to that used by Zhang *et al*.[15] for profiling potential biomarkers in the plasma of asthma patients. We first calibrated all the spectra (refer to the previous paragraph) and imported them to the CPT. The program calculates the areas of the most important peaks that account for statistical differences between the venom of the various species. These peaks are highlighted by the software, which uses them to generate a model to classify the spectra and eventually to assign any other new spectrum to a particular group. The settings we used for the analysis are reported in the tables. The values of the same peaks' areas were also used to perform a Stepwise Discriminant Analysis and to obtain graphs of the groups' distributions.

RESULTS AND DISCUSSION

The rapid analysis of the venom, consisting in its direct deposition on the MALDI plate followed by matrix application (see 'Venom collection and sample preparation A'), did not lead to any significative result. The samples appeared as a translucent surface, probably due to some interfering compounds (fats, sugars) present in the venom. These results are in agreement with previous findings (Dotimas and Hider[22] on honeybee), where it was shown that at least 7% of venom dry weight is composed of sugars and phospholipids. Consequently, the samples for MALDI-TOF analysis were obtained by dilution of the venom samples (see 'Venom collection and sample preparation B'). Under these experimental conditions only the soluble compounds present in the supernatant were analyzed.

Furthermore, the supernatant solution was filtered through a 3 kDa cutoff Centricon unit and the filtrate (see 'Venom collection and sample preparation C'), enriched in medium MW components, was prepared for MALDI-TOF.

In order to obtain statistically significant profiles, MALDI spectra of two different sample sets (20 venom samples from *P. dominulus* prepared as in 'Venom collection and sample preparation B', and 10 venom samples from *P. dominulus* prepared as in 'Venom collection and sample preparation C') were processed by the CPT software. CPT generates an average spectrum of the two sample sets: the comparison of the data obtained by the two approaches described above (simple dilution approach *vs* Centricon-based approach) is reported in Fig. 1.

As it can be observed, the spectra are almost superimposable: the same ions in the range m/z 900–3000 are present, with some differences in relative abundance. In particular, by using the Centricon-based method, a higher abundance of the ions at higher m/z values is observed.

Setting a signal-to-noise threshold of 3.0 (on average spectrum) and a relative threshold base peak of 1.0%, the software found 33 peaks suitable for the following elaboration of models (Table 1); the model produced with the Quick Classifier procedure discriminated correctly 97.5% of the samples with 97.6% for cross validation (a procedure which minimizes the risk of overfitting producing a model that leaves out a fraction of the total number of samples) (Table 2). The two different sample preparations can therefore be easily distinguished by the analysis. For these reasons all further investigations, aiming at finding possible differences at a specific level, have been performed using the Centricon-based approach.

CPT was then used to compare the spectra obtained from the individual samples ($N = 46$) of the five different species considered. The software found 28 peaks suitable for the elaboration of discriminative models. Figure 2 reports the average MALDI spectra for the five different species, whereas Table 3 (I model) lists the main peaks for each species. The main similarities were found between European

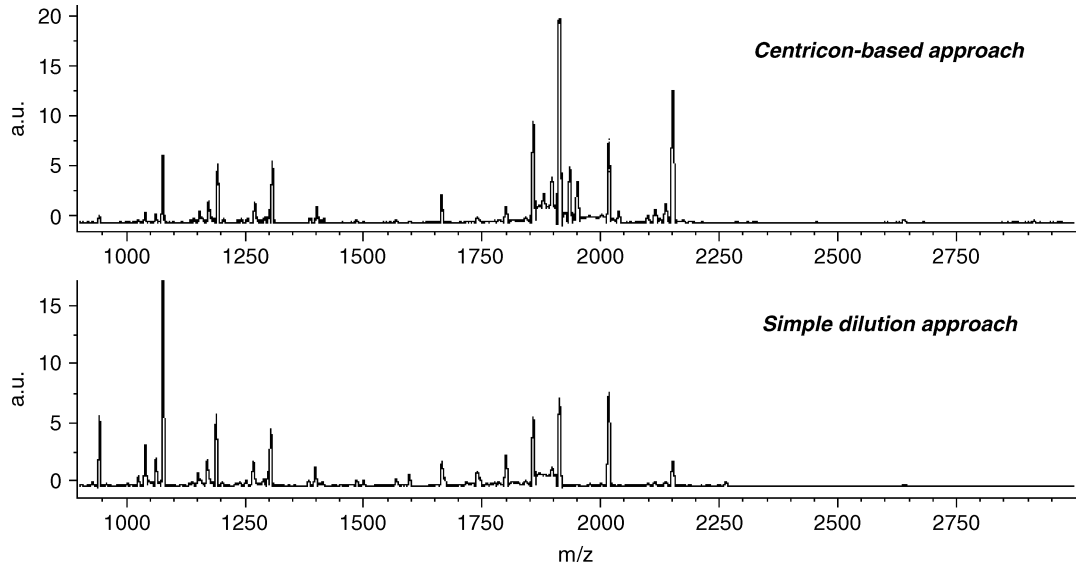

Figure 1. Average MALDI spectra of *P. dominulus* venom samples obtained from the venom, with the simple dilution approach ($N = 20$) and with the Centricon-based approach ($N = 10$).

DOI: 10.1002/jms

Table 1. List of the 33 main MALDI-TOF peaks, ranging from 900 to 3000 *m/z*, identified by the CPT in two sets of specimens of *P. dominulus* venom (simple dilution approach *vs* Centricon-based approach) for the creation of the discrimination model. As $z = 1$, values of *m/z* are in equivalent Daltons

Peaks m/z		
927.39	1484.09	1886.42
941.52	1498.79	1895.63
1023.34	1567.26	1903.05
1038.03	1594.86	1911.25
1060.47	1663.2	1933.2
1075.6	1737.98	1949.24
1168.69	1798.66	2015.31
1187.62	1856.14	2113.19
1266.04	1870.28	2135.24
1296.72	1878.35	2150.27
1396.74	1737.98	2638.35

Table 2. CPT model for recognition of *Polistes dominulus* individuals' venom prepared with two different methods (simple dilution method and Centricon-based method) and for recognition of *P. dominulus, P. gallicus, P. nimphus, P. exclamans* and *V. crabro* individuals' venom (prepared according to the Centricon-based method) for MALDI-TOF analysis. CPT parameters used for model generation for method discrimination and species discrimination analyses were: Peak width: 0.01; Smoothing (width: 5 Da, cycles: 1); Average Peak List Calculation (Relative Threshold Base Peak: 0.01, Signal-to-Noise Threshold: 3, Limit Peak Number: false); Area Calculation (Integration Type: end point level); Peak Selection (Use All Peaks: true, Sort Mode: *P*-value tta); Model Generation (Algorithm: Quick Classifier); Cross Validation (Percent Leave Out: 20%, Number of Iterations: 10)

	Recognition capability (%)	Cross validation (%)
Method discrimination		
Overall	97.5	97.6
P. dominulus – simple dilution method ($N = 20$)	100	100
P. dominulus – Centricon-based method ($N = 10$)	95	95.24
Species discrimination		
Overall	96	94.43
P. dominulus ($N = 10$)	100	90.48
P. gallicus ($N = 10$)	90	90
P. nimphus ($N = 10$)	90	91.67
P. exclamans ($N = 7$)	100	100
V. crabro ($N = 9$)	100	100

Polistes, while *P. exclamans* and *V. crabro* show completely different spectral patterns.

The model produced by the software (using the Quick Classifier algorithm) discriminated correctly 98% (99.17% with cross validation) of the samples into the right species

Table 3. Main peaks ranging from 900 to 3000 Da found for the five different wasp species (*P.n* = *Polistes nimphus*, *P.d* = *P. dominulus*, *P.g* = *P. gallicus*, *P.e* = *P. exclamans*, *V.c* = *Vespa crabro*). Some of these peaks are used for comparison and discrimination of specimens belonging to the five species (I model) and some for the discrimination of the specimens belonging to the European *Polistes* species (II model)

	I model					II model		
Species / Peak m/Z	*P. n*	*P. d*	*P. g*	*P. e*	*V. c*	*P. n*	*P. d*	*P. g*
940	X	X	X					
977					X			
1075	X	X	X					
1117				X				
1239				X				
1266			X					
1298					X			
1301		X						
1331					X			
1362				X				
1376	X					X		
1395					X		X	
1471				X				
1496					X			
1507					X			
1584				X				
1776				X				
1784								X
1855	X	X						
1870			X					X
1896			X					
1910	X	X						
2048	X					X		
2089				X				
2149		X					X	
2185				X				
2224				X				

(Table 2). Using a more traditional multivariate statistical analysis (Stepwise Discriminant Analysis) applied to the 28 peaks identified with CPT, we obtained 100% of the samples correctly assigned to the right species with 99.9% of the variance in the data set explained by the two first discriminant functions (Function 1: Wilks' Lambda = 0.000, $\chi^2 = 786.04$, $P < 0.001$; Function 2: Wilks' Lambda = 0.000, $\chi^2 = 430.39$, $P < 0.001$). The chemical distances of the various species are highlighted by the graph of Fig. 3.

However, when we tried to classify the venom 20 specimens of *P. dominulus* treated with the simple dilution approach protocol ('Venom collection and sample preparation B') using the CPT discriminatory model described above, we obtained only ten of them correctly classified in the right species, while the other ten were erroneously assigned to the other two European *Polistes*.

DOI: 10.1002/jms

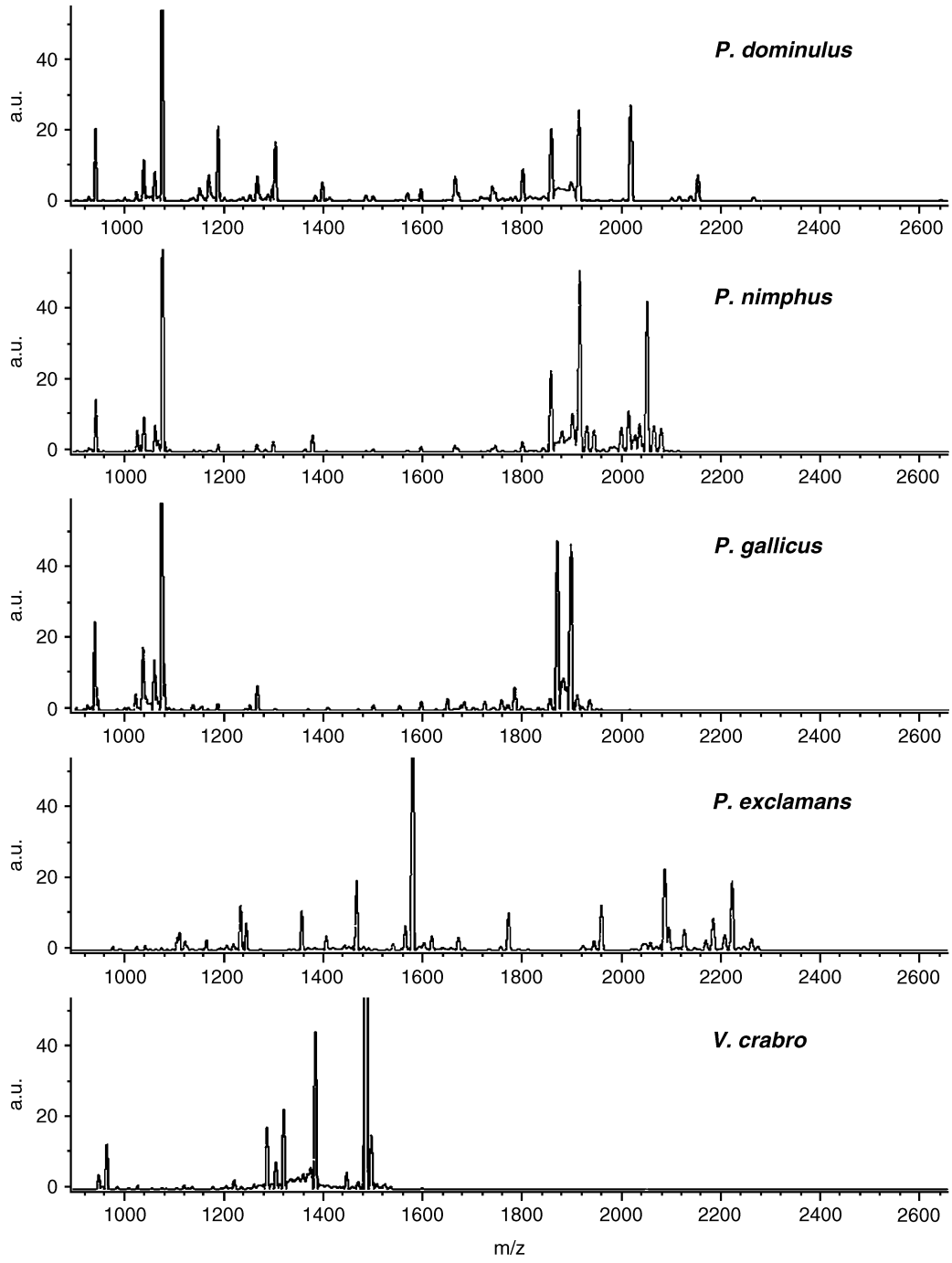

Figure 2. Average MALDI spectra of venom samples from the five examined species *P. dominulus*, *P. nimphus*, *P. gallicus* (10 samples each), *P. exclamans* (7 samples) and *V. crabro* (9 samples), obtained with the Centricon-based approach.

We then tried to obtain a CPT model only for the European *Polistes* species ($N = 30$). This time, however, we used the Gel View Facility supplied by the program in order to choose the most suitable peaks (i.e. the most representative peaks for each species) listed in Table 3 (II model) for a correct discrimination of the venom patterns. This is a rather subjective approach, but it is quite immediate and quick owing to the evident differences in the graphical representation (Fig. 4).

We used an alternative algorithm supplied by the CPT software (Genetic Algorithm), as it allows the use of the chosen peaks ('forcing' them into the model) to develop a discriminatory model. This new approach allowed a complete discrimination among the European *Polistes* species (100% recognition capability both with and without cross validation) and classified correctly all the *P. dominulus* samples obtained with the simple dilution approach (20 out of 20).

Chemical analyses for the identification of the peaks contributing to the discrimination model are still in progress: for two of these substances we already determined their peptidic nature and their sequence, 1854 Da and 1909 Da in *P. dominulus*.[3] The peptidic nature of some peaks of the other species was also confirmed, with the same technique as used by Turillazzi *et al*. (2006).[3]

DOI: 10.1002/jms

JMS

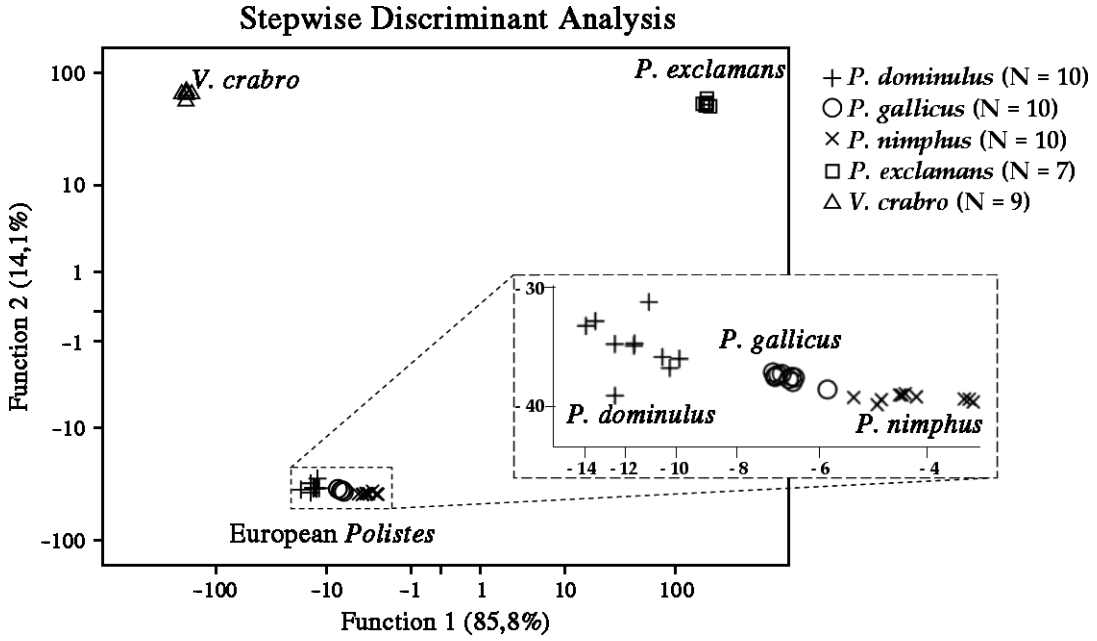

Figure 3. Plot of the scores of the two first Discriminant Functions obtained from the Stepwise Discriminant Analysis of the areas of 28 MALDI spectral peaks of the medium MW fraction of the venom of 46 wasps belonging to the five species examined.

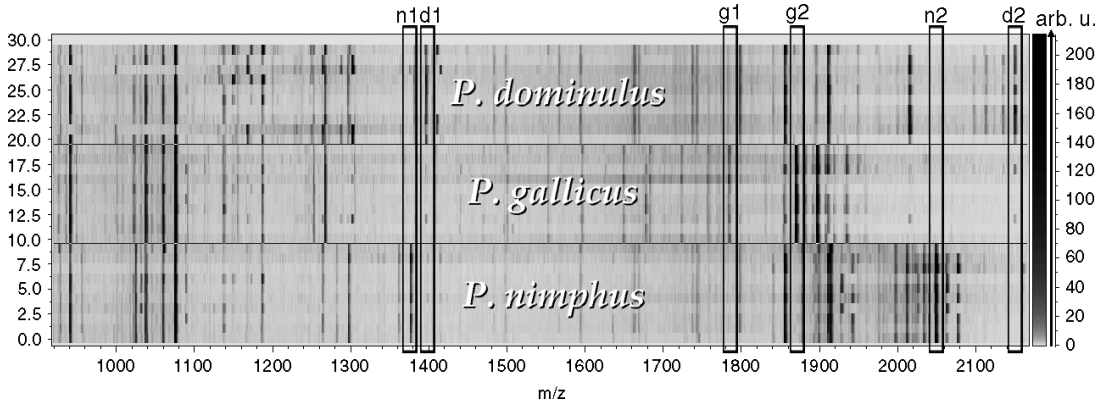

Figure 4. Gel View Facility supplied by the ClinProTools software in order to choose the most suitable peaks for discrimination of European *Polistes* venom. All the 30 samples of the three species analyzed are represented in the figure: the spectral pattern of each individual is shown as a horizontal line with color intensity standing for the relative abundance of the peaks. n1, n2, g1, g2, d1, d2 are the chosen representative peaks for *P. nimphus, P. gallicus* and *P. dominulus*, respectively, whose masses are reported in Table 3.

CONCLUSIONS

This research demonstrates that different species of social wasps have different venom composition in the MW fraction ranging from 900 to 3000 Da. Average spectral profiles of this fraction can be diagnostic for the identification of the species and the results are consistent with the relative taxonomical distances of the species. These differences are both qualitative and quantitative, and each species can be distinguished by a set of fundamental peaks. The identification of these peaks in future studies will be important for fully characterizing the chemistry of the venom of each species.

Differential preparations of venom can influence the corresponding spectral patterns but do not seriously affect the average profile and the classification of the species. This could be important also for quality control of commercial venoms before their use for VIT, assuming that the chemical preparation maintains the medium MW fraction of the secretion.

The variations that we observed between venoms of individuals belonging to the same species deserve a deeper investigation, as they could be related to differences in age, caste, etc. This opens interesting questions about the possibility to document the chemical dynamics of the venom and its correlation with colonial organization of these social insects. MALDI-TOF technique coupled with the CPT software has proved to be a powerful analytical system for the determination of markers discriminating different groups of samples to be used in a wide range of studies.

Acknowledgements

We thank Prof. Joan Strassmann, Rice University, Houston, TX, for providing the specimens of North American *Polistes*, and Prof. Gloriano Moneti, Dr Giuseppe Pieraccini (CISM, University of Florence) and Uwe Rapp for the revision of this paper. We thank

also Bruker Daltonics for the supply of CPT software and two anonymous referees for their criticisms and suggestions to improve the manuscript.

The Ente Cassa di Risparmio di Firenze is gratefully acknowledged for financial support in purchasing MALDI-TOF/TOF and for a grant award to Dr Simona Francese.

REFERENCES

1. Schoeters E, Billen J. Morphology and ultrastructure of a secretory region enclosed by the venom reservoir in social wasps (Insects, Hymenoptera). *Zoomorphology* 1995; **115**: 63.
2. Landolt PJ, Jeanne RL, Reed HC. Chemical communication in social wasps. In *Pheromone Communication in Social Insects*., Vander Meer RK, Breed MD, Winston ML, Espelie KE (eds). Westview Press: Boulder, CO, 1998; 216.
3. Turillazzi S, Mastrobuoni G, Dani FR, Moneti G, Pieraccini G, La Marca G, Bartolucci G, Perito B, Lambardi D, Cavallini V, Dapporto L. Dominulin A and B: two new antibacterial Peptides identified on the cuticle and in the venom of the social paper wasp *Polistes dominulus* using MALDI-TOF, MALDI-TOF/TOF, and ESI-Ion Trap. *J. Am. Soc. Mass Spectr.* 2006; **17**: 376.
4. Schmidt JO. Hymenopteran venoms: striving toward the ultimate defense against vertebrates. In *Insect Defenses*, Evans DL, Schmidt JO (eds). New York Press: Albany, 1990; 354.
5. Schmidt JO, Blum MS, Overal WL. Hemolytic activities of stinging insect venoms. *Arch. Insect Biochem.* 1983; **1**: 155.
6. Hoffman DR. Hymenoptera venoms: composition, standardization, stability. In *Monograph on Insect Allergy*, Levine MI, Lockey RF (eds). American Academy of Allergy, Asthma & Immunology: Milwaukee, WI, 2004; 37.
7. Golden DBK. Insect sting allergy and venom immunotherapy: a model and a mistery. *J. Allergy Clin. Immun.* 2005; **115**: 439.
8. King TP, Spangfort MD. Structure and biology of stinging insect venom allergens. *Int. Arch. Allergy Imm.* 2000; **123**: 99.
9. Nakajima T, Naoki H, Corzo G, Li D, Escoubas P, Yamaji N, Nagai H, Yasuda A, Andrianstiferana M, Haupt J, Oshiro N. A trial of Mass Spectrometric Characterization of femto-molar amount from subtropical islands. *J. Toxicol. Toxin. Rev.* 2003; **22**: 509.
10. Pimenta AMC, De Lima ME. Small peptides, big world: biotechnological potential in neglected bioactive peptides from arthropod venoms. *J. Pept. Sci.* 2005; **11**: 670.
11. Serrao Wermelinger L, Dutra DLS, Oliveira-Carvalho AL, Soares MR, Bloch C, Zingali RB. Fast analysis of low molecular mass compounds present in snake venom: identification of ten new pyroglutamate-containing peptides. *Rapid Commun. Mass Spectrom.* 2005; **19**: 1703.
12. Jakubowski JA, Kelley WP, Sweedler JV, Gilly WF, Schulz JR. Intraspecific variation of venom injected by fish-hunting *Conus* snails. *J. Exp. Biol.* 2005; **208**: 2873.
13. Kolarich D, Leonard R, Hemmer W, Altmann F. The N-glycans of yellow jacket venom hyaluronidases and the protein sequence of its major isoform in *Vespula vulgaris*. *FEBS J.* 2005; **272**: 5182.
14. Zhang X, Leung SM, Morris CR, Shigenaga MK. Evaluation of a novel, integrated approach using functionalized magnetic beads, bench-top MALDI-TOF-MS with prestructured sample supports, and pattern recognition software for profiling potential biomarkers in human plasma. *J. Biomol. Tech.* 2004; **15**: 167.
15. Ketterlinus R, Hsieh SY, Teng SH, Lee H, Pusch W. Fishing for biomarkers: analyzing mass spectrometry data with the new ClinProTools™ software. *Biotechniques* 2005; **38**: S37.
16. Bruschini C, Dani FR, Pieraccini G, Guarna F, Turillazzi S. Volatiles from the venom of five species of paper wasps (*Polistes dominulus, P. gallicus, P. nimphus, P. sulcifer* and *P. olivaceus*). *Toxicon* 2006; **47**: 812.
17. Bruschini C, Dani FR, Pieraccini G, Guarna F, Turillazzi S. Erratum to ''Volatiles from the venom of five species of paper wasps (*Polistes dominulus, P. gallicus, P. nimphus, P. sulcifer* and *P. olivaceus*)''. *Toxicon* 2006; **48**: 473.
18. Cervo R, Zacchi R, Turillazzi S. *Polistes dominulus* (Hymenoptera Vespidae) invading North America: some hypotheses for its rapid spread. *Insect. Soc.* 2000; **47**: 155.
19. Carpenter JM. Phylogeny and biogeography. In *Natural History and Evolution of Paper-Wasps*, Turillazzi S, West-Eberhard MJ (eds). Oxford University Press: 1990; 18.
20. Arevalo E, Zhu Y, Carpenter JM, Strassmann J. The phylogeny of the social wasp subfamily Polistinae: evidence from microsatellite flanking sequences, mitocondrial COI sequence, and morphological characters. *BMC Evol. Biol.* 2004; **4**: 8, (available at: http://www.biomedcentral.com).
21. Ross KG, Matthews RW (eds). *The Social Biology of Wasps*. Comstock: Ithaca, 1991.
22. Dotimas EM, Hider RC. Honeybee venom. *Bee World* 1987; **68**: 51.

2.5. Conclusions

This study demonstrates that different species of social wasps have different venom composition in the MW fraction ranging from 900 to 3000 Da. Average mass spectral profiles of this fraction can be diagnostic for the identification of the species and results are consistent with the relative taxonomical distances of the species. These differences are both qualitative and quantitative and each species can be distinguished by a set of fundamental peaks.

Different preparations of venom can influence the corresponding spectral patterns but do not seriously affect the average profile and the classification of the species. This could be important for quality control of commercial venoms before their use for Venom ImmunoTherapy, standing that the chemical preparation maintains the medium MW fraction of the secretion. The variations that we observed between venoms of individuals belonging to the same species deserve a deeper investigation as they could be related to differences like age, caste and so on.

Two of the discriminating peptides from *P. dominulus*, which were already found on female cuticle, have been characterized showing to be similar to some peptides included in the class of mastoparans, haemolytic tetradecapeptides which have from 7 to 10 hydrophobic amino acid residues and from 2 to 4 lysine residues in their primary sequence.[29,30,31] The molecular weights of Dominulins are similar to those of Apidaecins, inducible haemolymph peptides with antibiotic activities reported for several Hymenopterans.[32] However both the amino acid composition and sequence of Apidaecins strongly differ from Dominulins.

The venom should be the source of these peptides which are spread all over the cuticle by the frequent grooming movements of the female wasps. Since these peptides have an antimicrobial activity, their presence on the cuticle may constitute a first barrier against microbial infections. Moreover they may constitute a social protection for the whole colony when they are applied to the nest surface.

[29] Hirai Y., Kuwada M., Yasuhara T., Yoshida H., Nakajima T. *Chem. Pharm. Bull*. **1979,** *27,* 1945–1946.
[30] Dohtsu K., Okumura K., Hagiwara K.,; Palma MS., Nakajima T. *J. Nat. Toxins* **1993,** *1*, 271–276.
[31] Toki T., Yasuhara T., Nakajima T. *Eisei Dobutsu* **1988,** *39,* 105–111.
[32] Casteels P., Ampe C., Jacobs F., Vaeck M., Tempst P. *EMBO J.* **1989,** *8,* 2387–2391.

At present we are enlarging the range of tests against other species of bacteria and fungi, including well known pathogens for insects (and man), to verify the effective efficacy of these compounds in the colonial and individual protection of these wasps.

This study opens interesting questions about the possibility to document the chemical dynamics of the venom and its correlation with colonial organization of these social insects. MALDI ToF technique coupled with CPT software confirmed to be a powerful analytical system for the determination of markers discriminating different groups of samples to be used in a wide range of studies. In the future we plan to continue the characterization of discriminating peaks in wasp venoms and to extend their classification on the basis of proteic fraction.

3. METALLODRUG/PROTEIN INTERACTIONS REVEALED BY ESI MASS SPECTROMETRY

3.1. Introduction

3.1.1. Anticancer metallodrugs

Since the discovery in the 1960' of the antitumoral activity of (*cis*-[$PtCl_2(NH_3)_2$]), a compound named cisplatin, metal based drugs have been playing a major role in anticancer chemotherapeutic strategies. Research in the field is still very active and has been expanded in recent years to include a conspicuous number of non-platinum metallodrugs. During the last three decades, the interest of the scientific community working on anticancer metal compounds has mostly focused on their interactions with DNA, the commonly accepted "primary" target for platinum compounds, which were described and analysed in hundreds of papers.[33]In contrast, rather surprisingly, the reactions of platinum and non-platinum anticancer metallodrugs with proteins have received very little attention. Only a few biophysical studies have indeed dealt with the interactions of anticancer metallodrugs with proteins. These studies mostly concerned the two major serum proteins, albumin[34] and transferrin,[35,36,37] because they can play a fundamental role in clearance of the intravenously administered drug, as well as metallothioneins,[38,39,40] small cysteine-rich intracellular protein, primarily involved in soft metal ions storage and detoxification.[41] However, additional studies were carried out on a few model proteins such as ubiquitin,[42] haemoglobin,[43,44] myoglobin,[45] cytochrome c[46] and glutathione-S-transferase.[47]

---

[33] Wang D., Lippard SJ. *Nat. Rev. Drug. Discov*. **2005,** *4*, 307-320.
[34] Ivanov AI., Christodoulou J., Parkinson JA., Barnham KJ., Tucker A., Woodrow J., Sadler PJ. *J .Biol Chem*. **1998**, *273*, 14721-14730.
[35] Khalaila I., Allardyce CS., Verma CS., Dyson PJ., *Chem. Bio. Chem*. **2005,** *6*, 1788-1795.
[36] Allardyce CS,. Dyson PJ, Coffey J., Johnson N., *Rapid. Commun. Mass Spectrom*. **2002**, *16,* 933-5.
[37] Zhao YY., Mandal R., Li XF. *Rapid Commun Mass Spectrom*. **2005**, *19,* 1956-62.
[38] Hagrman D., Goodisman J., Dabrowiak JC.,. Souid AK, *Drug. Metab. Dispos*. **2003** , *31,* 916-23.
[39] Zhang B., Tang W., Gao S., Zhou Y., *J. Inorg. Biochem*. **1995**, *58*, 9-19.
[40] Knipp M.,. Karotki AV., Chesnov S., Natile G., Sadler P J., Brabec V., Vasak M., *Biochemistry* **2007** in the press.
[41] Chu G., *J. Biol. Chem*. **1994**, *269*, 787-790.
[42] Gibson D., Costello CE., *Eur. Mass. Spectrom*. **1999**, 5501-510.
[43] Mandal R., Kalke R., Li XF., *Chem Res Toxicol*. **2004**, *17,* 1391-1397.
[44] Mandal R., Teixeira C., Li XF., *Analyst*. **2003**, 128 629-34.
[45] Peleg-Shulman T., Najajreh Y., Gibson D*., J. Inorg. Biochem*. **2002**, *91*, 306-311.

For that reason this topic deserves more and more attention; it is in fact increasingly evident that the interactions of anticancer metallodrugs with proteins play crucial roles not only in their uptake and biodistribution processes but also in determining their overall toxicity profile. Even more interestingly, reactions of anticancer metallodrugs with proteins are likely to be involved in some crucial aspects of their mechanism of action. This latter statement is particularly true for non-platinum anticancer metallodrugs such as ruthenium and gold compounds for which DNA-independent mechanisms of action have been proposed and experimentally supported.[48,49] For instance, it was suggested that dimethylsulfoxide ruthenium(III) drugs might either interfere with specific proteins involved in signal transduction pathways or alter cell adhesion processes.[50] Direct antimitochondrial effects were demonstrated for a few cytotoxic gold complexes with gold in the oxidation states +1 and +3.[51]

Nowadays, the study of the interactions occurring between metallodrugs and proteins may take new and considerable advantage of the availability of very sophisticated and advanced analytical tools. For instance, a number of papers have highlighted the great potential of modern mass spectrometry ionization methods, in particular ESI and MALDI, to characterise metal-protein adducts at the molecular level.[52,53,54] On the other hand, X-ray diffraction studies of such adducts, although not easy, may result extremely valuable in providing detailed structural information on the formed metallodrug-protein species. On the whole, the integration between these complementary methods, as well as with NMR spectroscopy, has the potential to offer rather exhaustive descriptions of metallodrug/protein interactions when working on the purified components.

---

[46] Yang G., Miao R., Jin C., Mei Y., Tang H., Hong J., Guo Z., Zhu L., *J. Mass. Spectrom*. **2005**, *40*, 1005-16.

[47] Ang WH., Khalaila I., Allardyce CS., Juillerat-Jeanneret L., Dyson PJ., *J. Am. Chem. Soc*. **2005**, *127,* 1382-3.

[48] Dyson P J., Sava G., *Dalton Trans*. **2006**, 1929-1933.

[49] Gabbiani C., Casini A., Messori L., *Gold Bull*. **2007**, *40*,73-81.

[50] Pintus G., Tadolini B., Posadino AM., Sanna B., Debidda M., Bennardini F., Sava G., Ventura C., *Eur. J. Biochem*. **2002**, *269,* 5861-70.

[51] Barnard PJ., Berners-Price SJ., *Coord.Chem.Rev*. **2007**, *251,* 1889-1902.

[52] Cristoni S., Bernardi LR. *Mass. Spectrom*. **2003**, *22*, 369-406.

[53] Hartinger CG., Alexenko S., Timerbaev AR., Keppler BK., Published Title of colleted works, Novel approaches for the discovery and the development of anticancer agents, Vienna, CESAR, **2005**, P16.

[54] Mandal R., Li XF, *Rapid Commun.Mass Spectrom*. **2006**, *20,* 48-52.

3.1.2. Basic aspects of metallodrug/protein interactions

Remarkably, most of the above mentioned compounds are known to behave as pro-drugs, in other words an activation step is required before they can react with their biomolecular targets and cause their specific biological effects. Usually this step consists of the release of a weak ligand (the so called leaving group) and of its replacement by a water molecule. The resulting aqua species usually manifest a high propensity to react with protein side-chains. Alternatively, activation may take place through a redox process, for instance metal reduction, as it is the case for newly developed anticancer platinum(IV) compounds.[55] The reaction of activated metallodrugs with protein side chains leads to formation of metallodrug-protein complexes or adducts in which metallic fragments are covalently bound to proteins. These adducts usually manifest an appreciable stability.

Thus, it becomes fundamental to understand the reactions of metallodrugs with proteins at the molecular level, to identify common trends in these reactions, to characterise the nature of bound metal fragment and binding site in the protein, and to identify the most important intracellular protein targets for the various classes of anticancer metallodrugs.

3.2. Methods

3.2.1. Mass spectrometry

Although single crystal X-ray diffraction still represents the election tool to obtain high quality structural information on proteins, especially for those of medium to large size, up to now very few crystal structures have been solved to a high resolution for metallodrug-protein adducts. This situation may be principally ascribed to the intrinsic difficulty in obtaining good quality crystals for metallodrug/protein adducts. Also it is worth noting that crystal structures provide only a static vision of the metallodrug-protein derivative in the solid state. Information on the reactivity of the bound metal fragment is difficult to extract although it may be inferred indirectly.

In this respect mass spectrometry offers an alternative approach to the problem and may provide independent and complementary information

In electrospray ionization (ESI) a solution of the analyte is passed through a capillary which is held at high electric potential. As effect of the high electric field the emerging solution generates highly charged droplets which pass towards the analyser portion of the

[55] Wong E. and Giandomenico CM., *Chem Rev* **1999,** *99,* 2451–2466

mass spectrometer because of a potential and pressure gradient. During that transition, the droplets reduce in size by evaporation of the solvent or by "Coulomb explosion" (droplet subdivision resulting from the high charge density).[56] Ultimately, fully desolvated ions result from complete evaporation of the solvent. Nebulisation of the solution emerging from the capillary may be facilitated by a sheath flow of nebuliser gas, a technique for which the term "ionspray" was originally coined by its developers.[57]

The essential features of the experimental arrangement are shown in figure 4; the source can be coupled to a variety of MS analyzers, such as ion traps or Orbitrap, which are the ones used in the following studies.

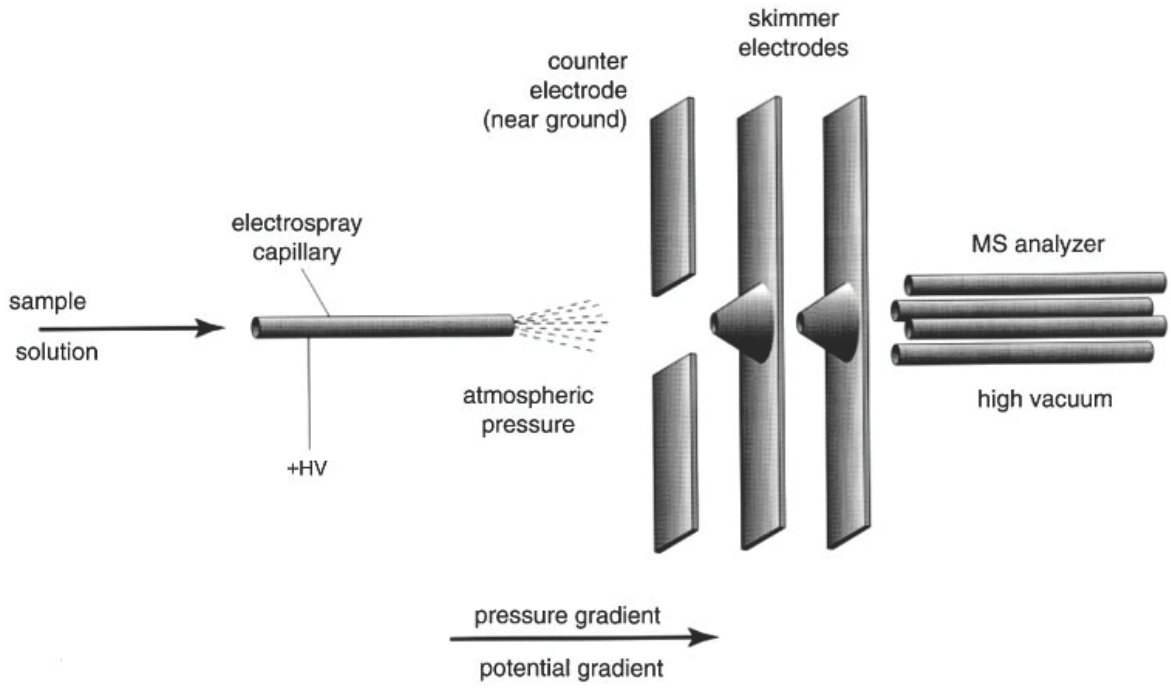

Figure 4. Scheme of ESI ion source.

ESI is a gentle ionization method, yielding no molecular fragmentation (unless induced in the atmosphere/vacuum interface) and allowing intact weakly bound complexes to be detected. Since its birth, it was evident that weakly bound complexes could be detected, but only some years later some researchers demonstrated that specific noncovalent interactions could be detected by ESI-MS.[58]

Today, thanks to the latest technological improvements ESI MS represents a very powerful method for the molecular characterisation of metallodrug-protein adducts. A series of pioneering studies carried out by Dani Gibson and co-workers during the 1990s

[56] Cech NB., Enke CG. *Mass Spectrom Rev*. **2001**, *20*, 362-87
[57] Bruins AP. *J Chromatogr*. **1991,** *554*, 39-46.
[58] Henion J., Li YT., Hsieh YL., Ganem B. *Ther Drug Monit*. **1993,** *6,* 563-9

and the early 2000s highlighted the advantages of this method and defined the experimental conditions for its application to simple metallodrug/protein systems. Most of his studies focused on the reactivity of cisplatin and analogues with ubiquitin, taken as the reference model protein. The careful interpretation of the ESI MS results collected under various experimental conditions allowed to assign the two main platinum binding sites in ubiquitin, to describe the time dependent evolution of the resulting platinum protein adducts and also to monitor the reactivity of the platinum protein adducts with other relevant biomolecules that are present intracellularly e.g. glutathione and various nucleobases.[59]

The high content of structural and functional information that could be derived from those early ESI MS studies prompted us to use a similar approach for the characterisation of metallodrug-protein systems hereafter described.

3.2.2. Selected model systems

As first step towards the understanding of protein/metallodrug reaction mechanisms it is mandatory to choose relatively simple experimental systems, in order to reduce the variables to be taken into account and to focus on analogies and differences between the various compounds in the presence of different proteins.

In this study the most relevant platinum complexes in clinical use have been considered i.e. cisplatin, carboplatin and oxaliplatin (figure 5) but also some new experimental platinum compounds bearing different structural motifs such as the well known platinum iminoethers recently developed at the University of Bari (figure 6).[60] Among ruthenium compounds we took in consideration the ruthenium(III) complex (imidazolium trans [tetrachloro(DMSO) (imidazole)ruthenate(III)]) NAMI A[61] (figure 7), now in phase II of

[59] Peleg-Shulman T., Najajreh Y., Gibson D., *J. Inorg. Biochem*. **2002,** *91*, 306-311.

[60] Coluccia M., Boccarelli A., Mariggio MA., Cardellicchio N., Caputo P., Intini FP., Natile G. *Chem Biol Interact*. **1995**, *98,* 251-66

[61] Alessio E., Mestroni G., Bergamo A., Sava G., *Curr. Top Med. Chem*. **2004**, *41,* 525-35

clinical trials,[62] but also a few ruthenium(II)–arene complexes developed at the École polytechnique fédérale de Lausanne by the group of Paul Dyson (figure 8).[63]

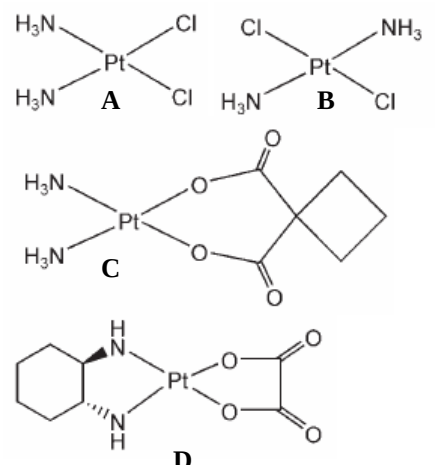

Figure 5. Structure of (A) cisPt, (B) transPt, (C) carboPt, (D) oxaloPt.

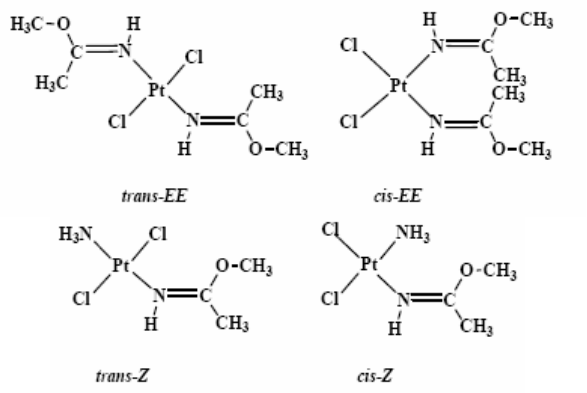

Figure 6. Structure of iminoether platinum complexes utilized.

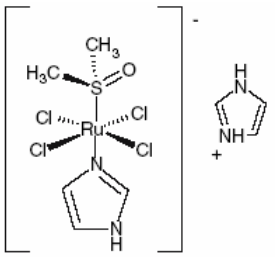

Figure 7.
Structure of NAMI A

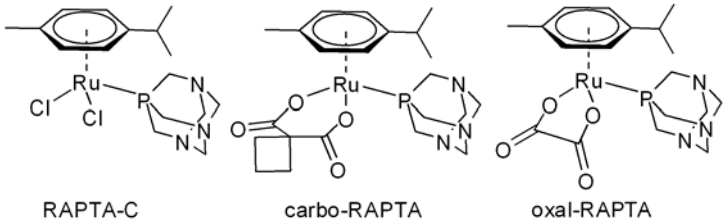

Figure 8.Structure of RAPTA complexes.

Proteins selected as suitable models to test reactivity with metallodrugs were the following: hen egg white lysozyme (HEWL), and horse heart cytochrome c (cyt c), mainly because they manifest a high stability in solution under physiological-type conditions, are commercially available, relatively cheap and water soluble. In addition these proteins exhibit in most cases a basic pI and are thus appropriate for ESI MS detection in the positive ion mode. All these features render experimental work on these model systems more comfortable.

[62] Rademaker-Lakhai J. M., van den Bongard D., Pluim D., Beijnen J H., Schellens J H., *Clin.Cancer Res.* **2004**, *10*, 3717-27.

[63] Scolaro C., Bergamo A., Brescacin L., Delfino R., Cocchietto M., Laurenczy G., Geldbach TJ., Sava G., Dyson PJ. *J Med Chem*. **2005**, *48,* 4161-71.

3.3. Results

In a first study the interactions of four classical platinum(II) drugs -namely cisplatin, its inactive isomer transplatin, carboplatin and oxaliplatin - with horse heart cytochrome c were analysed. Under the applied experimental conditions, the four compounds turned out to exhibit a roughly similar pattern of reactivity with cyt c. This finding was soon of particular interest and novelty, being in striking contrast with current opinions concerning the comparative reactivity of the investigated platinum drugs. Indeed, the four platinum compounds that were selected for our study are commonly known to exhibit greatly different stability and reactivity patterns under physiological-like conditions;[64,65,66,67.68] in fact carboplatin and oxaliplatin are reflected in a lower reactivity with DNA and with other proteins,[69,70,71,72,73,74] Thus, it was quite surprising finding that all tested platinum compounds produced substantially similar levels of cyt c platination. Accordingly, it can be deduced that cyt c should play a major role in enhancing the reactivity of the kinetically stable carboplatin and oxaliplatin compared to cisplatin and transplatin.

Representative ESI MS spectra of the cyt c adducts with cisplatin or carboplatin are reported in figure 9 A and C.

In all cases the ESI MS spectra clearly show the formation of the adduct, but the free protein still dominates the spectrum; however, after longer incubation time (168 h) the peak of free protein is barely visible (figure 9 B and D), pointing out that nearly complete protein platination has truly occurred.

---

[64] Treskes M., Holwerda U., Klein I., Pinedo HM., van der Vijgh WJ., *Biochem. Pharmacol*. **1991**, *42*, 2125 –2130

[65] Andersson A., Hedenmalm H., Elfsson B., Ehrsson H., *J. Pharm. Sci.* **1994**, *83*, 859 –862

[66] Jerremalm E., Videhult P., Alvelius G., Griffiths WJ., Bergman T., Eksborg S., Ehrsson H., *J. Pharm. Sci*. **2002**, *91*, 2116– 2121.

[67] Raymond E., Faivre S., Chaney S., Woynarowski J., Cvitkovic E., *Mol. Cancer Ther*. **2002**, *1*, 227 –235.

[68] Cheung YW., Cradock JC., Vishnuvajjala BR., Flora KP., *Am. J. Hosp. Pharm*. **1987**, *44*, 124 –130.

[69] Boulikas T., Vougiouka M., *Oncol. Rep*. **2003**, *10*, 1663 –1682.

[70] Knox RJ., Friedlos F., Lydall DA., Roberts JJ., *Cancer Res*. **1986**, *46*, 1972 -1979.

[71] Heudi O., Mercier-Jobard S., Cailleux A., Allain P., *Biopharm. Drug Dispos*. **1999**, *20*, 107-116.

[72] Gaver R. C., George A. M., Deeb G., *Cancer Chemother. Pharmacol*. **1987**, *20*, 271 -276.

[73] van der Vijgh W. J., Klein I., *Cancer Chemother. Pharmacol*. 19**8**6, *18*, 129 -132.

[74] Xie R., Johnson W., Rodriguez L., Gounder M., Hall G.S.,. Buckley B.A, *Anal. Bioanal. Chem*. **2007**, *387*, 2815-22

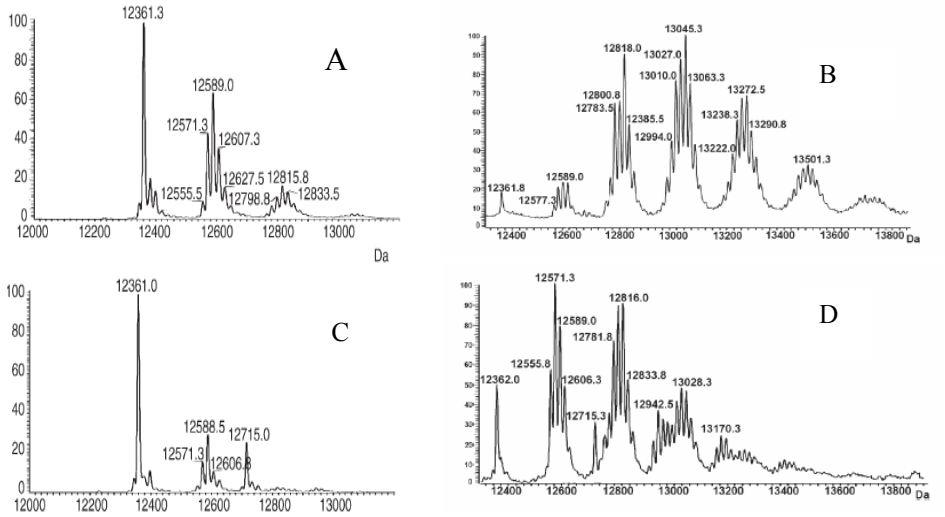

Figure 9. Spectrum of adducts between cyt c and cisPt or carboPt after 24 h (panels A and C) or 168 h (panels B and D) of incubation.

The same investigative approach was applied to platinum adducts of HEWL and even in this case ESI MS measurements turned out very valuable to monitor the process of metallodrug-lysozyme adduct formation and to elucidate the exact nature of the protein bound metallic fragments. Differently from previous case, it was observed that under the employed solution conditions, platinum-HEWL adduct formation is rather slow, that cisplatin is by far the most efficient platinum compound in producing HEWL platination and that monoplatinated species are the predominant ones, again suggesting the presence of a highly preferential platinum binding site. This hypothesis was then confirmed by solving the crystal structure of cisplatin-HEWL complex above, indicating the imidazole ring of His15 as primary binding site (figure 10).

In addition, it is worth noting that the ESI MS spectrum of the HEWL cisplatin derivative (figure 11) shows two peaks of similar intensity at 14569 and 14605 Da that formally correspond to either $[Pt(NH_3)_2Cl]^+$ or intact cisplatin bound to the native protein. A similar situation was formerly described by Dyson and co-workers in the case of the cisplatin-transferrin system and interpreted in terms of a two-step cisplatin to protein binding

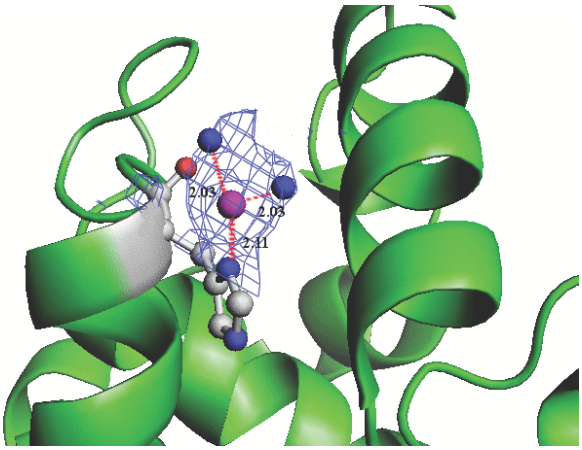

Figure 10. X-ray structure of cisplatin/HEWL adduct, covering platinum(II) (magenta) that interacts with Nε of His15 and with two ammonia ligands (blue) and the relative bond lengths (Å).

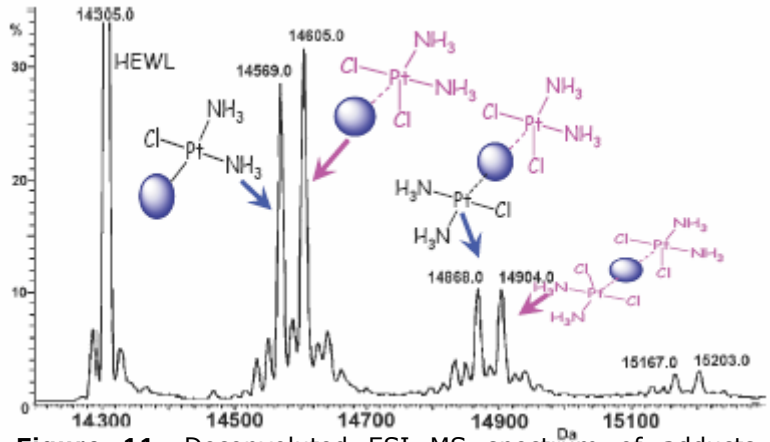

Figure 11. Deconvoluted ESI MS spectrum of adducts formed between HEWL and cisplatin, after 48 h incubation at 37 °C. The initial ruthenium/protein stoichiometry of each sample is 3:1.

process.[75]

This approach was then extended to monitor the reactions of some novel anticancer platinum(II) iminoether complexes, namely *trans*- and *cis*-*EE* (*trans*- and *cis*-$[PtCl_2\{(E)$-$HN{=}C(OCH_3)CH_3\}_2]$, respectively) and *trans*- and *cis*-*Z* (*trans*- and *cis*-$[PtCl_2(NH_3)\{(Z)$-$HN{=}C(OCH_3)CH_3\}]$, respectively), with horse heart cytochrome c.

From this study it has emerged very clearly that interactions with this cyt c do profoundly alter the intrinsic reactivity of the various platinum iminoethers, leading to the observation of rather unexpected chemical transformations at the level of the platinum ligands. In addition, the kinetics of degradation of the platinum complexes could be measured and found to be largely influenced by the interactions with this protein. Remarkably, a profoundly different pattern of reactivity was identified for the *trans* isomers with respect to the *cis*. Valuable information for the platinum binding site assignment was achieved through a partial proteolysis experiment by using the endoproteinase Asp-N. The comparative analysis of the obtained results with those previously reported for classical platinum(II) anticancer drugs made us confident that Met 65 is the major binding site for platinum(II) iminoethers on cyt c.

Independent data obtained from NMR, ICP-OES (Inductively Coupled Plasma-Optical Emission Spectroscopy)and absorption electronic spectroscopies gave strong support to these observations, being in concordance with MS data.

Following the satisfactory results obtained for platinum-protein adducts, the study went on with the characterisation of adducts formed between the same model proteins and some important non platinum metallodrugs. Ru(II)-arene complexes (RAPTA compounds) share a common structural motif consisting of a ruthenium(II) centre bound to both an arene (cymene in this case) and to a 1,3,5-triaza-7-phosphaadamantane (PTA) ligand. They only

[75] Khalaila, I., Allardyce CS., Verma CS., Dyson PJ., *Chem. Bio. Chem.* **2005**, *6*, 1788-1795.

differ in the nature of the ligands located at the two remaining coordination positions. The first representative member of this family is [Ru(η^6-cymene)(pta)Cl_2] (RAPTA-C). Replacement of the two chloride groups with bidentate ligands [either oxalate - to form Ru(η^6-cymene)(pta)(C_2O_4) (oxalo-RAPTA) - or cyclobutane dicarboxylate (CBD) - to give Ru(η^6-cymene)(pta)($C_6H_6O_4$) (carbo-RAPTA)] - greatly reduces the rate of aquation, thus modifying their overall solution behaviour, without affecting cytotoxicity.[76] The three investigated complexes essentially manifested a similar cell-growth inhibition activity against a number of representative cancer cell lines. The binding of a wide range of RAPTA derivatives to oligonucleotides was formerly studied but no direct correlation between oligonucleotide binding and cytotoxicity could be established.[77,78] This finding might suggest that protein targets are of great importance in producing the observed cytotoxic effects.

As expected, the substitution of chloride ligands with bidentate ligand as oxalate or CDB greatly reduces the rate of substitution of these ligands with protein residues.

In second place, the analysis of the adducts formed by cyt c and RAPTA-C suggests that the protein has two distinct anchoring sites, one larger that can host Ru plus arene and PTA ligand, and a smaller one that can host Ru plus only arene ligand.

When incubated with lysozyme the same compounds showed a much lower reactivity, pointing out the strong influence that the chemical microenvironment strongly exerts on the drug reactivity.

The obtained results could be subsequently confirmed by high resolution mass spectrometry measurements, carried out on an LTQ FT-Orbitrap instrument. The obtained experimental data perfectly match theoretical expectations, thus confirming our hypotheses on the chemical nature of the resulting protein bound fragments.

Finally, this ESI MS approach was applied to the well known antimetastatic ruthenium(III) complex NAMI A developed in Trieste, Italy, by Mestroni, Alessio and Sava. Although the main features of interaction between NAMI A and some serum protein were determined in some initial studies, molecular details of the binding processes could

---

[76] Ang WH., Daldini E., Scolaro C., Scopelliti R., Juillerat-Jeannerat L., Dyson PJ., *Inorg. Chem*. **2006**, *45*, 9006-9013.

[77] Dorcier A., Dyson PJ., Gossens C., Rothlisberger U., Scopelliti R., Tavernelli, I. *Organometallics* **2005**, *24*, 2114-2123.

[78] Scolaro C., Geldbach T. J., Rochat S., Dorcier A., Gossens C., Bergamo A., Cocchietto M., Tavernelli I., Sava G., Rothlisberger U., Dyson PJ. *Organometallics* **2006**, *25*, 756-765.

not be fully elucidated due to the relatively high molecular weight of the mentioned proteins and to failure to obtain high resolution X-ray crystal structures for the resulting ruthenium-protein adducts.

In our work NAMI A was reacted either with cyt c or HEWL and the resulting products were analysed through ESI MS. Quite unexpectedly, two substantially different modes of metallodrug-protein interaction clearly emerged in the two cases. In fact, lysozyme gave rise, predominantly, to non-covalent binding with either intact or mono-hydrolyzed NAMI A, most likely mediated by electrostatic interactions. Protein binding appeared to be largely reversible. Remarkably, these interactions greatly slowed down intrinsic NAMI A degradation processes.

In contrast, cyt c was found to enhance NAMI A degradation by facilitating the progressive detachment of the various ligands from the ruthenium centre. Most likely, this process is favoured by an initial electrostatic interaction between the negatively charged NAMI A "core" and this small basic protein.[79]

It is worth mentioning that the reactivity of NAMI A with the above proteins was monitored through a variety of independent physico-chemical methods including optical spectroscopy, ^{1}H NMR and ICP OES. The combined use of the mentioned analytical techniques complemented and confirmed the information obtained through ESI MS.

[79] Andersson T., Thulin E., Forsén S., *Biochemistry* **1979**, *18,* 2487-93.

3.4. Publications

DOI: 10.1002/cmdc.200500079

Exploring Metallodrug–Protein Interactions by ESI Mass Spectrometry: The Reaction of Anticancer Platinum Drugs with Horse Heart Cytochrome c

Angela Casini,[a] Chiara Gabbiani,[a] Guido Mastrobuoni,[b] Luigi Messori,*[a] Gloriano Moneti,[b] and Giuseppe Pieraccini[b]

Since DNA is commonly believed to be the primary target for platinum metallodrugs,[1–4] researchers' interest has mainly focused on the characterisation of platinum–nucleic acid adducts while devoting much less attention to platinum–protein adducts. However, protein-bound platinum fragments probably represent truly active anticancer species—rather than mere drug-inactivation products—provided that metal transfer among distinct binding sites is kinetically allowed.[4] Moreover, platination of specific side chains, which can affect the function of biologically crucial proteins or enzymes through the formation of tight coordinative bonds, might play a relevant role in the overall mechanism and toxicity of platinum drugs.[5] The state of the art of platinum–protein interactions is described in a few articles and reviews;[6–8] in any case, this issue warrants further experimental work.

Thanks to the latest improvements, electrospray ionisation mass spectrometry (ESI-MS) today represents a very powerful method for exploring metallodrug–protein interactions.[6] Owing to the introduction of "soft" ionisation methods, it is possible to transfer the intact metal–protein adduct—whole, in the gas phase—to determine its molecular mass with high accuracy and, thus, obtain its full molecular characterisation. However, much work is still required for the optimisation and the standardisation of experimental ESI-MS procedures directed at these systems. A great variability in ESI-MS responses is generally found in the current literature that depends on many factors, such as the nature of the protein, the nature of the metal, the specific solution conditions, the nature of the metal-bound ligands, pH and the kind of buffer.[9] Apparently, the intrinsic "fragility" of the metal–protein coordination bonds represents a major obstacle, often leading to extensive bond cleavage during ionisation and to loss of chemical information.

[a] Dr. A. Casini, Dr. C. Gabbiani, Prof. L. Messori
Department of Chemistry, University of Florence
Via della Lastruccia 3, 50019 Sesto, Fiorentino (Italy)
Fax: (+39) 055-457-3385
E-mail: luigi.messori@unifi.it

[b] Dr. G. Mastrobuoni, Prof. G. Moneti, Dr. G. Pieraccini
Mass Spectrometry Centre, University of Florence
Via U. Schiff 6, 50019 Sesto Fiorentino (Italy)

Supporting information for this article is available on the WWW under http://www.chemmedchem.org or from the author.

Some pioneering ESI-MS studies of platinum–protein interactions were reported a few years ago by Gibson and co-workers, who used either ubiquitin or myoglobin as model proteins.[10] A number of platinum–protein adducts were identified and characterised in detail. Afterwards, a few additional ESI-MS studies of various metallodrug–protein adducts were reported by other research groups.[11]

Cytochrome c is a small electron-carrier heme protein, localised in the mitochondria, that plays a crucial role in apoptotic pathways.[12] Cytochrome c is also known to be an excellent ESI-MS probe and has been the subject of a number of investigations.[13] This led us to choose cytochrome c as the model protein for our study. The following classical platinum drugs were selected: cisplatin, transplatin, carboplatin and oxaliplatin (Scheme 1).

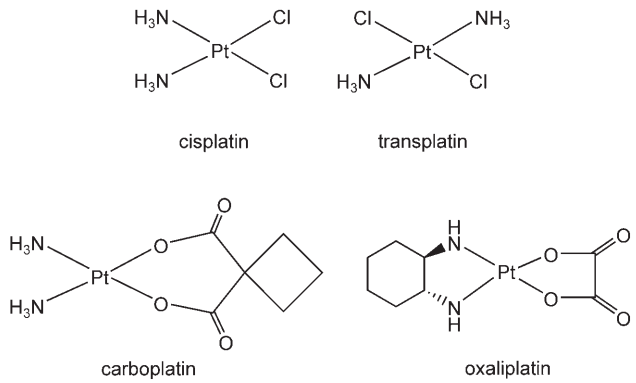

Scheme 1. Schematic drawing of selected anticancer platinum complexes.

Cytochrome c presents, indeed, a number of favourable features: it is a small protein suitable for ESI-MS studies (M_W = 12362), it shows spectroscopically useful and intense absorption bands in the visible region, it possesses a covalently linked heme moiety, it is known to produce well-resolved ESI-MS spectra in the *m/z* 1000–2000 region,[13] a few "free" sites are available on its surface that may specifically react with transition metal ions, that is, His26, His33 and Met65.

Platinum–protein adducts were prepared as follows. Horse heart cytochrome c (cyt c) was treated at physiological pH with each platinum compound at various metal/protein ratios, as described in the Experimental Section,[14] for different incubation times (24–168 h). After extensive dialysis, the resulting platinum–protein adducts were analysed by visible absorption spectroscopy, inductively coupled plasma optical emission spectroscopy (ICP-OES) and ESI-MS.

UV-visible spectra show that, under aerobic conditions, cyt c is stable in its oxidised state. Addition of the various platinum drugs, even at relatively high molar ratios, did not appreciably modify the main visible bands at 400 and 550 nm (Figure S1 in the Supporting Information); this indicates that the protein chromophore is not affected. Conversely, ICP-OES determinations of platinated cyt c samples suggest substantial association of platinum to the protein, even after extensive dialysis against the buffer (vide infra).

The ESI-MS spectral profiles for cyt c and its platinum adducts are shown in Figure 1, with the respective deconvoluted spectra in Figure 2. Very satisfactory S/N ratios were obtained for all ESI-MS profiles and for the deconvoluted spectra. Under the nondenaturing experimental conditions used here, cyt c shows a spectral pattern that is dominated by the +8 multicharged species;[13] the relative intensities of the adjacent +9 and +7 peaks are in line with previous observations.[13] The obtained molecular mass of 12362 Da closely matches the theoretical mass of cyt c (i.e. apocytochrome c plus the heme group). Treatment with platinum drugs produced, in all cases, the appearance of new ESI-MS features that are diagnostic of the formation of stable platinum–protein adducts. All shown spectral profiles refer to samples treated for 72 h with a threefold excess of Pt drug and then extensively dialysed. Indeed, these conditions afforded a significant degree of cyt c platination (platination levels ranging from 1.2 to 1.5 Pt moles per cyt c were determined by ICP-OES for all platinum-treated samples).

No substantial modifications of the distribution pattern of the multicharged ions were observed in the platinum–cyt c adducts; this implies that the overall protein conformation is not significantly affected. Remarkably, the peak corresponding to non-platinated cyt c is still observed in all cases; this indicates that platination of cyt c, even after 72 h incubation, is not complete. However, the intensity of this peak is found to greatly decrease (until disappearance) as the incubation times or the applied Pt/cyt c ratios are further increased (see, for instance, Figure 3, below).

The deconvoluted ESI-MS spectrum of the cisplatin derivative (Figure 2B) shows an intense multiplet centred at 12589 Da that corresponds to an adduct in which a single $[Pt(NH_3)_2]^{2+}$ fragment is coordinated to the native holoprotein. An additional multiplet is observed around 12816 Da that corresponds to a 2:1 platinum–protein stoichiometry (the latter mass is just the sum of cyt c plus two $[Pt(NH_3)_2]^{2+}$ fragments). Some additional weak signals, observed around 13062 Da, are assigned to an adduct with a 3:1 Pt/protein ratio. Overall, these results point out that cisplatin forms various kinds of cyt c derivatives with platinum–protein stoichiometries ranging from 1:1 to 3:1.

The pattern of the multiplet centred at 12589 Da deserves some further comments. Remarkably, the relative positions and intensities of the four main peaks within this multiplet are nearly identical to those found by Gibson et al. in the case of the cisplatin adduct of ubiquitin.[10] Thus, it is straightforward to assign the peaks at 12626, 12607, 12589 and 12571 Da to protein binding of the molecular fragments $[Pt(NH_3)_2Cl]^+$, $[Pt(NH_3)_2H_2O]^{2+}$, $[Pt(NH_3)_2]^{2+}$ and $[Pt(NH_3)]^{2+}$, respectively. A similar reasoning may be applied to the description of the ESI-MS multiplets observed in the spectra of the other platinum–protein adducts, reported later.

The ESI-MS spectrum of the transplatin derivative, shown in Figure 2C, again evidences a multiplet centred around 12589 Da, similar in shape to that of cisplatin and consistent with the anchoring of a $[Pt(NH_3)_2]^{2+}$ fragment to cyt c. However, at variance with the case of cisplatin, no signs of the 2:1

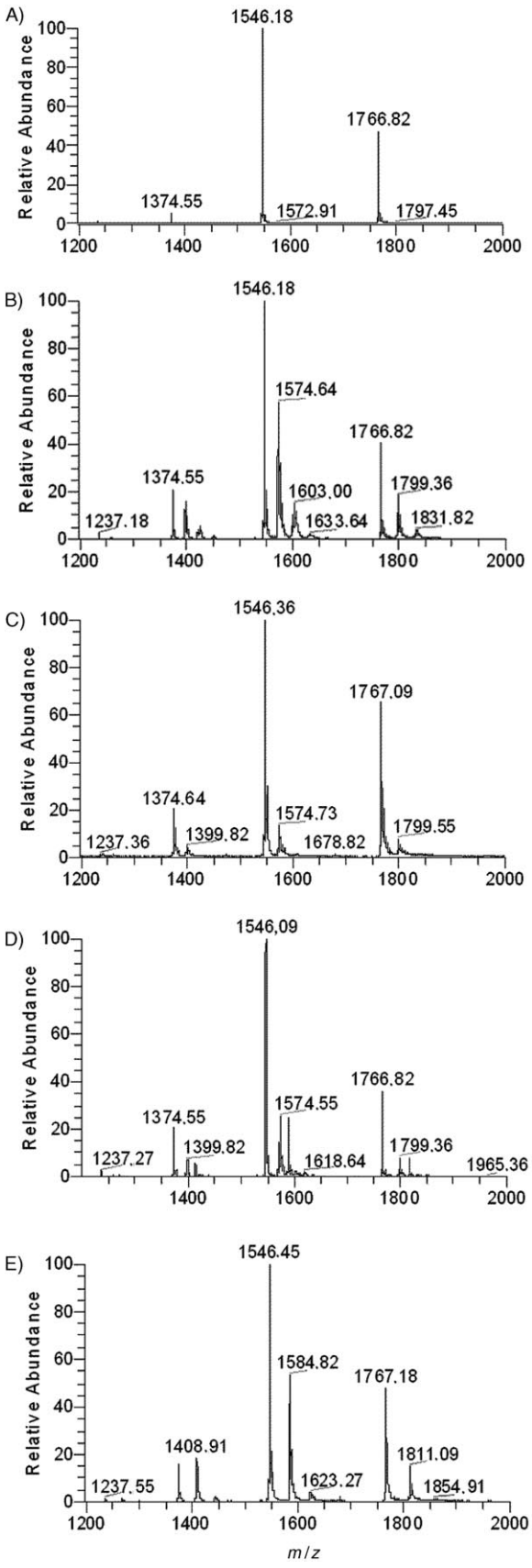

Figure 1. ESI-MS spectral profiles for A) cytochrome c and its platinum adducts: B) cisplatin, C) transplatin, D) carboplatin, E) oxaliplatin. The stoichiometry of each platinum/protein adduct is 3:1.

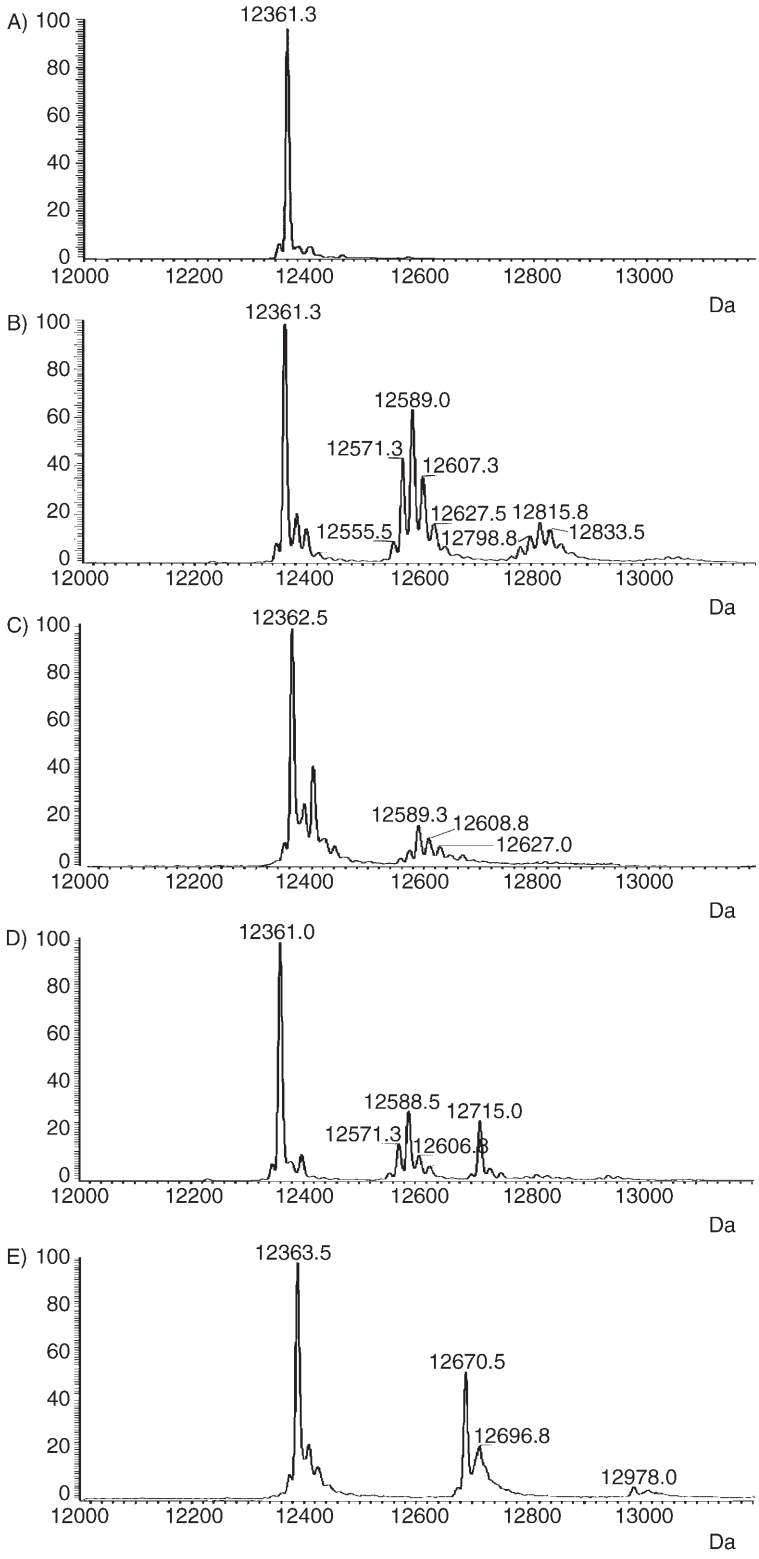

Figure 2. Deconvoluted ESI-MS spectra of A) cytochrome c and its platinum adducts: B) cisplatin, C) transplatin, D) carboplatin, E) oxaliplatin. The stoichiometry of each platinum/protein adduct is 3:1.

and 3:1 platinum–protein adducts are detected under the applied solution conditions (72 h incubation, 3:1 Pt/protein ratio).

Analysis of the ESI-MS spectrum obtained for the carboplatin derivative reveals a rather different situation (Figure 2D). Indeed, two clearly distinct adducts are observed, both manifesting a 1:1 platinum/protein stoichiometry, while adducts with a higher platinum content are not detected. In detail, we observe a first multiplet centred at 12589 Da, similar in shape to that found in the cisplatin derivative, and a second one, at 12715 Da of comparable intensity. The latter most likely corresponds to addition of a $[Pt(NH_3)CBD]$ (CBD = *cis*-(1,1-cyclobutanedicarboxylato)) fragment to the protein. Failure to observe the peak of a doubly platinated protein adduct suggests that binding of the two distinct platinum fragments to cyt c is competitive for the same site (most likely Met65; see below). Notably, for longer incubation times, the peak at 12715 becomes much weaker while the peak at 12589 Da increases its intensity; this suggests progressive release of the *cis*-(1,1-cyclobutanedicarboxylato) ligand from the protein-bound platinum centre.

Finally, the ESI-MS spectrum of the oxaliplatin derivative is shown in Figure 2E. An intense peak is observed at 12670 Da that might well correspond to the binding of a $[Pt(R{=}(NH_2)_2)]^{2+}$ (R = cyclohexane) moiety to cyt c. Moreover, the peak of a 2:1 adduct, in which two fragments of the above kind are associated to the protein, is clearly observed at 12977 Da.

Additional ESI-MS measurements were performed on Pt–cyt c adducts prepared under more drastic conditions (Pt/cyt c ratio of 10:1; 168 h incubation time, 37 °C). In all cases these conditions led to formation of adducts with greater Pt/cyt c stoichiometries and to substantial decreases in the peaks of the native protein and of the monoplatinated adduct. A representative example is shown in Figure 3. The ESI-MS spectrum of a cyt c sample incubated for one week with a tenfold molar excess of cisplatin is dominated by three peaks of comparable intensity corresponding to the 2:1, 3:1 and 4:1 Pt–cyt c adducts. Remarkably, a very weak peak corresponding to the free protein can only just be observed at 12361.8 Da; this suggests that almost complete protein platination has occurred.

Overall, the results reported above provide quite detailed insight into the reactivity of the various platinum complexes with cyt c, as judged from the nature of the resulting products. It is shown that all tested platinum compounds, when presented to the protein in a 3:1 molar excess for 72 h at 37 °C generate a certain number of stable platinum–protein adducts, with a net predominance of the monoplatinated ones. Very similar cyt c platination levels were afforded following treatment with the four different platinum compounds under identical conditions. In addition, higher but still comparable platination levels were obtained for cyt c samples treated for one week with a tenfold molar

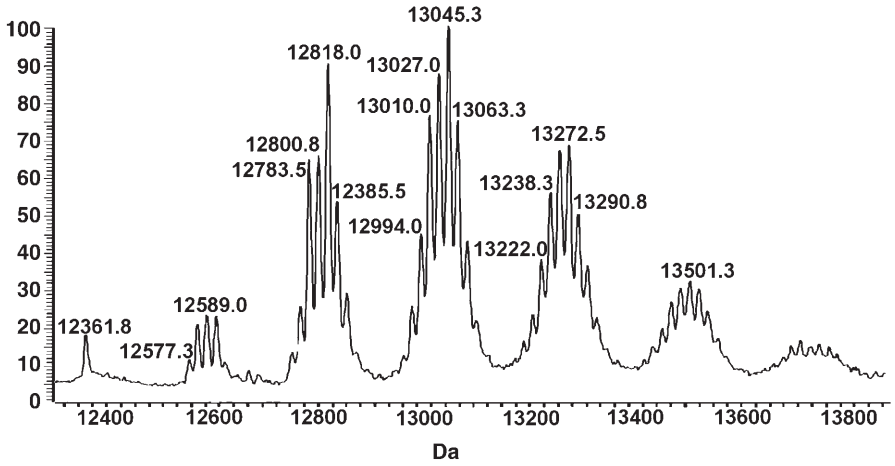

Figure 3. Deconvoluted ESI-MS spectra of the cisplatin adduct with cyt c in a 10:1 ratio, incubation time 168 h at 37 °C.

excess of either cisplatin or carboplatin. In fact, platination levels of 6.7 ± 0.5 and 5.0 ± 0.5 Pt moles per cyt c were found for cisplatin and carboplatin, respectively.

Thus, under the present experimental conditions, the four investigated platinum compounds turn out to exhibit a roughly similar pattern of reactivity with cyt c. This finding is of particular interest and novelty, being in striking contrast to current opinions concerning the comparative reactivity of the investigated platinum drugs. Indeed, the four platinum compounds selected for our study are known to exhibit greatly different stability patterns under physiological-like conditions.[15] For instance, carboplatin has been reported to hydrolyse about 100-fold less rapidly than cisplatin.[15] Equally, oxaliplatin has been shown to hydrolyse far more slowly than cisplatin.[15] The higher stabilities of carboplatin and oxaliplatin towards are generally reflected in a lower reactivity with DNA and with other proteins.[16] Thus it is really surprising that all the platinum compounds tested here were found to platinate cyt c at a substantially similar level. It can be inferred that cyt c plays some active role in enhancing the reactivity of the kinetically stable carboplatin and oxaliplatin.

The specific sites of protein platination still require unambiguous identification. It is known, from divalent platinum solution chemistry, that complexes of the "soft" platinum(II) ion display high affinity for sulfur-containing groups: they are expected to bind readily to cysteine and methionine sulfurs and, with lower affinity, to the imidazole nitrogens of histidines.[17] In cyt c, only Met65, His26 and His33 are freely available for platinum coordination. In line with the reported higher affinity of platinum(II) complexes for sulfur ligands, and previous spectroscopic results concerning the interaction of cisplatin with cyt c,[18] we propose that Met65 represents the primary binding site for the tested platinum drugs, while the imidazole groups of His26 and His33 offer secondary binding sites. The above analysis of the ESI-MS spectral features of the various platinum derivatives highlights predominant formation of monoadducts in which the platinum fragments are most likely coordinated to Met65. Interestingly, the two distinct monoplatinated adducts obtained upon reacting cyt c with carboplatin imply that both fragments compete for the strong Met65 "primary" site rather than binding to "secondary" His sites.

In conclusion, we have shown that classical platinum(II) drugs produce cyt c adducts sufficiently stable to survive the soft ionisation procedures of the ESI-MS experiment. The stoichiometry of the individual adducts and the nature of the protein-bound metal fragments have been fully characterised by interpreting their respective ESI-MS spectra. Remarkably, and surprisingly, all tested platinum(II) drugs were found to exhibit roughly comparable reactivity profiles towards this protein. We suggest that Met65 represents the primary anchoring site for platinum(II) compounds.

Beyond the specific information gained on platinated cyt c derivatives, the present study further exploits the ESI-MS technique as an election and direct method for the accurate molecular description of weak but biologically relevant metal–protein adducts. Valuable information on the comparative reactivity of families of metallodrugs towards protein targets can be straightforwardly derived from the application of the described experimental approach.

Acknowledgements

MIUR and Ente Cassa di Risparmio di Firenze are gratefully acknowledged for financial support. We also acknowledge support by COST Action D20. We thank Prof. D. Gibson (Department of Medicinal Chemistry, Hebrew University of Jerusalem) for critical reading of the ESI-MS results and valuable suggestions.

Keywords: antitumor agents · cytochromes · ESI-MS · platinum · reaction mechanisms

[1] B. Lippert, *Cisplatin: Chemistry and Biochemistry of a Leading Anticancer Drug*, Wiley, New York, **1999**.
[2] V. Brabec, *Prog. Nucleic Acid Res. Mol. Biol.* **2002**, *71*, 1–68.
[3] D. Wang, S. J. Lippard, *Nat. Rev. Drug Discov.* **2005**, *4*, 307–320.
[4] J. Reedijk, *Proc. Natl. Acad. Sci. USA* **2003**, *100*, 3611–3616.
[5] Special Issue on Medicinal Inorganic Chemistry, *Chem. Rev.* **1999**, *99*, 2201–2842.
[6] "Interactions of Antitumor Metal Complexes with Serum Proteins. Perspectives for Anticancer Drug Development", F. Kratz in *Metal Complexes in Cancer Chemotherapy* (Ed.: B. K. Keppler), VCH, Weinheim, **1993**, pp. 391–429.
[7] A. I. Ivanov, J. Christodoulou, J. A. Parkinson, K. J. Barnham, A. Tucker, J. Woodrow, P. J. Sadler, *J. Biol. Chem.* **1998**, *273*, 14721–14730.
[8] B. P. Espósito, R. Najjar, *Coord. Chem. Rev.* **2002**, *232*, 137–149.
[9] a) M. Mann, R. C. Hendrickson, A. Pandey, *Annu. Rev. Biochem.* **2001**, *70*, 437–473; b) A. P. Jonsson, *Cell. Mol. Life Sci.* **2001**, *58*, 868–884; c) S. Cristoni, L. R. Bernardi, *Mass Spectrom.* **2003**, *22*, 369–406; d) J. A. Loo,

Mass Spectrom. Rev. **1997**, *16*, 1 – 23; e) P. Hu, Q. Z. Ye, J. A. Loo, *Anal. Chem.* **1994**, *66*, 4190 – 4194.

[10] a) T. Peleg-Shulman, Y. Najajreh, D. Gibson, *J. Inorg. Biochem.* **2002**, *91*, 306 – 311; b) D. Gibson, C. E. Costello, *Eur. Mass Spectrom.* **1999**, *5*, 501 – 510; c) T. Peleg-Shulman, D. Gibson, *J. Am. Chem. Soc.* **2001**, *123*, 3171 – 3172.

[11] a) F. Wang, J. Bella, J. A. Parkinson, P. J. Sadler, *J. Biol. Inorg. Chem.* **2005**, *10*, 147 – 155; b) J. Zou, P. Taylor, J. Dornan, S. P. Robinson, M. D. Walkinshaw, P. J. Sadler, *Angew. Chem.* **2000**, *112*, 3054 – 3057; *Angew. Chem. Int. Ed.* **2000**, *39*, 2931 – 2934; c) C. S. Allardyce, P. J. Dyson, J. Coffey, N. Johnson, *Rapid Commun. Mass Spectrom.* **2002**, *16*, 933 – 935; d) "The Binding of Platinum Complexes to Human Serum Albumin Studied by Electrospray Ionization-Ion Trap-Mass Spectrometry (ESI-IT-MS)", C. G. Hartinger, S. Alexenko, A. R. Timerbaev, B. K. Keppler in *Novel Approaches for the Discovery and the Development of Anticancer Agents*, CESAR, Vienna, **2005**, p. 16.

[12] X. Jiang, X. Wang, *Annu. Rev. Biochem.* **2004**, *73*, 87 – 106.

[13] a) M. Samalikova, I. Matecko, N. Muller, R. Grandori, *Anal. Bioanal. Chem.* **2004**, *378*, 1112 – 1123; b) M. Samalikova, R. Grandori, *J. Am. Chem. Soc.* **2003**, *125*, 13 352 – 13 353.

[14] Cisplatin, transplatin, carboplatin and oxaliplatin were purchased from Sigma–Aldrich. Horse heart cytochrome c was also from Sigma. Samples were prepared in ammonium carbonate buffer (25 mM, pH 7.4) with a protein concentration of 5×10^{-4} M, and platinum-to-protein ratios ranging from 3:1 to 10:1. The reaction mixtures were incubated for different time intervals (24 h, 72 h and 1 week) at 37 °C. Samples were extensively ultrafiltered by using Centricon YM-3 (Amicon Bioseparations, Millipore Corporation) in order to remove the unbound platinum complex. After the samples had been diluted 100-fold with MilliQ water, ESI-MS spectra were recorded by direct introduction at a flow rate of 3 μL min^{-1} in a LTQ linear ion trap (Thermo, San Jose, CA) equipped with a conventional ESI source. The specific conditions used for these experiments were as follows: spray voltage = 3.5 kV, capillary voltage = 40 V and the capillary temperature was kept at 353 K. The sheath gas was set at 13 (arbitrary units) whereas sweep gas and auxiliary gas were kept at 0 (arbitrary units). ESI spectra were acquired by using Xcalibur software (Thermo), and deconvolution was obtained by using Bioworks software (Thermo). The mass-step size in deconvolution calculation was 0.25 Da, and the spectrum range considered was 1100–2000 *m/z*. The same experiments were repeated at various capillary temperatures from 90 to 180 °C, but the peak patterns and relative abundances were not influenced (data not shown). ICP-OES spectra of the samples were recorded on an Optima 2000 instrumentation (Perkin–Elmer).

[15] a) M. Treskes, U. Holwerda, I. Klein, H. M. Pinedo, W. J. van der Vijgh, *Biochem. Pharmacol.* **1991**, *42*, 2125 – 2130; b) A. Andersson, H. Hedenmalm, B. Elfsson, H. Ehrsson, *J. Pharm. Sci.* **1994**, *83*, 859 – 862; c) E. Jeremalm, P. Videhult, G. Alvelius, W. J. Griffiths, T. Bergman, S. Eksborg, H. Ehrsson, *J. Pharm. Sci.* **2002**, *91*, 2116 – 2121; d) E. Raymond, S. Faivre, S. Chaney, J. Woynarowski, E. Cvitkovic, *Mol. Cancer Ther.* **2002**, *1*, 227 – 235; e) Y. W. Cheung, J. C. Cradock, B. R. Vishnuvajjala, K. P. Flora, *Am. J. Hosp. Pharm.* **1987**, *44*, 124 – 130.

[16] a) T. Boulikas, M. Vougiouka, *Oncol. Rep.* **2003**, *10*, 1663 – 1682; b) R. Mandal, R. Kalke, X. F. Li, *Chem. Res. Toxicol.* **2004**, *17*, 1391 – 1397; c) R. J. Knox, F. Friedlos, D. A. Lydall, J. J. Roberts, *Cancer Res.* **1986**, *46*, 1972 – 1979; d) O. Heudi, S. Mercier-Jobard, A. Cailleux, P. Allain, *Biopharm. Drug Dispos.* **1999**, *20*, 107 – 116; e) R. C. Gaver, A. M. George, G. Deeb, *Cancer Chemother. Pharmacol.* **1987**, *20*, 271 – 276; f) W. J. van der Vijgh, I. Klein, *Cancer Chemother. Pharmacol.* **1986**, *18*,129 – 132.

[17] J. Reediijk, *Chem. Rev.* **1999**, *99*, 2499 – 2510.

[18] J. Lijuan, C. Yu , T. Guozi, T. Wenxia, *J. Inorg. Biochem.* **1997**, *65*, 73 – 77.

[19] During the preparation of this article, a paper appeared reporting an ESI-MS investigation of the carboplatin/cytochrome c system. ("Determination of Binding Sites in Carboplatin-Bound Cytochrome c Using Electrospray Ionization Mass Spectrometry and Tandem Mass Spectrometry": G. Yang, R. Miao, C. Jin, Y. Mei, H. Tang, J. Hong, Z. Guo, L. Zhu, *J. Mass. Spectrom. A* **2005**, *40*, 1005 – 1016). The results obtained by these authors under different solution conditions are in good agreement with those obtained in our study.

Received: November 14, 2005
Published online on February 27, 2006

ESI mass spectrometry and X-ray diffraction studies of adducts between anticancer platinum drugs and hen egg white lysozyme

Angela Casini,[a] Guido Mastrobuoni,[b] Claudia Temperini,[a] Chiara Gabbiani,[a] Simona Francese,[b] Gloriano Moneti,[b] Claudiu T. Supuran,[a] Andrea Scozzafava[a] and Luigi Messori*[a]

Received (in Cambridge, UK) 3rd August 2006, Accepted 11th October 2006
First published as an Advance Article on the web 26th October 2006
DOI: 10.1039/b611122j

The interactions of cisplatin and its analogues, transplatin, carboplatin and oxaliplatin, with hen egg white lysozyme were analysed through ESI mass spectrometry, and the resulting metallodrug–protein adducts identified; the X-ray crystal structure of the cisplatin lysozyme derivative, solved at 1.9 Å resolution, reveals selective platination of imidazole Nε of His15.

The interactions of anticancer platinum complexes with proteins have attracted renewed interest during the last few years as they are considered crucial for the pharmacokinetics, the biodistribution, the resistance processes and the toxicity of these metallodrugs.[1,2]

Powerful analytical methods are required to unravel the extreme complexity of platinum–protein interactions; thus, relevant progresses in this field were eventually recorded following the implementation of the latest mass spectrometry techniques and of advanced metalloproteomics protocols.[3,4] Notably, newly reported studies of platinum–protein adducts have highlighted peculiar features of platinum reactions with proteins such as the occurrence of large kinetic differences in the protein platination profiles (strictly dependent on the nature of both the protein and the metal complex)[5] and the eventual release of ammonia ligands from platinum, following protein complexation.[6–8]

Within this frame, we have investigated the interactions of classical platinum drugs (Scheme 1) with hen egg white lysozyme (HEWL), used here as a model protein. Indeed, lysozyme, owing to its small size and to the prevalence of positively charged groups, is a particularly suitable protein for ESI MS investigations as previously shown.[9,10] Moreover, HEWL is well known among crystallographers as a protein very prone to crystallisation, thus turning out very appropriate for X-ray diffraction studies of its metallodrug adducts.[11,12]

In the present study, the platinum–lysozyme interactions were primarily addressed through ESI MS measurements owing to the ease, the rapidity, the sensitivity and the relevant information content of this technique.[3,5,7] Fig. 1 shows the deconvoluted ESI MS spectra of HEWL adducts with cisplatin, transplatin, carboplatin and oxaliplatin, taken after 72 h incubation, at 37 °C.†

A number of observations can be made upon inspection of these ESI-MS spectra. Notably, the ESI-MS peak corresponding to the non-platinated enzyme, at 14 305 Da, is always the one of higher intensity, implying that protein metallation takes place only partially even after challenging the protein with a three fold excess of the metallodrug over long incubation times. This observation was confirmed by ICP-OES (inductively coupled optical emission spectroscopy) measurements† that revealed rather low platination levels for all platinum protein adducts; indeed platination levels of about 50% were measured in the case of cisplatin while values lower than 15% were afforded in all the other cases (oxaliplatin, carboplatin and transplatin). On the other hand, detection of well resolved ESI-MS peaks, with mass values falling in the 14 500/15 000 Da interval, provided unambiguous evidence for adduct formation, also giving detailed information on the nature of protein bound metallic fragments.

The ESI-MS spectrum of the cisplatin derivative (Fig. 1A) shows two peaks of similar intensity at 14 569 and 14 605 Da that formally correspond to either $[Pt(NH_3)_2Cl]^+$ or intact cisplatin bound to the native protein. A similar situation was formerly described by Dyson and coworkers in the case of the cisplatin–transferrin system and interpreted in terms of a two-step cisplatin to protein binding process.[13,14] In our case, additional peaks of similar shape but lower intensitiy are observed at 14 868 and 14 904 Da consistent with the corresponding doubly platinated species. The ESI-MS spectrum of the carboplatin (Fig. 1B) adduct reveals a multiplet centered at 14 676 Da; such a mass corresponds to the addition of a $[Pt(NH_3)_2CBD]$ (CBD = *cis*-(1,1-cyclobutanedicarboxylate)) fragment to the protein, most likely as the result of a classical ring opening process. The ESI-MS spectrum of the oxaliplatin derivative (Fig. 1C) exhibits a main peak at 14 612 Da

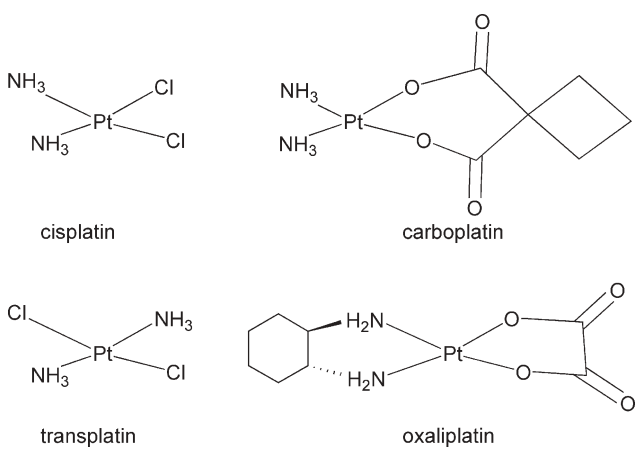

Scheme 1 Schematic drawings of selected anticancer platinum complexes.

[a]*Department of Chemistry, University of Florence, Via della Lastruccia 3, 50019, Sesto Fiorentino, Italy. E-mail: luigi.messori@unifi.it; Fax: +39 055 4573385; Tel: +39 055 4573284*
[b]*Mass Spectrometry Center, University of Florence, Via U. Schiff 6, 50019, Sesto Fiorentino, Italy*

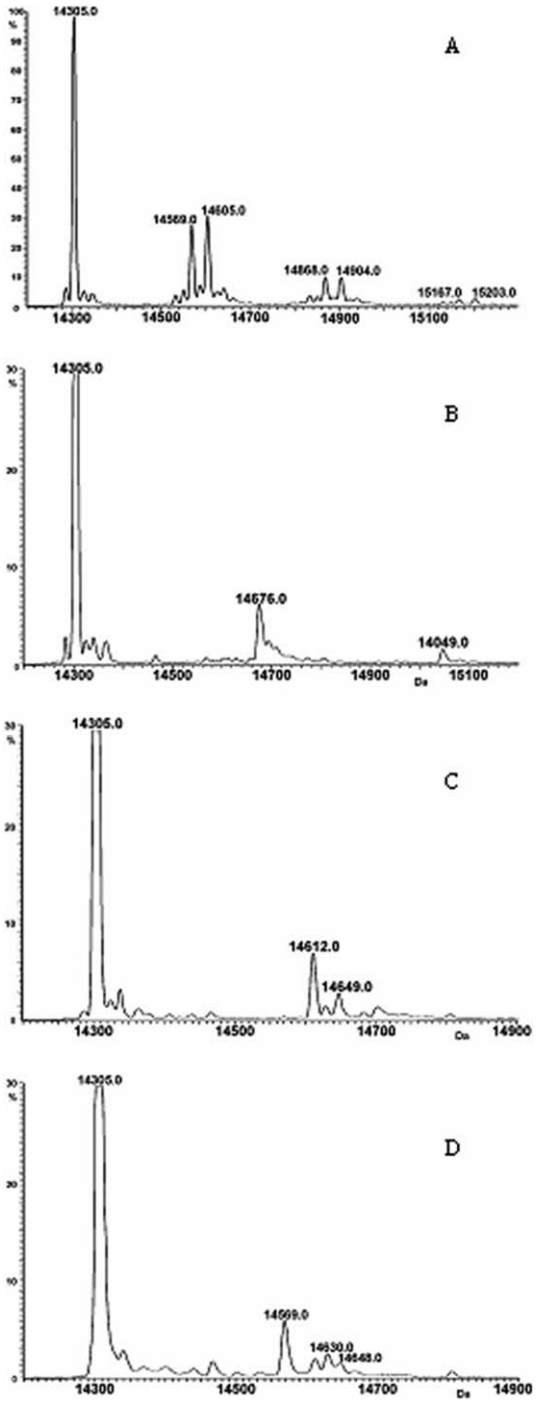

Fig. 1 Deconvoluted ESI-MS spectra of lysozyme adducts with the selected platinum complexes recorded in H_2O after 72 h incubation at 37 °C: (A) cisplatin, (B) carboplatin, (C) oxaliplatin, (D) transplatin. The stoichiometry of each platinum/protein adduct is 3 : 1.

that well corresponds to the binding of a $[Pt(R(NH_2)_2)]^{2+}$ (R = cyclohexane) moiety to HEWL (with concomitant release of the oxalate ligand). This is in accordance with a previous report on the interaction of oxaliplatin with cytochrome *c*.[5] Finally, the mass spectrum of the adduct formed between HEWL and transplatin (Fig. 1D) evidences a peak at 14569 Da that corresponds to protein binding of a $[Pt(NH_3)_2Cl]^+$ fragment (264 Da) after release of a single chloride ligand.

Thus, the above ESI-MS measurements have turned out very valuable to monitor the processes of metallodrug–lysozyme adduct formation and to elucidate the exact nature of the protein bound metallic fragments. We have learned that, under the employed solution conditions, adduct formation is rather slow, that cisplatin is by far the most efficient in producing HEWL platination, that monoplatinated species are the predominant ones, thus suggesting the presence of a highly preferential platinum binding site.

Afterward, in order to gain more precise molecular information on the formed adducts and on the possible sites of metal binding, soaking experiments were carried out in which HEWL crystals were incubated with an excess of each selected platinum drug. Crystals suitable for X-ray diffraction analysis were obtained only in the case of cisplatin. These crystals were subject to X-ray data collection and the structure of the adduct solved at 1.9 Å resolution. Details of data collection and structure refinement are given below.‡

The structure of the cisplatin–HEWL adduct is very similar to that of the native protein (193 L). Platination occurs at the only histidine residue, His 15, which is situated on the surface of the protein and is highly accessible (Fig. 2). Indeed, the analysis of the electron density maps reveals a specific binding of the platinum ion to the Nε of the imidazole ring of His15. In contrast, no other significant modifications of the electron density map were observed ruling out the presence of additional (secondary) binding sites. Particular attention was paid to monitoring the local environment of the two methionine residues (Met 12 and Met 105) that commonly represent preferred anchoring sites for platinum(II) compounds; no significant modifications could be appreciated at these sites in agreement with their scarce accessibility. Platinum binding to HEWL active site (see ref. 12) could be ruled out as well.

We tried to refine the local environment of the protein bound platinum(II) center by assuming a classical square planar geometry and the presence of only nitrogen/oxygen ligands. Within these assumptions the platinum(II) ion appears to bind the protein with an occupancy value of 0.3. The resulting, moderately distorted, square planar coordination environment is represented in Fig. 3. The platinum atom is bound to the the Nε of His 15 and, tentatively, to the nitrogens of two ammonia molecules in cisplatin. The fourth ligand is not detectable: it might well correspond to a loosely bound/disordered platinum coordinated water molecule. A careful analysis of the thermal factors and of the interaction distances suggests that the platinum center, once bound to the protein, retains its ammonia groups. In fact, if the ligands are refined with the assumption that the coordination positions are occupied by nitrogen atoms, the B-factor value goes down to a realistic value (around 22.0). Furthermore, the resulting distances between the platinum atom and the ammonia groups (2.03 Å) is well comparable to usual values for Pt–N distances (around 2.1 Å). Conversely, the presence of chloride ligands coordinated to the platinum center, as it was previously found for the cisplatin/superoxide dismutase derivative,[6] can be ruled out in this case. In a way, this finding contrasts with ESI-MS results of cisplatin–lysozyme showing the persistence of one, or even two, chloride ligands on the protein bound platinum center; however this apparent contradiction might be due to the intrinsic differences of the two experimental approaches.

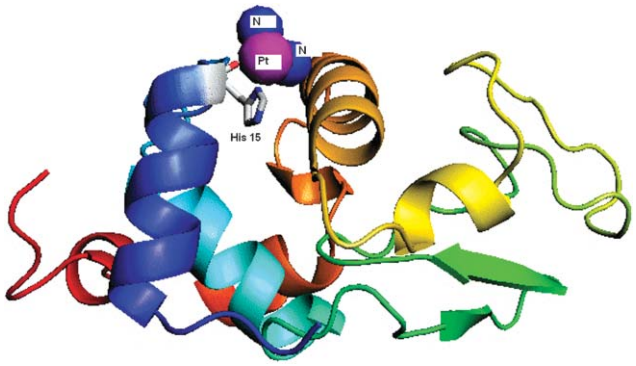

Fig. 2 Schematic representation of the asymmetric unit describing the surface interaction of cisplatin with hen egg white lysozyme; the side chain of His 15 is shown along with platinum, ammonia ligands.

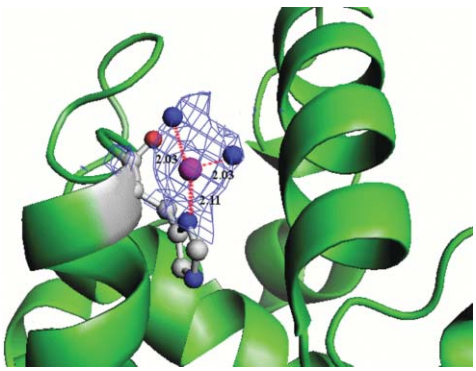

Fig. 3 $2F_o - F_c$ map at 1σ covering cisplatin that interacts with Nε of His15 and with two ammonia ligands and the relative bond lengths (Å).

Overall, the present study has highlighted some relevant features of the interactions of platinum drugs with the model protein HEWL. All tested compounds are able to form specific adducts with lysozyme although these metallation processes appear to be less efficient than in the case of cytochrome *c*, previously reported.[5] The nature of the protein bound metallic fragments has been determined, being in good accord with results obtained on similar systems.[5] Very interestingly, in the case of cisplatin, the crystal structure of its adduct with HEWL has been solved at 1.9 Å resolution. Although details of platinum coordination have not been fully solved, it is evident that platinum is anchored to the imidazole Nε of His 15, in agreement with previous structural results of ruthenated lysozyme.[11] It is very likely that this residue-His15- represents a general binding site for platinum drugs and other late transition metal complexes. Remarkably, the present structure is one of the few reported examples of crystal structures of cisplatin–protein adducts.

CIRCMSB, MIUR and Ente Cassa di Risparmio di Firenze are gratefully acknowledged for financial support.

Notes and references

† *Analysis by positive-ion electrospray ionisation mass spectrometry.* Cisplatin, transplatin, carboplatin and oxaliplatin were purchased from Sigma-Aldrich (Codes P4394, P1525, C2538 and O9512 respectively). Hen egg white lysozyme was also from Sigma (Code L7651). HEWL adducts were prepared in ammonium carbonate buffer 25 mM, pH 7.4, with a protein concentration of 10^{-4} M, and a platinum to protein ratio of 3 : 1. The reaction mixtures were incubated for different time intervals, over a period of 72 h, at 37 °C. Samples were extensively ultrafiltered using Centricon YM-3 (Amicon Bioseparations, Millipore Corporation) in order to remove the unbound platinum complex. After a 100 fold dilution with MilliQ water, ESI MS spectra were recorded by direct introduction at a 3 μl min^{-1} flow rate in a LTQ linear ion trap (Thermo, San Jose, California), equipped with a conventional ESI source. The specific conditions used for these experiments were as follows: the spray voltage was 3.5 kV, the capillary voltage was 32 V and the capillary temperature was kept at 353 K. Sheath gas was set at 16 (arbitrary units) whereas sweep gas and auxiliary gas were kept at 0 (arbitrary units). ESI spectra were acquired using Xcalibur software (Thermo) and deconvolution was obtained using Bioworks software (Thermo). The mass step size in deconvolution calculation was 1 Da and the spectrum range considered was 1100–2000 *m*/*z*. The same experiments were repeated varying capillary temperature (180 °C), but the peak patterns and relative abundances were not influenced (data not shown). ICP-OES analysis of the platinum content in each sample were recorded using an Optima 2000 instrument (Perkin Elmer, Europe).

‡ *Crystallization and X-ray data collection.* HEWL crystals were grown at 277 K using the hanging drop method. The reservoir buffer contained 5 mM sodium acetate buffer, pH 6.5 and 0.05 M NaCl, and the drop contained hen egg white lysozyme (10 mg ml^{-1}) in acetate buffer (5 μl) and reservoir solution (5 μl). After 5 days lysozyme crystals were formed, we soaked them with a solution of cisplatin. Final concentration of cisplatin in solution was 10 times higher than the lysozyme. After 3 days of incubation at 277 K, a monochromatic experiment at the Cu-α wavelength was performed on a selected crystal by the rotation method on a PX-Ultra sealed tube diffractometer (Oxford Diffraction) at 100 K. Data were processed using the programs MOSFLM[15] and SCALA. The initial structure was solved using a reported lysozyme structure (pdb code 193 L), and refinement performed using the program REFMAC5.[16] Model building and map inspections were performing using the COOT program.[17] The coordinates have been deposited in the Protein Data Bank (PDB) under the accession code 2I6Z. Data statistics: space group, $P4_32_12$; unit cell, 77.45 Å, 77.45 Å, 37.35 Å, 90°, 90°, 90°; resolution range: 20–1.90 Å; observed reflections (unique) = 18677 (2476); I/σ (I) = 13.2 (4.7); completeness = 97.4% (90.0%); R_{merge} = 5.2% (31.5%). Refinement: R_{fact}, 18.9%, R_{free} 24.8%; rms bonds = 0.008 Å, rms angles (°) = 1.068. Values in parenthesis relate to the highest resolution shell (2.00–1.90).

1 K. R. Barnes and S. J. Lippard, *Met. Ions Biol. Syst.*, 2004, **42**, 143–77.
2 J. Reedijk, *Proc. Natl. Acad. Sci. U. S. A.*, 2003, **100**, 3611–3616.
3 A. R. Timerbaev, C. G. Hartinger, S. S. Aleksenko and B. K. Keppler, *Chem. Rev.*, 2006, **106**(6), 2224–48.
4 E. K. Yim, K. H. Lee, C. J. Kim and J. S. Park, *Int. J. Gynecol. Cancer*, 2006, **16**(2), 690–7.
5 A. Casini, C. Gabbiani, G. Mastrobuoni, L. Messori, G. Moneti and G. Pieraccini, *Chem. Med. Chem.*, 2006, **1**(4), 413–417.
6 V. Calderone, A. Casini, S. Mangani, L. Messori and P. L. Orioli, *Angew. Chem., Int. Ed.*, 2006, **45**(8), 1267–9.
7 T. Peleg-Shulman, Y. Najajreh and D. Gibson, *J. Inorg. Biochem.*, 2002, **91**(1), 306–11.
8 J. K. Lau and D. V. Deubel, *Chemistry*, 2005, **11**(9), 2849–55.
9 M. Samalikova and R. Grandori, *J. Mass Spectrom.*, 2005, **40**(4), 503–10.
10 M. Salmain, B. Caro, F. Le Guen-Robin, J. C. Blais and G. Jaouen, *ChemBioChem*, 2004, **5**(1), 99–109.
11 I. W. McNae, K. Fishburne, A. Habtemariam, T. M. Hunter, M. Melchart, F. Wang, M. D. Walkinshaw and P. J. Sadler, *Chem. Commun.*, 2004, **16**, 1786–7.
12 S. J. Li, *Biopolymers*, 2006, **81**(2), 74–80.
13 C. S. Allardyce, P. J. Dyson, J. Coffey and N. Johnson, *Rapid Commun. Mass Spectrom.*, 2002, **16**(10), 933–5.
14 I. Khalaila, C. S. Allardyce, C. S. Verma and P. J. Dyson, *ChemBioChem*, 2005, **6**(10), 1788–95.
15 A. G. W. Leslie, *MOSFLM Users' Guide*, MRC-LMB, Cambridge, UK, 1994.
16 T. A. Jones, J. Y. Zhou, S. W. Cowan and M. Kjeldoard, *Acta Crystrallogr., Sect. A: Fundam. Crystallogr.*, 1991, **47**, 110–119.
17 P. Emsley and K. Cowtan, *Acta Crystallogr., Sect. D: Biol. Crystallogr.*, 2004, **60**, 2126–2132.

DOI: 10.1002/cmdc.200600258

ESI–MS Characterisation of Protein Adducts of Anticancer Ruthenium(II)-Arene PTA (RAPTA) Complexes

Angela Casini,[a] Guido Mastrobuoni,[b] Wee Han Ang,[c] Chiara Gabbiani,[a] Giuseppe Pieraccini,[b] Gloriano Moneti,[b] Paul J. Dyson,[c] and Luigi Messori*[a]

Metal-based drugs are playing an increasing role in the field of modern anticancer pharmacology. Indeed, following the clinical success of cisplatin in the treatment of various cancer forms, several other metal complexes, both platinum and nonplatinum, were designed, prepared, and tested as experimental anticancer drugs.[1] Among them, ruthenium-based metallodrugs look very promising. Remarkably, two ruthenium(III) complexes, that is, KP1019 (indazolium *trans*-[tetrachlorobis(1H-indazole)ruthenate(III)]) and NAMI-A (imidazolium *trans*-[tetrachloro(DMSO) (imidazole)ruthenate(III)]), were reported to exhibit outstanding anticancer and/or antimetastatic properties in vivo and are currently undergoing clinical trials.[2,3] In addition, a number of ruthenium(II) arene compounds were shown to possess very encouraging cytotoxic and antitumour properties in preclinical models[4] and are being intensely investigated.

As the mechanisms of action of ruthenium-based anticancer compounds are still largely unexplored and controversial,[5] it is of particular interest to develop specific methods to analyse in detail their reactivity toward potential biomolecular targets, in particular proteins. In fact, in contrast to classical platinum drugs that are known to target genomic DNA, the true targets of ruthenium drugs are not yet well defined; for instance, it was suggested that DMSO ruthenium(III) drugs might either directly interfere with specific proteins involved in signal transduction pathways or alter cell adhesion processes.[6]

In recent years, electrospray ionisation mass spectrometry (ESI–MS) has emerged as an extremely valuable and powerful method to monitor the formation of protein adducts of classical platinum drugs at the molecular level, and to identify the precise nature of the resulting metallic fragments attached to protein side chains.[7] However, to the best of our knowledge, only very few ESI–MS studies have dealt with protein adducts formed by nonplatinum anticancer drugs.[8] We report here an ESI–MS investigation of the reactions of three arene-capped ruthenium(II) compounds,[9] belonging to the RAPTA family, with two small proteins, namely horse heart cytochrome c (cyt c) and hen egg white lysozyme. Cyt c is an important protein crucially involved in apoptotic pathways,[10] whereas lysozyme is relevant in certain defence mechanisms.[11] Moreover, their size and overall properties render these proteins particularly suitable for ESI–MS studies.

Owing to the intrinsic high quality of the obtained ESI–MS spectra, a rapid and unambiguous assignment of the resulting metallodrug/protein adducts could be achieved as well as a straightforward identification of the nature of metal-containing molecular fragments, attached to these proteins. In addition, the presence of distinct metal binding sites on these proteins was revealed, favouring formation of different types of metallo-fragments.

The ruthenium compounds used in this investigation are shown . All of them share a common structural motif consisting of a ruthenium(II) centre bound to both an arene (cymene in this case) and to a 1,3,5-triaza-7-phosphaadamantane (pta) ligand. They only differ in the nature of the ligands located at the two remaining coordination positions. Notably, replacement of the two chloride groups (that are present in RAPTA-C) with bidentate ligands [either oxalate—to form Ru(η^6-cymene)(pta)(C_2O_4) (oxalo-RAPTA)—or cyclobutane dicarboxylate—to give Ru(η^6-cymene)(pta)($C_6H_6O_4$) (carbo-RAPTA)]—greatly reduces the rate of the aquation processes, thus modifying their overall solution behaviour, without adversely affecting cytotoxicity.[12] The three investigated complexes essentially manifest a similar cell-growth inhibition activity against a number of representative cancer cell lines (HT29 colon carcinoma, the A549 lung carcinoma, and the T47D and MCF7 breast carcinoma). The binding of a wide range of RAPTA derivatives to oligonucleotides was formerly studied but no direct correlation between oligonucleotide binding and cytotoxicity could be observed.[13] This finding might suggest that protein targets are of greater importance in producing the observed cytotoxic effects.

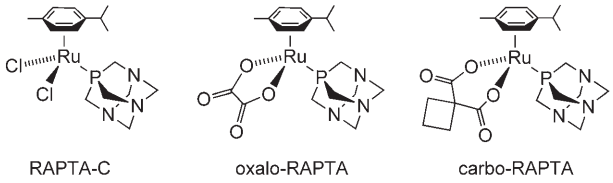

Adducts of RAPTA complexes with cyt c were prepared by incubating each RAPTA compound with horse heart cytochrome c, under the solution conditions described in the experimental section. The resulting ruthenium-protein adducts were analysed by visible absorption spectroscopy or ESI–MS. Even

[a] Dr. A. Casini, Dr. C. Gabbiani, Prof. L. Messori
Department of Chemistry, University of Florence
Via della Lastruccia 3, 50019 Sesto Fiorentino (Italy)
Fax: (+39) 055-457-3385
E-mail: luigi.messori@unifi.it

[b] Dr. G. Mastrobuoni, Dr. G. Pieraccini, Prof. G. Moneti
Mass Spectrometry Centre, University of Florence
Via U. Schiff 6, 50019 Sesto Fiorentino (Italy)

[c] W. H. Ang, Prof. P. J. Dyson
Institut des Sciences et Ingénierie Chimiques,
Ecole Polytechnique Fédérale de Lausanne (EPFL),
CH-1015 Lausanne (Switzerland)

Supporting information for this article is available on the WWW under http://www.chemmedchem.org or from the author.

under aerobic conditions, cyt c, in the presence of RAPTA-C or carbo-RAPTA, undergoes partial reduction, with time, to the ferrous species, as may be inferred from the typical modifications of the Q bands, around 500–550 nm in the UV-Vis spectra. Figure 1 shows the progressive changes of the absorption spectra of cyt c, observed after addition of 1 equivalent RAPTA-C, over a period of 24 h. When the equilibrium is reached (after 24 h at 25 °C) about 30% of total cyt c is present in its reduced form. Similar spectral effects are observed for carbo-RAPTA but not for oxalo-RAPTA. Notably, this phenomenon was not observed for free cyt c, in the absence of ruthenium complexes, working under identical experimental conditions. Such behaviour is in line with spectrophotometric effects produced by other ruthenium compounds (unpublished results from our laboratory).

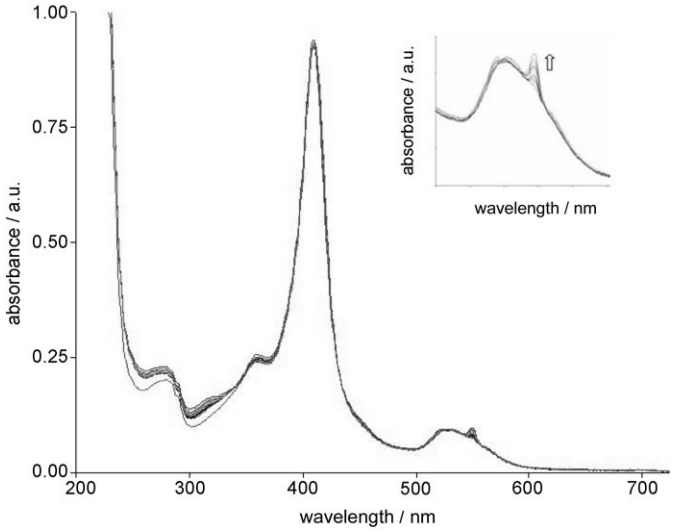

Figure 1. Absorption UV-visible spectra of cytochrome c a) before and b) after addition of 3 equivalents of RAPTA-C. Spectra were recorded at different times over 24 h at 25 °C. The inset shows the detail of the modification of the Q bands in the spectra with time due to the reduction of the iron center.

Deconvoluted ESI–MS spectra, recorded after 48 h incubation of cyt c with the three RAPTA compounds, are shown in Figure 2. The obtained ESI–MS spectra exhibit a very favourable signal to noise ratio; the presence of a limited number of well resolved peaks, with mass values higher than the native protein, renders their assignment to specific metallodrug/protein adducts rather straightforward. By comparing the intensity of the peak of the native protein with that of the main monoruthenated species it is evident that the reaction of cyt c with RAPTA-C results in extensive protein metallation; moderate protein ruthenation is observed in the case of carbo-RAPTA, whereas only a very low amount of ruthenated adducts are formed in the case of oxalo-RAPTA. These large differences in adduct formation are tentatively ascribed to intrinsic differences in the ability of the various RAPTA species to release their leaving groups and subsequently react with protein side chains. In fact, RAPTA-C is known to hydrolyse rather rapidly,

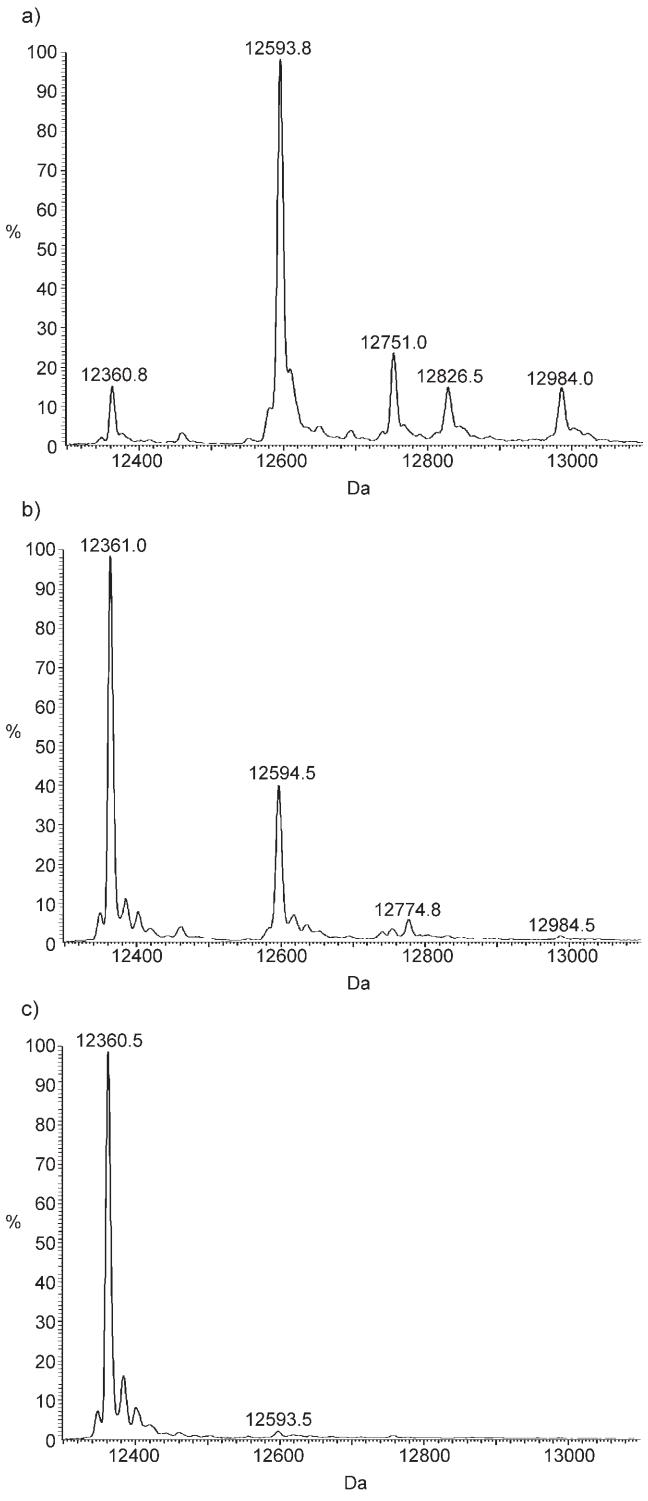

Figure 2. Deconvoluted ESI–MS spectra of adduct formed between cytochrome c and a) RAPTA-C, b) carbo-RAPTA and c) oxalo-RAPTA respectively, after 48 h incubation at 37 °C. The initial ruthenium/protein stoichiometry of each sample is 3:1.

whereas ligand substitution reactions are comparatively slower for carbo-RAPTA and much slower for oxalo-RAPTA.[12]

Notably, in the case of RAPTA-C, four distinct adducts with cyt c are formed; two of them are assigned to monoruthenat-

ed species whereas the other two are assigned to doubly ruthenated species. In more detail, the deconvoluted ESI–MS spectrum of the RAPTA-C derivative shows an intense peak at 12594 Da that corresponds to an adduct in which a single [(η^6-cymene)Ru] fragment is bound to the native holoprotein and another rather intense peak at 12751 Da, corresponds to the binding of a [(η^6-cymene)(pta)Ru] fragment.

Two additional intense peaks, of higher *m/z* value, are observed (see Figure 2a), at 12826 and 12984 Da, that correspond to 2:1 ruthenium–protein adducts; their masses exactly match the sum of cyt c plus two [(η^6-cymene)Ru] fragments or cyt c plus one [(η^6-cymene)Ru] and one [(η^6-cymene)(pta)Ru] fragment, respectively. The pattern of the observed ESI–MS peaks suggests that two distinct anchoring sites for ruthenium exist on cyt–c: the first one is able to accommodate a [(η^6-cymene)(Ru] moiety, favouring the release of the pta ligand, whereas the second one may bind either a [(η^6-cymene)(pta)Ru] or a [(η^6-cymene)(Ru] moiety.

Carbo-RAPTA exhibits a peak for the monometallated species at 12594 Da, analogous to RAPTA C, and an additional peak at ~12775 Da that may be tentatively assigned as a [Ru(pta)($C_6H_6O_4$)(OH)] adduct, that is, an adduct in which the η^6-cymene has been lost instead of the carboxylate ligand. In addition, because of the loss of the cymene ligand which uses three coordination sites on the ruthenium centre, a water or hydroxide ligand is also present in such a way to reduce coordinative unsaturation.[13] Loss of the η^6-cymene in the place of the carboxylate ligand is not an unexpected feature being in agreement with a previous study describing the binding of ruthenium(II) arene complexes to oligonucleotides.[13] In contrast, only one peak, of very low intensity, is observed at 12984 Da that may be ascribed to a bis-ruthenated species, in line with the lower reactivity of carbo-RAPTA.

In the case of oxalo-RAPTA a peak of very low relative intensity at 12593 Da is seen that corresponds to a monoruthenated, [(η^6-cymene)Ru], species.

Additional experiments were then carried out to monitor the binding process in more detail. In particular, protein metallation was investigated by collecting ESI–MS at increasing time intervals after mixing (see Supporting Information). From comparison of the relative intensities of the peak of the native protein with that of the major monoruthenated species a rough estimate of the binding kinetics could be obtained. In the case of the RAPTA-C/cyt c (3:1) system we observed that the percentage of ruthenation, three hours after mixing, is only 30% whereas, after 24 h, protein ruthenation is nearly complete.

Some of the above results (namely those concerning the RAPTA-C derivative) were subsequently confirmed by high resolution mass spectrometry measurements, carried out on an Orbitrap instrument. In Figure 3 observed and theoretical spectra of 8^+ charged state are shown for a) cyt c (I), b) cyt c + [(η^6-cymene)Ru] fragment (II) and c) cyt c + [(η^6-cymene)(pta)Ru] fragment (III) . Remarkably, the obtained experimental data perfectly match theoretical expectations, thus confirming our hypotheses on the chemical nature of protein bound fragments.

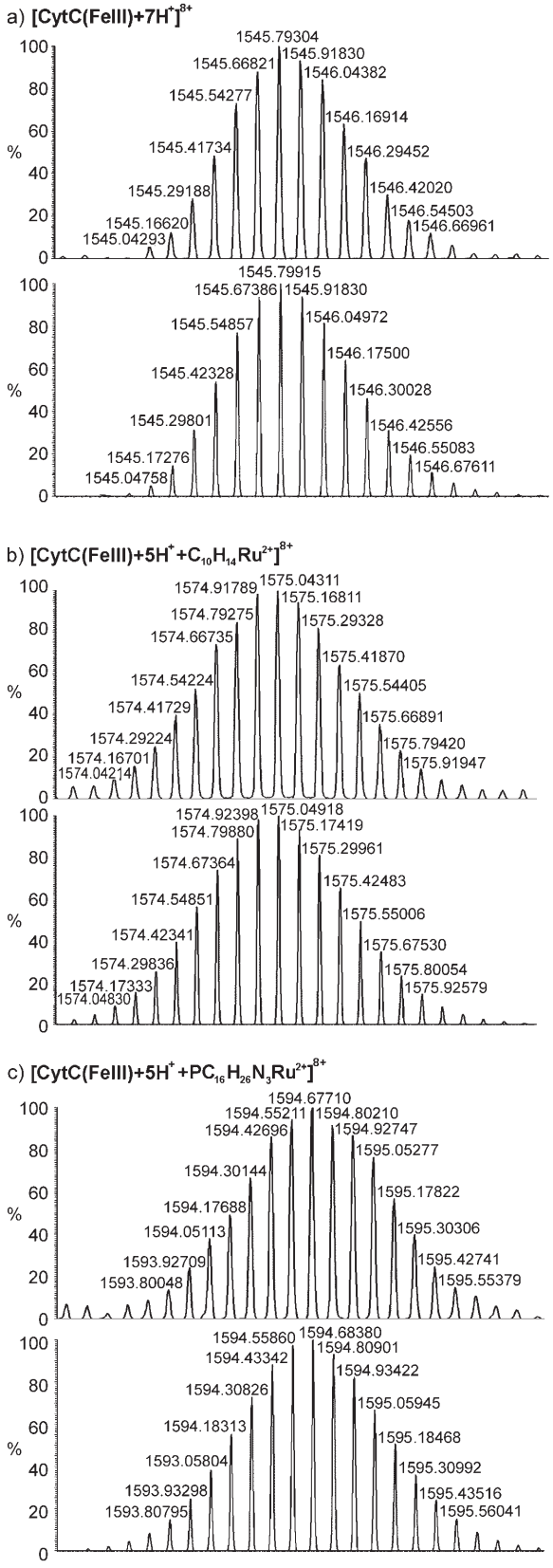

Figure 3. Comparison between the observed (upper) and theoretical (lower) spectra of 8^+ charge state of a) cyt c (I), b) cyt c + [(η^6-cymene)Ru] fragment (II), and c) cyt c + [(η^6-cymene)(pta)Ru] fragment (III). Data were recorded with an Orbitrap high-resolution mass spectrometer (Thermo, San Jose, CA).

A comparison of the protein binding behaviour of these three RAPTA complexes with that of related, clinically-proven, platinum drugs, such as cisplatin, carboplatin, and oxaliplatin, is worth making. In keeping with the RAPTA series, cisplatin shows more extensive binding to cyt c than the other derivatives.[14] Under essentially equivalent conditions cisplatin forms mono-, bis-, and tris-adducts whereas only mono- and bis-adducts are formed with RAPTA-C. Carboplatin and oxaliplatin produce only monoplatinated adducts closely resembling the reactivity pattern observed for the ruthenium analogues reported herein.

It is worth noting that incubation of [Ru(η^6-biphenyl)(en)Cl][PF_6] (where en = ethylenedianime) with cyt c (10:1 ratio) monitored by ESI–MS analysis showed the formation of only monoruthenated species,[15] which appear to be less abundant than those of RAPTA-C, possibly reflecting the difference in the sites that can undergo hydrolysis, that is, [Ru(η^6-biphenyl)(en)Cl][PF_6] has one chloride that can hydrolyse whereas RAPTA-C has two chloride ligands that can potentially be substituted by water.

For comparative purposes, these three RAPTA complexes were reacted with lysozyme and the resulting reaction products analysed by ESI–MS. The deconvoluted ESI–MS spectrum of the RAPTA-C adduct, after 48 h incubation at 37 °C, is shown in Figure 4. The spectrum is diagnostic of appreciable adduct formation. Two monoruthenated adducts are observed at 14538 Da for the [(η^6-cymene)Ru] fragment and 14694 Da for the [(η^6-cymene)(pta)Ru] adduct. Thus, analysis of the ESI–MS provides clear evidence for the presence of identical metallic fragments to those seen in the case of cyt c. Overall, the three RAPTA complexes show a markedly lower reactivity with lysozyme compared to cyt c. The structure of a Ru-η^6-cymene adduct of lysozyme was previously characterised by X-ray diffraction;[16] a [(η^6-cymene)$RuCl_2$] fragment was found to be coordinated to His 15. The sample preparation reported in that paper is somewhat different to that used herein, involving a chloride saturated solution; nevertheless, the X-ray data and the ESI–MS data are in reasonable agreement.

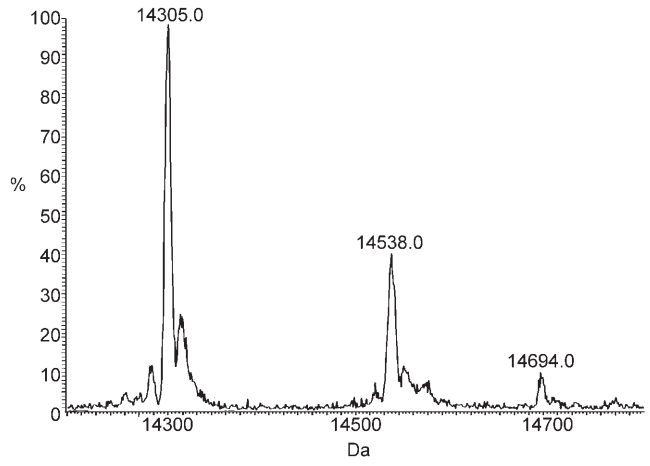

Figure 4. Deconvoluted ESI–MS spectra of lysozyme-adduct with the RAPTA-C complex after 48 h incubation at 37 °C. The initial ruthenium/protein stoichiometry is 3:1.

Previous studies had specifically addressed the interactions of a variety of ruthenium complexes and ruthenium anticancer drugs with proteins. For instance, extensive spectroscopic and crystallographic studies were reported on the reactions of Keppler-type anticancer ruthenium(III) complexes, in particular KP1019, with the major serum proteins serum albumin and serum transferrin. These studies clearly pointed out that preferential binding sites for Ru^{III} are histidine residues located on the protein surface.[17] Analogous studies were carried out on NAMI-A/serum protein adducts leading to similar results.[18]

Gray and co-workers had previously reported that a stable pentaammineruthenium(III)-histidine-33 complex is formed in the reaction between aquopentaammineruthenium(II) and horse heart ferricytochrome c.[19] HPLC analysis of the tryptic hydrolysate of the modified protein was employed to identify the pentaammineruthenium binding site. Spectroscopic measurements showed that the integrity of the native structure in the vicinity of the heme c group is maintained in the ruthenium-modified protein. We have repeated this investigational approach on our system. The cytochrome c RAPTA-C derivative was digested with trypsin and the resulting peptides analysed by direct mass (see Experimental Section for full details). A pattern of tryptic peptides fully consistent with that reported by Gray et al. was obtained. Remarkably, difference spectra of the free and ruthenium-bound digest patterns revealed a new parent ion carrying a double charge with an *m/z* value of 701 in the ruthenium-treated protein (see Figure b in the Supporting Information). Further analysis showed that the parent ion with *m/z* 701 had an isotope distribution characteristic of ruthenium. Notably, the molecular mass of this new fragment corresponds to the cyt c peptide ^{28}Thr-Gly-Pro-Asn-Leu-His-Gly-Leu-Phe-Gly-Arg^{38} bearing a Ru^{II}-η^6-(cymene) moiety. This observation strongly supports the idea that His 33 is a major interaction site for RAPTA-C.

In conclusion, our study has demonstrated the importance and the value of the ESI–MS method to gain specific and rapid information on the reactions of ruthenium metallodrugs with two representative small proteins. Formation of stable adducts could be unambiguously assessed and the nature of the protein bound metallic fragments fully elucidated. Preferential binding of ruthenium metallofragments to surface histidines has been shown. The reported experimental approach has the potential to be extended to larger proteins that are believed to be actual macromolecular targets for ruthenium metallodrugs, taking advantage of the rapid progresses of this analytical method.

Experimental Section

Materials. Horse heart cytochrome c and chicken egg white lysozyme were obtained from Sigma (Code C7752 and L7651, respectively).

RAPTA-C, carbo-RAPTA, and oxalo-RAPTA were prepared according to literature procedures.[20,12]

UV-visible absorption spectroscopy. The interaction of horse heart cytochrome c (10^{-5} M) with the ruthenium complexes, was monitored in H_2O MilliQ pH 5–6, at 25 °C, at different times over a

period of 24 h. The ruthenium/protein adducts were prepared in 1:1 ratio. Spectra were recorded on a Perkin–Elmer Lambda 20 Bio instrument.

ESI–MS analysis. Samples were prepared in H_2O MilliQ pH 5–6, with a protein concentration of 10^{-4} M, and a ruthenium to protein ratio of 3:1. The reaction mixtures were incubated for different time intervals (3, 6, 24 and 48 h) at 37 °C. Samples were extensively ultrafiltered using Centricon YM-3 (Amicon Bioseparations, Millipore Corporation) to remove the unbound complex. After a 100-fold dilution with MilliQ water, ESI–MS spectra were recorded by direct introduction at 3 μL min^{-1} flow rate in a LTQ linear ion trap (Thermo, San Jose, California), equipped with a conventional ESI source. The specific conditions used for these experiments were as follows: the spray voltage was 3.2 kV, the capillary voltage was 32 V, and the capillary temperature was kept at 353 K. Sheath gas was set at 15 (arbitrary units), the sweep gas and auxiliary gas were kept at 0 (arbitrary units). ESI spectra were acquired using Xcalibur 2.0 software (Thermo) and deconvolution was obtained using Bioworks 3.2 software (Thermo). The mass step size in deconvolution calculation was 0.25 Da and the spectrum range was 1100–2000 *m/z*.

Spectra of the same samples were also recorded on an Orbitrap high-resolution mass spectrometer (Thermo, San Jose, CA) and the obtained results were fully consistent (data not shown). The instrument was equipped with a conventional ESI source. The working conditions were the following: spray voltage was 2.3 kV, capillary voltage 20 V, and capillary temperature was kept at 403 K. Sheath gas was set at 16 (arbitrary units), the sweep gas and auxiliary gas were kept at 0 (arbitrary units). For acquisition, Xcalibur 2.0 software (Thermo) was used and monoisotopic and average deconvoluted masses were obtained by using integrated Xtract tool. For spectra acquisition a nominal resolution (at *m/z* 400) of 10 000 was used.

For tryptic digestion analysis 40 μL of cytochrome c (10^{-4} M), either free or reacted with RAPTA-C, were diluted in 10 mM ammonium bicarbonate and bovine trypsin was added in a ratio of 1:50 (*w/w*). The mixture was incubated for 16 h at 37 °C. Then, the trypsin digested samples were separated with an Ultimate3000 system (Dionex) coupled to the LTQ Orbitrap mass spectrometer (Thermo). In detail, 0.5 μL of each sample were loaded on a Vydac C4 column (150 mm × 300 μm, 5 μm pore size) by using 100% solution A (95% water, 5% acetonitrile, 0.01% formic acid) and eluted using a linear gradient up to 40% solution B (95% acetonitrile, 5% water, 0.01% formic acid) in 35 min.

Acknowledgements

MIUR and Ente Cassa di Risparmio di Firenze are gratefully acknowledged for financial support. AIRC is acknowledged for a grant to Dr. Angela Casini.

Keywords: anticancer drugs · complexes · high-resolution ESIMS · proteins · ruthenium arene

[1] K. R. Barnes, S. J. Lippard, *Met. Ions Biol. Syst.*. **2004**, *42*, 43 – 77.
[2] a) E. Alessio, G. Mestroni, A. Bergamo, G. Sava, *Curr. Top. Med. Chem.* **2004**, *4*,1525 – 1535; b) J. M. Rademaker-Lakhai, D. van den Bongard, D. Pluim, J. H. Beijnen, J. H. Schellens, *Clin. Cancer Res.* **2004**, *10*, 3717 – 3727.
[3] a) M. Galanski, V. B. Arion, M. A. Jakupec, B. K. Keppler, *Curr. Pharm. Des.* **2003**, *9*, 2078 – 2089; b) C. G. Hartinger, S. Zorbas-Seifried, M. A. Jakupec, B. Kynast, H. Zorbas, B. K. Keppler, *J. Inorg. Biochem.* **2006**, *100*, 891 – 904.
[4] a) Y. K. Yan, M. Melchart, A. Habtemariam, P. J. Sadler, *Chem. Commun.* **2005**, 4764 – 4776; b) W. Han Ang, P. J. Dyson, *Eur. J. Inorg. Chem.* **2006**, 4003 – 4018.
[5] P. J. Dyson, G. Sava, *Dalton Trans.* **2006**, 1929 – 1933.
[6] G. Pintus, B. Tadolini, A. M. Posadino, B. Sanna, M. Debidda, F. Bennardini, G. Sava, C. Ventura, *Eur. J. Biochem.* **2002**, *269*, 5861 – 5870.
[7] a) I. Khalaila, C. S. Allardyce, C. Verma, P. J. Dyson, *ChemBioChem* **2005**, *6*, 1788 – 1795; b) A. Casini, G. Mastrobuoni, C. Temperini, C. Gabbiani, S. Francese, G. Moneti, C. T. Supuran, A. Scozzafava, L. Messori, *Chem. Commun.* **2007**, *2*, 156 – 158; c) T. Peleg-Shulman, Y. Najajreh, D. Gibson, *J. Inorg. Biochem.* **2002**, *91*, 306 – 311.
[8] A. R. Timerbaev, C. G. Hartinger, S. S. Aleksenko, B. K. Keppler, *Chem. Rev.* **2006**, *106*, 2224 – 2248.
[9] C. Scolaro, A. Bergamo, L. Brescacin, R. Delfino, M. Cocchietto, G. Laurenczy, T. J. Geldbach, G. Sava, P. J. Dyson, *J. Med. Chem.* **2005**, *48*, 4161 – 4171.
[10] X. Jiang, X. Wang, *Annu. Rev. Biochem.* **2004**, *73*, 87 – 106.
[11] H. A. McKenzie, F. H. White, *Adv. Protein Chem.* **1991**, *41*, 173 – 315.
[12] W. H. Ang, E. Daldini, C. Scolaro, R. Scopelliti, L. Juillerat-Jeannerat, P. J. Dyson, *Inorg. Chem.* **2006**, *45*, 9006 – 9013.
[13] a) A. Dorcier, P. J. Dyson, C. Gossens, U. Rothlisberger, R. Scopelliti, I. Tavernelli, *Organometallics* **2005**, *24*, 2114 – 2123; b) C. Scolaro, T. J. Geldbach, S. Rochat, A. Dorcier, C. Gossens, A. Bergamo, M. Cocchietto, I. Tavernelli, G. Sava, U. Rothlisberger, P. J. Dyson, *Organometallics* **2006**, *25*, 756 – 765.
[14] A. Casini, C. Gabbiani, G. Mastrobuoni, L. Messori, G. Moneti, G. Pieraccini, *ChemMedChem* **2006**, *1*, 413 – 417.
[15] F. Wang, J. Bella, J. A. Parkinson, P. J. Sadler, *J. Biol. Inorg. Chem.* **2005**, *10*, 147 – 155.
[16] I. W. McNae, K. Fishburne, A. Habtemariam, T. M. Hunter, M. Melchart, F. Wang, M. D. Walkinshaw, P. J. Sadler, *Chem. Commun.* **2004**, 1786 – 1787.
[17] a) C. A. Smith, A. J. Sutherland-Smith, B. K. Keppler, F. Kratz, E. N. Baker, *J. Biol. Inorg. Chem.* **1996**, *1*, 424; b) F. Piccioli, S. Sabatini , L. Messori, P. Orioli, C. Hartinger, B. K. Keppler, *J. Inorg. Biochem.* **2004**, *98*, 1135 – 1142.
[18] a) L. Messori, P. Orioli, D. Vullo, E. Alessio, E. Iengo, *Eur. J. Biochem.* **2000**, *267*, 1206 – 1213; b) A. Bergamo, L. Messori, F. Piccioli, M. Cocchietto, G. Sava, *Invest. New Drugs* **2003**, *21*, 401 – 411.
[19] K. M. Yocom, J. B. Shelton, J. R. Shelton, W. A. Schroeder, G. Worosila, S. S. Isied, E. Bordignon, H. B. Gray, *Proc. Natl. Acad. Sci. USA* **1982**, *79*, 7052 – 7055.
[20] C. S. Allardyce, P. J. Dyson, D. J. Ellis, S. L. Heath, *Chem. Commun.* **2001**, 1396 – 1397.

Received: November 3, 2006
Revised: January 26, 2007
Published online on March 16, 2007

J Biol Inorg Chem
DOI 10.1007/s00775-007-0280-4

ORIGINAL PAPER

Ruthenium anticancer drugs and proteins: a study of the interactions of the ruthenium(III) complex imidazolium *trans*-[tetrachloro(dimethyl sulfoxide)(imidazole)ruthenate(III)] with hen egg white lysozyme and horse heart cytochrome *c*

Angela Casini · Guido Mastrobuoni · Mattia Terenghi · Chiara Gabbiani · Enrico Monzani · Gloriano Moneti · Luigi Casella · Luigi Messori

Received: 13 June 2007 / Accepted: 18 July 2007

Abstract The interactions with protein targets of the ruthenium(III) complex imidazolium *trans*-[tetrachloro(dimethyl sulfoxide)(imidazole)ruthenate(III)], NAMI-A, an effective anticancer and antimetastatic agent now in clinical trials, deserve great attention as they are believed to be at the basis of the mechanism of action of this innovative molecule. Here, we report on the reactions of NAMI-A with two well-known model proteins, namely, hen egg white lysozyme and horse heart cytochrome *c*; these reactions were investigated by a variety of physicochemical methods, including optical spectroscopy, ^{1}H NMR and electrospray ionization mass spectrometry. The combined use of the analytical techniques mentioned resulted in a rather exhaustive description of the NAMI-A–protein interactions; in particular, the formation of fairly stable metal–protein adducts was clearly documented and the nature of the resulting protein-bound metallic fragments ascertained in most cases. Notably, greatly different patterns of interaction were found to be operative for NAMI-A toward these two proteins. The biological implications of the present findings are discussed.

Keywords Ruthenium metal complexes · Cancer · Proteins · NMR · Electrospray ionization mass spectrometry

A. Casini · C. Gabbiani · L. Messori (✉)
Department of Chemistry,
University of Florence,
Via della Lastruccia 3,
50019 Sesto Fiorentino, Italy
e-mail: luigi.messori@unifi.it

G. Mastrobuoni · G. Moneti
Mass Spectrometry Center,
University of Florence,
Via U. Schiff 6,
50019 Sesto Fiorentino, Italy

M. Terenghi · E. Monzani · L. Casella
Department of Chemistry,
University of Pavia,
Via Taramelli 12,
27100 Pavia, Italy

Introduction

The ruthenium(III) complex [ImH][$RuCl_4$(DMSO)(Im)] (DMSO is dimethyl sulfoxide, Im is imidazole), nicknamed NAMI-A (Fig. 1), is a very promising anticancer metallodrug developed, in Trieste, by Enzo Alessio, Giovanni Mestroni and Gianni Sava [1, 2].

In spite of a very low intrinsic cytotoxicity, NAMI-A surprisingly manifested outstanding antimetastatic effects in experimental in vivo models; in particular such favorable effects were extensively documented for mice with Lewis lung carcinoma [3]. The extremely encouraging antimetastatic profile of NAMI-A, associated with a relatively low systemic toxicity, has already resulted in it being brought into clinical trials [4]. Phase I studies were indeed successfully completed, while phase II studies are currently in progress. Notably NAMI-A together with indazolium *trans*-[tetrachlorobisindazole ruthenate(III)] KP1019, a structurally related ruthenium(III) compound, developed in Vienna by Keppler et al. [5, 6], are the only ruthenium compounds presently undergoing clinical trials as anticancer drugs. Although these ruthenium(III) compounds are very similar to each other, both formally and structurally, some significant differences were nonetheless detected in their chemical reactivity that result in largely diverse biological and pharmacological profiles.

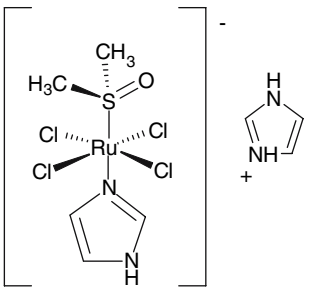

Fig. 1 Structure of the complex imidazolium *trans*-[tetrachloro (dimethyl sulfoxide)(imidazole)ruthenate(III)] (NAMI-A)

Despite intensive in vitro and in vivo studies, the precise molecular mechanisms of the biological and pharmacological actions of NAMI-A are still largely unknown and controversial [7, 8]. In any case, they seem to be profoundly different from those of cisplatin and its analogues that are known to target and damage genomic DNA [9–11]. Some specific proteins such as integrins and collagen were claimed as probable biomolecular targets for NAMI-A, but no conclusive evidence has yet been gathered [12, 13]. Moreover, specific interferences of NAMI-A with crucial signal transduction pathways such as MEK/ERK were revealed as well [14, 15]. Yet, the detailed molecular mechanisms through which NAMI-A reacts with proteins are poorly understood; this latter issue represents, therefore, the main goal of the present investigation.

Some previous spectroscopic work was directed at the analysis of the interactions of NAMI-A with typical serum proteins like serum albumin and serum transferrin [16, 17]. Although the gross features of NAMI-A–serum protein interactions were determined in those studies, molecular details of the binding processes could not be fully elucidated owing to the relatively high molecular weight of the proteins mentioned and to failure to obtain high-resolution X-ray crystal structures for the resulting ruthenium–protein adducts.

These arguments led us to focus attention on the reactions of NAMI-A with two smaller proteins, namely, hen egg white lysozyme (HEWL) and horse heart cytochrome *c* (cyt *c*), acting here as "model proteins", with the aim of obtaining a detailed description of the interactions occurring. In any case, it is worthwhile remembering that cyt *c* is a protein crucially involved in the apoptotic pathways [18], while HEWL is relevant for a number of host defense mechanisms [19]. Their sizes and overall properties render these proteins particularly suitable for electrospray ionization (ESI) mass spectrometry (MS) studies [20, 21] as well as for ^{1}H NMR studies [22]. Accordingly, the reactions of NAMI-A with either cyt *c* or HEWL were primarily analyzed by these two techniques, but also by electronic absorption spectroscopy and inductively coupled plasma optical emission spectroscopy (ICP-OES). The joint application of these various methods has afforded a rather detailed description of the metallodrug–protein interactions, at the molecular level.

Materials and methods

NAMI-A and proteins

Horse heart cyt *c* and HEWL were obtained from Sigma (codes C7752 and L7651, respectively). NAMI-A was prepared according to standard procedures [23] and its purity was checked by elemental analyses and UV–vis spectroscopy.

UV–vis absorption spectroscopy

The interaction of HEWL (10^{-4} M) with NAMI-A was monitored either in Milli-Q water, pH 5−6, or in phosphate-buffered solution (10 mM pH 7.5) at 25 °C, at different times over a period of 24 h. The ruthenium–protein adducts were prepared in 1:1 ratio. Spectra were recorded using a PerkinElmer Lambda 20 Bio instrument. In the case of the adducts with cyt *c* the concentrations of the protein and NAMI-A were 10^{-5} M owing to the high absorption of the Soret band.

Electrospray ionization mass spectrometry

Samples were prepared in Milli-Q water, pH 5–6, with a protein concentration of 10^{-5} M, and a ruthenium-to-protein ratio of 1:1. The reaction mixtures were incubated for different time intervals (0, 3, 6, 24 and 48 h) at 37 °C. Samples were extensively ultrafiltered using Centricon devices (Amicon Bioseparations, Millipore Corporation) in order to remove the unbound complex. After a 100-fold dilution with Milli-Q water, ESI-MS spectra were recorded by direct introduction at 3 μL/min flow rate in an LTQ linear ion trap (Thermo, San Jose, CA, USA), equipped with a conventional ESI source. The specific conditions used for these experiments were as follows: the spray voltage was 3.2 kV, the capillary voltage was 32 V and the capillary temperature was kept at 80 °C. The sheath gas setting was15 (arbitrary units), and the settings for the sweep gas and the auxiliary gas were kept at 0 (arbitrary units). ESI spectra were acquired using Xcalibur 2.0 software (Thermo) and deconvolution was obtained using Bioworks 3.2 software (Thermo). The mass step size in the deconvolution calculation was 0.25 Da and the spectrum range was 1,100–2,000 *m*/*z*.

Spectra of the same samples were also recorded using an LTQ Orbitrap high-resolution mass spectrometer (Thermo, San Jose, CA, USA); the results obtained were fully consistent with the previous ones. The instrument was equipped with a conventional ESI source. The working conditions were the following: the spray voltage was 2.3 kV, the capillary voltage was 20 V and the capillary temperature was kept at 130 °C. The sheath gas setting was 16 (arbitrary units), and the settings for the sweep gas and the auxiliary gas were kept at 0 (arbitrary units). For acquisition, Xcalibur 2.0 software (Thermo) was used and monoisotopic and average deconvoluted masses were obtained by using the integrated Xtract tool. For spectra acquisition, a nominal resolution (at *m*/*z* 400) of 10,000 was used.

NMR spectroscopy

All the NMR experiments were performed using a Bruker AVANCE 400 spectrometer operating at a ^{1}H frequency of 400.13 MHz and at temperature of 20 °C.

Samples to be analyzed by NMR spectroscopy contained the protein (1 mM) dissolved in D_2O or 50 mM deuterated phosphate buffer, pH 7.4. Correct volumes of NAMI-A predissolved in stock solutions under the same conditions were added to obtain 1:1 stoichiometric ratio with protein.

^{1}H spectra for the NAMI-A–protein systems were recorded by acquiring 1,600 scans with a 80,000-Hz spectral window, and suppressing the water signal by presaturation for 0.3 s. In the case of NAMI-A, ^{1}H spectra were obtained by cumulating 160 scans, in a spectral window of 14,000 Hz, centered at −5 ppm. The time dependence of the integral of the NMR peaks was obtained by using, for calibration, the integrals of the first spectra recorded. Owing to the relatively long acquisition time of a single NMR spectrum (approximately 10 min), the analysis of the rate constants was performed assuming the time value to be the middle time of the acquisition.

ICP-OES analysis

To determine the amount of ruthenium bound to each selected protein, samples were prepared with a protein concentration of 10^{-4} M, and a ruthenium-to-protein ratio of 1:1, either in Milli-Q water, pH 5–6, or in phosphate-buffered solution (10 mM, pH 7.5). Then, the samples were incubated at different times over 72 h at 37 °C and extensively ultrafiltered using Centricon devices (Y-3M, molecular mass cutoff 3,000 Da, Amicon Bioseparations, Millipore Corporation) in order to remove the unbound complex. Finally the ruthenium content in each sample, and in its corresponding low molecular mass fractions (ultrafiltrate), was determined through ICP-OES analysis, using an Optima 2000 instrument (PerkinElmer Europe).

Results and discussion

It was previously reported that NAMI-A, when dissolved in aqueous media, may undergo a variety of ligand-substitution reactions by water molecules, hydroxide anions, and/or by other buffer components, giving rise to a number of alternative degradation pathways [24, 25]. Notably, with time, not only chloride, but also DMSO and imidazole are progressively detached from the ruthenium(III) center, some of these processes largely overlapping. Formation of oligomeric and/or polymeric ruthenium species was described as well, primarily associated with solution aging [26]. Ligand-replacement reactions, in the case of NAMI-A, may be further compounded by concomitant redox processes owing to the relatively high reduction potential of the Ru(III)/Ru(II) couple; thus, even in the presence of mild reducing agents such as ascorbic acid, the one-electron reduction of the ruthenium(III) center was reported to take place [27–29]. Detailed spectroscopic investigations of the various ligand-substitution and/or redox processes, and of the resulting reaction products, showed that the choice of one of the possible degradation pathways is strongly dependent on the experimental conditions applied (for instance, the pH of the medium, the presence of reducing agents, the nature of the buffer). Remarkably, a first density functional theory study of the NAMI-A aquation processes appeared very recently providing theoretical support to experimental results [30].

The above observations led us to standardize very carefully the solution conditions of the various spectroscopic experiments, initially working on NAMI-A alone. Afterward, we investigated whether the addition of either HEWL or cyt *c* might affect the kinetics and the nature of the resulting NAMI-A degradation processes in comparison to NAMI-A alone. Reactions taking place in solution were primarily analyzed by optical absorption spectroscopy, NMR spectroscopy and ESI-MS. The results obtained for the two proteins investigated are detailed in the following sections.

Lysozyme

The reaction of NAMI-A with HEWL was initially studied by electronic absorption spectroscopy. The reaction was carried out either in water (pH ∼ 5–6) or in 50 mM phosphate buffer (pH 7.4) and monitored continuously,

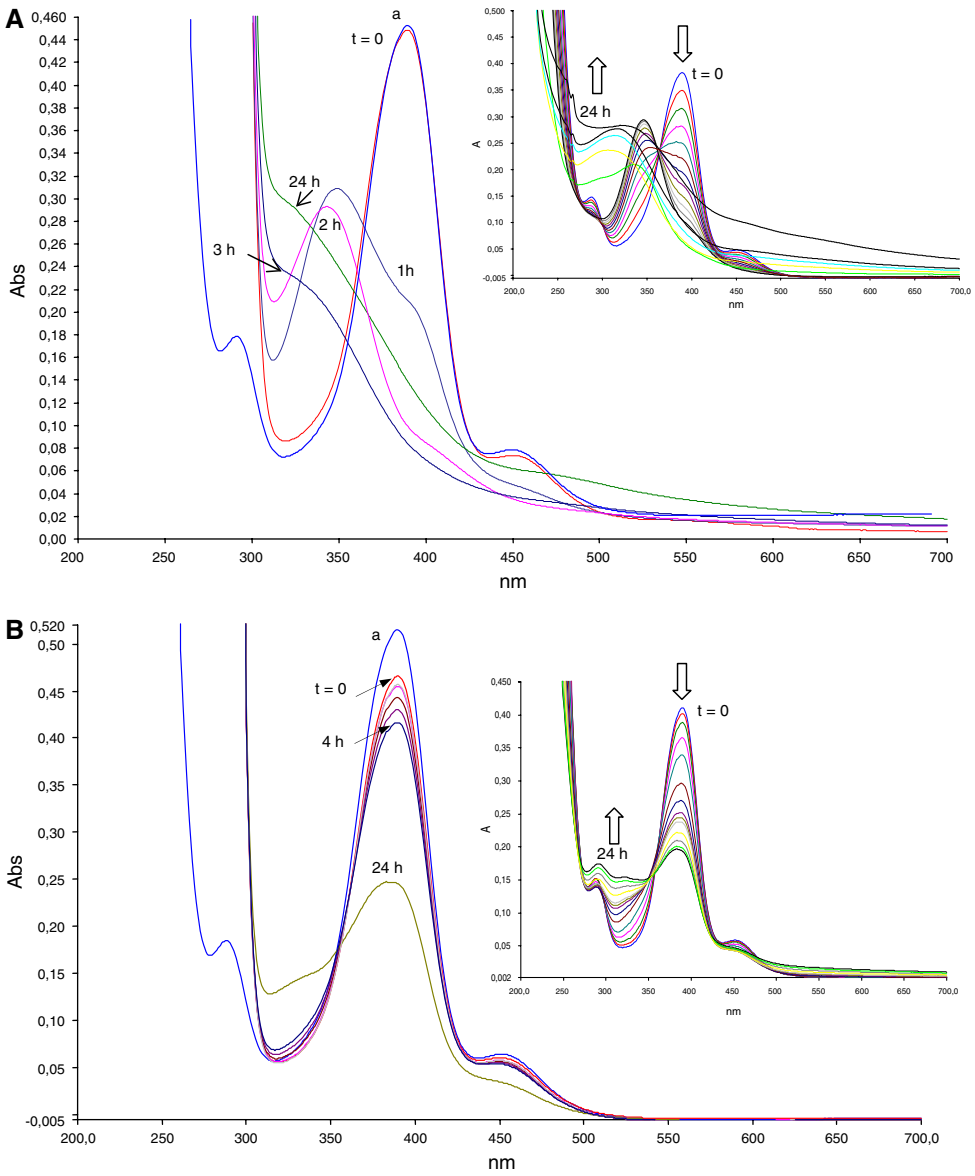

Fig. 2 Absorption UV–vis spectra of NAMI-A 10^{-4} M in 50 mM phosphate buffer pH 7.4 (**a**) or in water (pH ~ 5–6) (**b**), before (trace *a*) and after addition of 1 equiv of hen egg white lysozyme (HEWL). Spectra were recorded at different times over 24 h at 25 °C. *Insets* show the spectral behavior of NAMI-A alone in the same solution conditions. *Arrows* indicate the development of the absorption during time over 24 h

over 24 h, at room temperature (25 °C). For comparison purposes, the time-dependent spectrophotometric behavior of NAMI-A alone was investigated under identical solution conditions. The resulting spectral profiles are shown in Fig. 2.

The UV–vis spectrum of NAMI-A, in aqueous solution, shows a main band centered at 390 nm, which decreases progressively with time, being replaced by a similarly intense absorption at approximately 340 nm. These spectral changes were previously assigned to the replacement of a first chloride ligand by a water molecule [24, 25]. Replacement of a second chloride by water was also described, again accompanied by characteristic spectral changes (namely, the disappearance of the absorption at 340 nm). Further aquation and/or oligomerization processes take place afterward.

It was previously ascertained that the kinetics of the first aquation process is much faster at pH 7 than at acidic pH [24, 25]. Accordingly, we observed that the $t_{½}$ for the disappearance of the absorption band at 390 nm for NAMI-A alone (working at 10^{-4} M) is about 25 min in phosphate buffer; in contrast, in unbuffered water (pH ~ 5–6), the process is significantly slower, with a $t_{½}$ of about 22 h.

Remarkably, we found that addition of HEWL, at 1:1 molar ratio, greatly affects the rate of the first NAMI-A aquation process, in phosphate buffer, with an increase of $t_{½}$ from 25 min to about 1 h. At variance, the kinetic effects of the presence of HEWL are less evident when measured in water.

Protein ruthenation was quantitated by independent ICP-OES determinations after extensive sample ultrafiltration. Under the experimental conditions applied, the protein

metallation process was found to be relatively fast. Indeed, relevant HEWL metallation levels were already attained after 1 h incubation, at 37 °C (about 40% of the total ruthenium is associated to the protein), and then increased only marginally over far longer incubation times. Even after 72 h incubation, ruthenium levels never exceeded a ruthenium-to-HEWL molar ratio of 0.5.

The main features of the NAMI-A–HEWL interaction were independently monitored through ^{1}H NMR spectroscopy. This technique is particularly suitable for the present system as paramagnetic NAMI-A is known to exhibit well-resolved, isotropically shifted signals, mainly lying in the upfield region, that can be straightforwardly monitored even in the presence of the complex envelope of protein ^{1}H NMR signals. Thus, ^{1}H NMR spectra were collected for the 1:1 NAMI-A–HEWL system (10^{-3} M) over 24 h at room temperature, either in 50 mM phosphate buffer (pH 7.4) or in D_2O (pH ∼ 5–6), as described in "Materials and methods." For comparison purposes ^{1}H NMR spectra of NAMI-A alone were also recorded under the same solution conditions (data not shown). For NAMI-A a few hyperfine signals are observed in the upfield region, and are assigned to protons of the ruthenium(III) ligands in accordance with previous reports [24, 25]. In detail, immediately after dissolution of the complex, a broad signal at about −15.5 ppm is detected that is assigned to ruthenium(III)-coordinated DMSO, while signals at −3.5, −5.6 and −7.8 ppm are assigned to H_5 and $H_{2,4}$, respectively, of the imidazole ligand. Upon release of the first chloride, the resonances of NAMI-A are replaced by a new set of hyperfine signals. In particular, a new broad resonance appears at about −11.5 ppm, previously attributed to the protons of the DMSO ligand in the first hydrolysis product of NAMI-A, i.e., $[RuCl_3(DMSO)HIm(H_2O)]$. This latter species, in turn, undergoes further progressive aquation until it completely disappears; however, no new hyperfine resonances belonging to subsequent hydrolytic products could be detected.

In contrast, in the presence of HEWL, at equimolar ratios, no significant evolution of the NAMI-A hyperfine ^{1}H NMR features was detected over 24 h observation, implying that HEWL causes a drastic slowing down of NAMI-A aquation/degradation processes, in qualitative agreement with the above-reported optical behavior (Fig. 3). Discrepancies between the kinetic profiles obtained through the two different methods might be ascribed to concentration-dependent effects as recently suggested by Brindell et al. [29].

In a way, both the absorption and the ^{1}H NMR spectra point out that the ruthenium(III) center of NAMI-A does not coordinate to HEWL side chains as might have been reasonably expected on the basis of previous reports of similar ruthenium(III) protein systems [5]; instead,

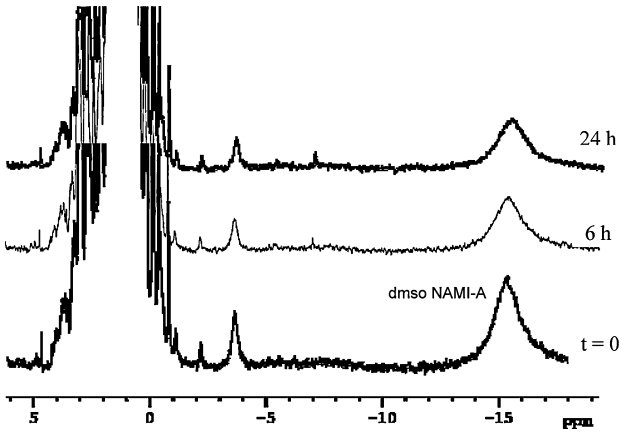

Fig. 3 400 MHz ^{1}H NMR spectra recorded over 24 h at 25 °C on a sample of HEWL after addition of NAMI-A in a 1:1 ratio. The sample was prepared in 50 mM phosphate buffer, pH 7.4

noncovalent metallodrug–protein interactions appear to be the dominant binding mode, most likely governed by strong electrostatic interactions between the negative tetrachlororuthenate "core" of NAMI-A and a patch of positively charged residues on the surface of lysozyme. Indeed, HEWL is known to be a very basic protein (pI = 9.3). Lysozyme basicity confers the protein outstanding anion binding properties as previously described [31, 32].

To give further support to this picture, ESI-MS spectra were obtained for the NAMI-A–HEWL system. Owing to the strict requirements of the ESI-MS technique, these latter experiments were recorded only in water. In these solution conditions (Milli-Q water, pH ∼ 5–6) the multicharged spectra of HEWL alone showed the predominance of the +8 charged species (data not shown). Representative, deconvoluted ESI-MS spectra of a 1:1 NAMI-A–HEWL sample, monitored over 24 h, are shown in Fig. 4. After mixing, besides the peak of the native protein, at 14,303 Da, another peak located at approximately 14,695 Da (peak 1a) shows up, whose molecular mass exactly matches that of HEWL plus an intact $[RuCl_4(DMSO)(Im)]^-$ monoanionic moiety. A secondary peak at approximately 14,657 Da (peak 2a) is indicative of the formation of a "potentially" covalent adduct between HEWL and a $[RuCl_3(DMSO)(Im)]$ fragment. At higher mass values (approximately 15,085 Da) another peak (peak 3a), of far lower intensity, is barely observed, corresponding to the "bis adduct" of HEWL with two $[RuCl_4(DMSO)(Im)]^-$ moieties. These spectral features, and the relative intensities of the peaks, are substantially conserved over the following 24 h, while the sample is kept at room temperature, suggesting that the adducts formed possess an appreciable stability. Table 1 provides the detailed assignment of the abovementioned ESI-MS peaks.

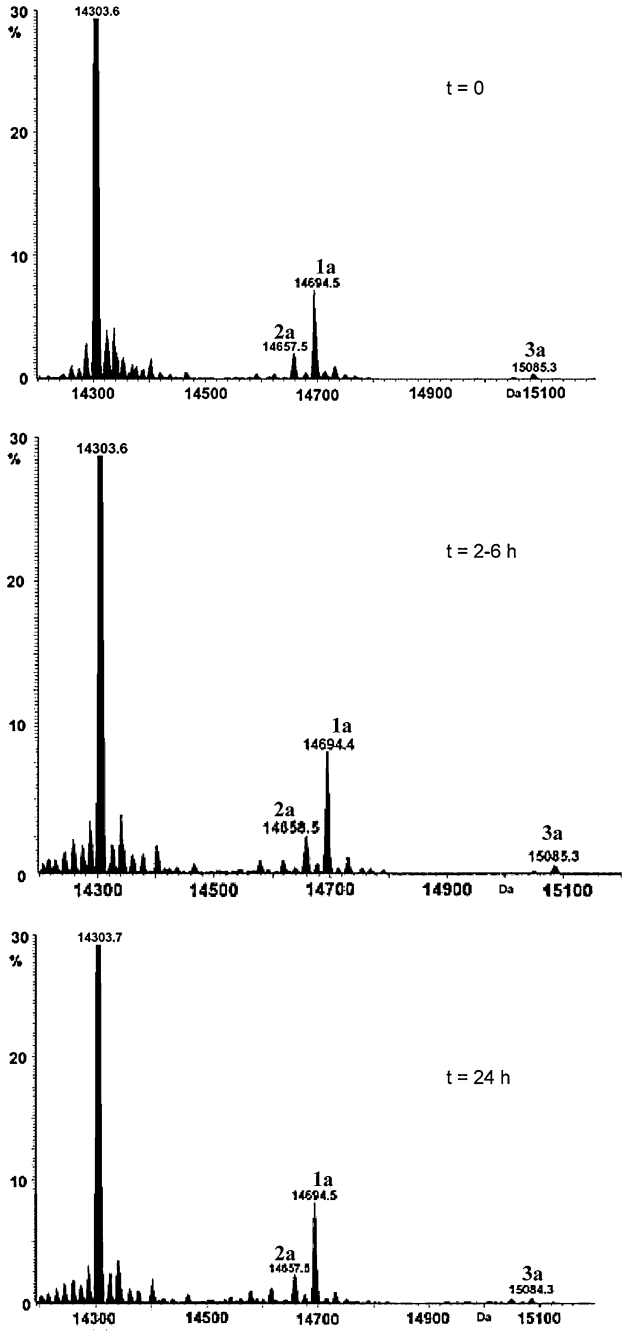

Fig. 4 Deconvoluted electrospray ionization mass spectrometry (ESI-MS) spectra of the NAMI-A adduct with HEWL in 1:1 ratio, at different incubation times (t = 0, 2–6 and 24 h, respectively) in Milli-Q water pH 5–6, at 37 °C. The assignment of the peaks is given in Table 1

Cytochrome *c*

The reaction of NAMI-A with horse heart cyt *c* was investigated through a similar experimental approach. We started again from time-dependent spectrophotometric studies of the 1:1 NAMI-A–cyt *c* system. Notably, in this case, the absorption spectra are dominated by the intense visible bands associated with the heme group of cyt *c*. It is well known that cyt *c*, in its oxidized form, exhibits an intense Soret band at approximately 405 nm and weaker Q bands in the 500–560-nm region [33]. Although these heme bands cover almost completely those far weaker bands typical of NAMI-A, we nonetheless recorded the absorption spectra of the 1:1 NAMI-A–cyt *c* system over 24 h, at room temperature, either in water or in phosphate-buffered solution. As expected, the absorption bands of NAMI-A are hardly detected owing to severe band overlap.

Table 1 Adducts formed between imidazolium *trans*-[tetrachloro(dimethyl sulfoxide)(imidazole)ruthenate(III)] and hen egg white lysozyme (*HEWL*) or cytochrome *c* (*cyt c*) as determined by electrospray ionization mass spectrometry

Adduct number	Mass (Da)	HEWL–Ru adduct	Cyt *c*–Ru adduct
1a	14,694	$[RuCl_4(dmso)Im]^-$	
2a	14,657	$[RuCl_3(dmso)Im]$	
3a	15,085	$2 \times [RuCl_4(dmso)Im]^-$	
1b	12,746		$[RuCl_4(dmso)Im]^-$
2b	12,725		$[RuCl_3OH(dmso)Im]^-$
3b	12,710		$[RuCl_3(dmso)Im]$
4b	12,674		$[RuCl_2(dmso)Im]^+$
5b	12,634		$[RuCl(dmso)Im]^{2+}$
6b	12,622		Ru-containing fragment not attributed

dmso dimethyl sulfoxide, *Im* imidazole

However, the analysis of the temporal evolution of the resulting spectra, in unbuffered water, allowed us to reveal relevant progressive changes of the spectral features characteristic of cyt *c*. In particular, the progressive appearance, with time, of Q bands typical of reduced cyt *c* was noticed, indicative of the occurrence of (at least partial) reduction at the heme iron center. On the basis of a semiquantitative analysis of the observed spectral changes at 550 nm, one can state that about 60% of the iron(III) centers undergo reduction to the ferrous species within 6–7 h after NAMI-A addition (in equimolar amounts) (Fig. 5). These spectral changes are specifically induced by NAMI-A through yet poorly understood mechanisms; however, it is tempting to hypothesize that cyt *c* reduction is the consequence of ruthenium binding to a specific protein site, capable of modulating the redox properties of the heme center, in line with previous observations (see later in the "Conclusions").

The ICP-OES data resemble those obtained in the case of HEWL adducts. Relevant protein metallation levels were readily achieved after 1 h incubation at 37 °C (about 40% of the total ruthenium is associated to the protein);

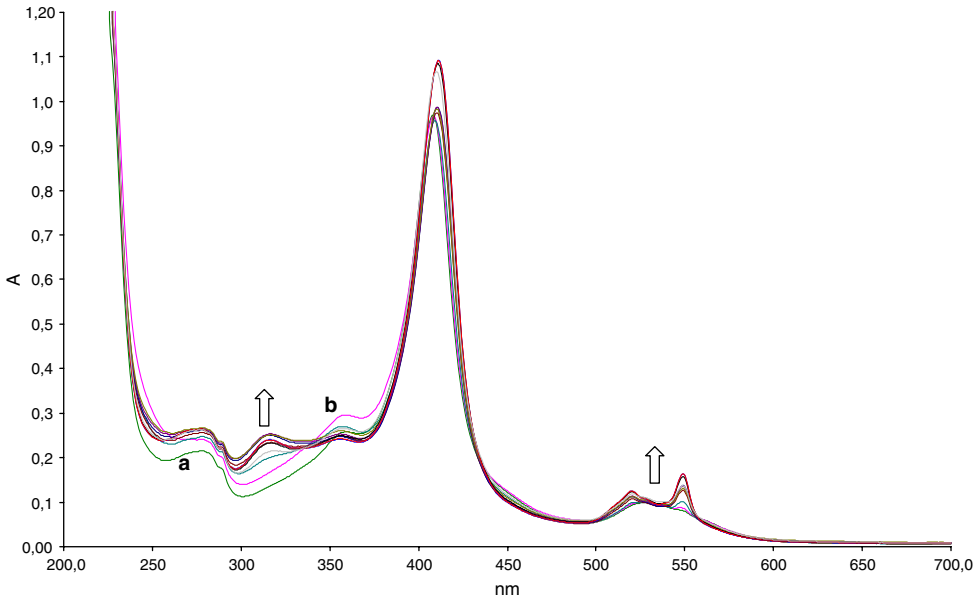

Fig. 5 Absorption UV–vis spectra of 10^{-5} M cytochrome *c* 1 in Milli-Q water (pH ~ 5–6), before (*a*) and after (*b*) addition of 1 equiv of NAMI-A. Spectra were recorded at different times over 24 h at 25 °C. *Arrows* indicate the development of the absorption with time

afterward, very marginal increases were measured even after very long incubation times (up to 50% in 24 h).

Independent information on NAMI-A aquation processes, in the present system, was subsequently gained from analysis of time-dependent ^{1}H NMR spectra. ^{1}H NMR spectra were collected on the 1:1 NAMI-A–cyt *c* system (10^{-3} M) at regular intervals over 24 h (at room temperature), either in 50 mM phosphate buffer (pH 7.4) or in D_2O (pH ~ 5–6). Fortunately, the hyperfine signals characteristic of oxidized cyt *c*, mostly lying in the downfield region, do not appreciably overlap with the few intense hyperfine signals of NAMI-A, falling upfield. For comparison purposes ^{1}H NMR spectra of NAMI-A alone were also recorded under the same solution conditions (data not shown). Accurate monitoring of the resonances at −15.5 ppm and at about −11.5 ppm, previously discussed, allowed us to evaluate the kinetics of NAMI-A aquation in the presence of cyt *c* in comparison with free NAMI-A. Changes in the intensity of the DMSO resonances for NAMI-A, either alone or in the presence of cyt *c*, at −15.5 and −11.5 ppm, are reported in Fig. 6.

For NAMI-A alone, in phosphate buffer (pH 7.4), the proton signals of ruthenium(III)-bound DMSO disappear in less than 3 h ($t_{½}$ ~ 60 min), and are replaced by the signals typical of coordinated DMSO in [$RuCl_3$(DMSO)Im(H_2O)] (NAMI - A_{H_2O} hereafter). Notably, in the millimolar concentration range employed for the NMR experiments, the lifetime of NAMI-A appears to be far longer with respect to what is observed in the UV–vis absorption spectroscopy experiments (at 10^{-4} M, $t_{½}$ = 25 min) [24, 25]. After 3–4 h this mono-hydrolyzed species continues its degradation process until it disappears completely after approximately 6 h, at room temperature. In the case of the NAMI-A–cyt *c* system, the first hydrolysis step is faster and reaches completion within about 1 h ($t_{½}$ ~ 15 min). Then, the resonances of the NAMI - A_{H_2O} species progressively decrease, till complete disappearance after about 6 h (Fig. 7).

Notwithstanding, a precise evaluation of the rate constants is prevented by the long acquisition time required to collect each spectrum (approximately 10 min). In any case, Fig. 6 clearly shows that the hydrolysis process occurs through two consecutive steps, the second being slightly slower. In the case of the NAMI-A–cyt *c* system, the halftime of NAMI - A_{H_2O} was estimated to be approximately 130 min.

The proposed two-step mechanism for the hydrolysis process is also confirmed by the analysis of the time

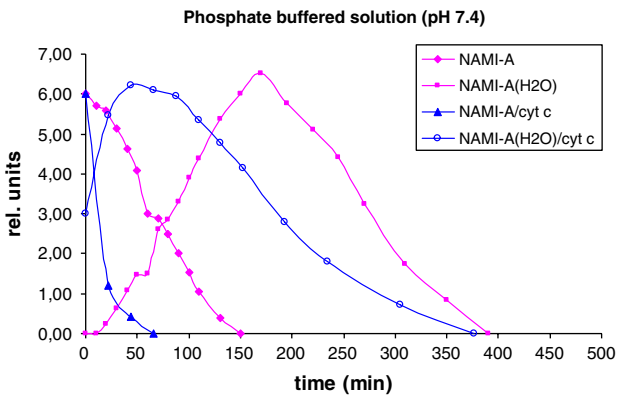

Fig. 6 Hydrolysis species formed at pH 7.4 in phosphate buffer, monitored through integration of the dimethyl sulfoxide (DMSO) resonances at −15.5 ppm for NAMI-A and at −11.5 ppm for [$RuCl_3$(DMSO)Im(H_2O)] (NAMI - A_{H_2O}) in the ^{1}H NMR spectra. *Im* imidazole

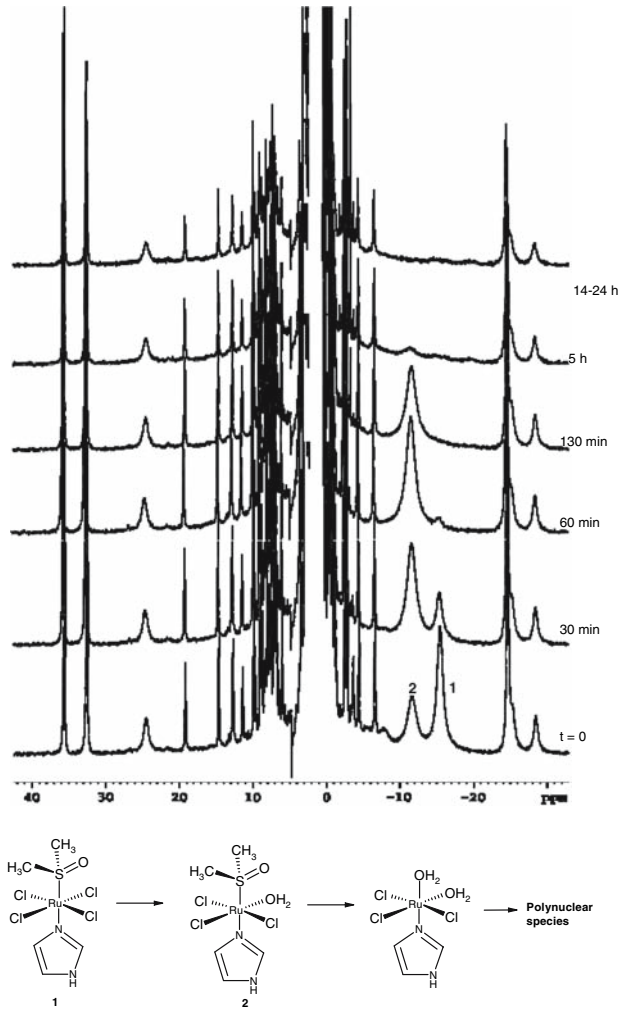

Fig. 7 400 MHz ^{1}H NMR spectra recorded over 24 h at 25 °C on a sample of horse heart cytochrome *c* after addition of NAMI-A in a 1:1 ratio. The sample was prepared in 50 mM phosphate buffer, pH 7.4. The scheme *below the spectra* represents the hydrolysis species of NAMI-A and the corresponding DMSO resonances

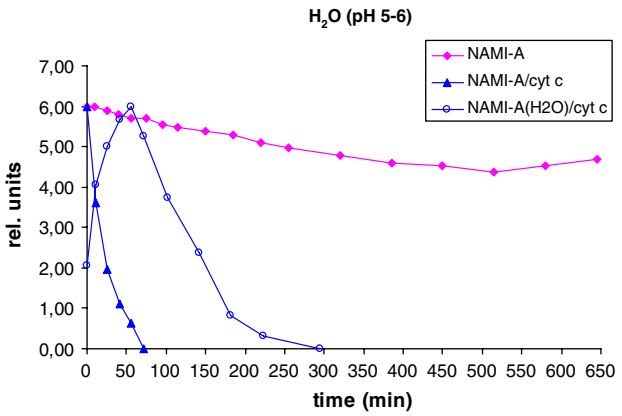

Fig. 8 Hydrolysis species formed at pH 5–6 in D_2O, monitored through integration of the DMSO resonances at −15.5 ppm (NAMI-A) and −11.5 ppm (NAMI - A_{H_2O}) in the ^{1}H NMR spectra

evolution of the signal of free DMSO (at 2.6 ppm), showing a peculiar sigmoidal behavior (data not shown), and thus indicating that DMSO is released only by NAMI - A_{H_2O} and not by NAMI-A.

When dissolved in water, at pH ∼ 5–6, NAMI-A, alone, is very stable as may be inferred from the persistence of the signal at −15.5 ppm over 24 h, indicative of "intact" NAMI-A (Fig. 8). However, this behavior changed drastically following addition of equimolar amounts of cyt *c*. In fact, in this latter case, NAMI-A undergoes fast hydrolysis to give the monoaqua species NAMI - A_{H_2O} (Fig. 8). The process reaches completion in about 1 h ($t_{½}$ ∼ 16 min) as in the case of phosphate buffered solutions. Then, the decrease of the NMR hyperfine signal at −11.5 ppm indicates that NAMI - A_{H_2O} again decomposes gradually ($t_{½}$ ∼ 60 min).

The occurrence of ruthenium reduction to diamagnetic ruthenium(II) could be ruled out here owing to the persistence of the characteristic hyperfine signals assigned to ruthenium(III) ligands. Conversely, time-dependent ^{1}H NMR spectra confirmed progressive cyt *c* reduction in agreement with the above-reported spectrophotometric results. Such a phenomenon was monitored through the careful analysis of time-dependent changes in the intensity of hyperfine signals, typical of oxidized cyt *c*. Both the porphyrin methyl groups and the Met80 S–CH_3 group strongly feel the paramagnetic effect of the low-spin iron(III) metal center; while the former –CH_3 groups are downfield-shifted, the latter is upfield-shifted. Their chemical shifts are in the order 8-CH_3 > 3-CH_3 > 5-CH_3 > 1-CH_3 ≫ Met80 S–CH_3 [34] Among them, the 8-CH_3 (35.7 ppm), the 3-CH_3 (32.8 ppm) and the Met80 S–CH_3 (−24.7 ppm) peaks, lying in a clear part of the spectrum, are suitable for studying the precise redox state of cyt *c*. Figure 9 clearly shows a decrease in the NMR intensity of these groups with time, owing to iron(III) to iron(II) protein active-site reduction It is worth noting that with the cyt *c* and NAMI-A concentrations employed in the NMR experiments, the reduction process does not reach completion and only accounts for approximately 50% of total iron.

Finally, ESI-MS measurements were carried out on NAMI-A–cyt *c* samples, prepared in water. Relevant deconvoluted spectra are shown in Fig. 10. From analysis of these data detailed information on the evolution of the system may again be derived (see Table 1 for a detailed description of the main peaks). At mixing, the peak of the native protein at 12,358 Da is the dominant one. A secondary peak at approximately 12,746 Da (peak 1b) corresponding to a $[RuCl_4(DMSO)(Im)]^-$ moiety is detected as well, as in the case of the HEWL adduct.

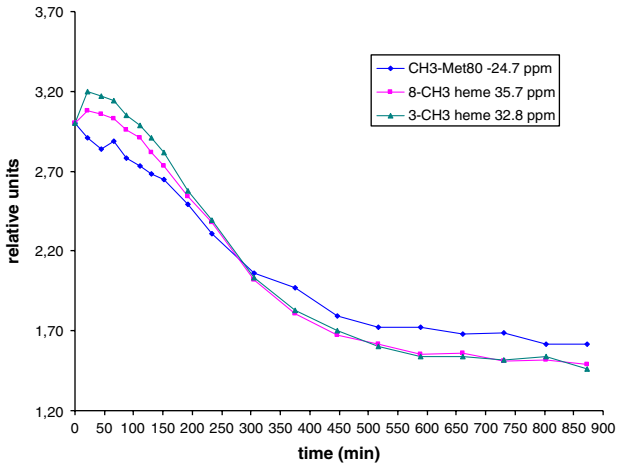

Fig. 9 Time dependence of the integral of the resonances at 35.7 (8-CH_3), 32.8 (3-CH_3) and −24.7 ppm (Met80 S–CH_3) in 50 mM deuterated phosphate buffer, pH 7.4

An ESI-MS spectrum of the same sample, acquired 2 h after mixing, revealed the occurrence of significant changes. The peak at 12,746 Da still persists, but is now accompanied by a group of peaks, of lower mass (falling in the 12,600–12,730-Da range), that correspond to NAMI-A hydrolysis products. High-resolution ESI-MS data demonstrate that these additional peaks (peaks 2b–5b) are attributed to distinct ruthenium-containing species arising from the sequential replacement of up to three chloride ligands by water (hydroxide) molecules. After 24-h incubation, the ESI-MS spectra show the presence of a single main peak, at 12,623 Da (peak 6b), assigned to a protein-bound ruthenium fragment of approximately 264 Da. This latter fragment most likely corresponds to a hydrated ruthenium center that has lost most of its original ligands, in particular the DMSO and the imidazole ligands. Remarkably, the same fragment, of mass approximately 264 Da, was obtained when cyt *c* was reacted with other structurally diverse ruthenium(III) complexes such as methylimidazolium *trans*-[tetrachloro (DMSO) (methylimidazole)ruthenate(III)] or thiazole *trans*-[tetrachloro(DMSO)(thiazole)ruthenate(III)] (unpublished results from our laboratory, data not shown).

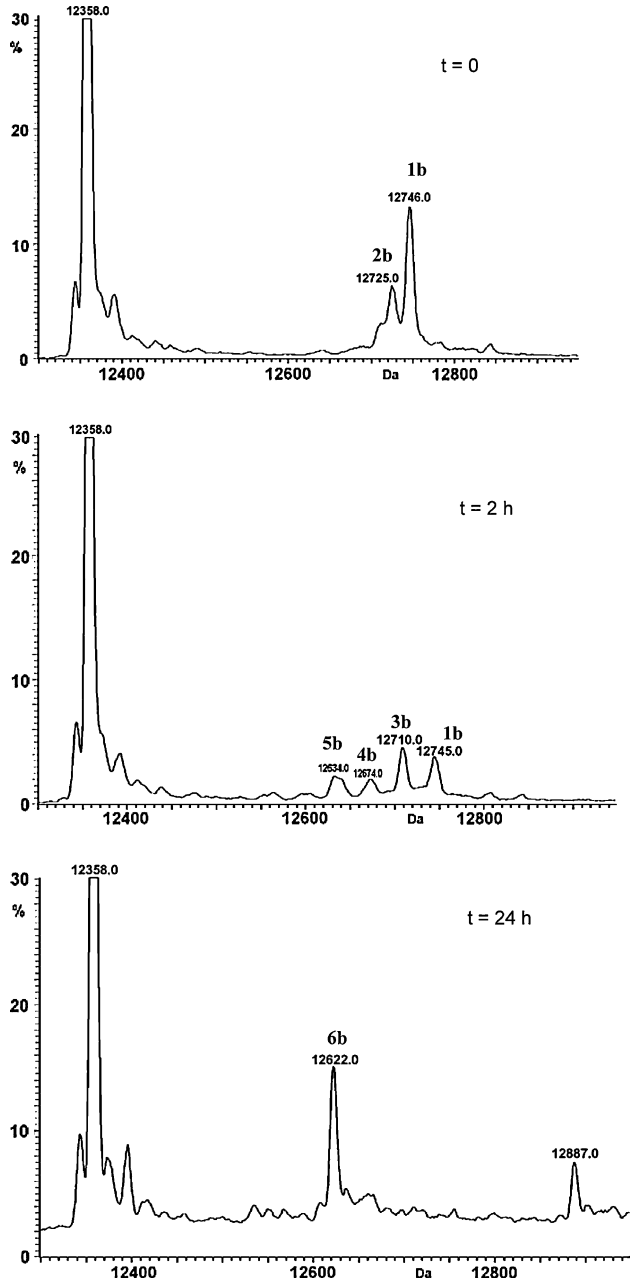

Fig. 10 Deconvoluted ESI-MS spectra of the NAMI-A adduct with horse heart cyt *c* in 1:1 ratio, at different incubation times (*t* = 0, 2 and 24 h, respectively) in Milli-Q water, pH 5–6 at 37 °C. The assignment of the peaks is given in Table 1

Conclusions

There is great interest today in understanding the interactions of metallodrugs with proteins at the molecular level, for their relevant impact on the overall biological, pharmacological and toxicological profile of these fascinating compounds. The available knowledge on this topic is relatively scarce owing to the limited number of published papers and to the intrinsic technical difficulties in identifying the most important metallodrug–protein complexes and elucidating their structure and biological role.

However, a series of recently published papers has provided new valuable insight into the formation process and the structural features of adducts formed between a few metallodrugs and some representative proteins [35, 36]. A recent review by Timerbaev et al. [37] has offered a detailed description of the present state of the art. Remarkably, new physicochemical methods, in particular a

few modern separation and analytical techniques, are being continuously implemented and exploited to gain insight into these complex systems, often with excellent results.

Within this general frame, we have carried out a detailed investigation of the interactions that take place in solution, under physiological-like conditions, between the experimental anticancer drug NAMI-A and two small model proteins, lysozyme and cyt *c*. The combined application of electronic absorption spectroscopy, ^{1}H NMR and ESI-MS has allowed a rather deep insight into the reactions of NAMI-A with these protein targets at the molecular level. Complementary, independent information was derived from ICP-OES measurements.

Quite unexpectedly, two substantially different modes of metallodrug–protein interaction clearly emerged in the two cases. In fact, lysozyme appears to give rise, predominantly, to noncovalent binding with either intact or monohydrolyzed NAMI-A, most likely mediated by electrostatic interactions. Binding appears to be largely reversible as witnessed by ICP-OES and ultrafiltration experiments. Remarkably, these interactions greatly slow down intrinsic NAMI-A degradation processes.

In contrast, cyt *c* was found to enhance NAMI-A degradation, accelerating the progressive detachment of the various ligands from the ruthenium center. Most likely, this process is facilitated by an initial electrostatic interaction between the negatively charged NAMI-A "core" and this small basic protein (indeed, similarly to lysozyme, cyt *c* is a highly cationic protein at physiological pH with a p*I* of approximately 9.59 and is very prone to interact with anions) [38]. Such initial interaction is then progressively replaced by coordinative binding of the ruthenium(III) center to the protein. Eventually, a highly degraded ruthenium-containing species in which most of the original metal ligands have been lost was found to remain associated to the protein. The masses of the various protein-bound ruthenium-containing fragments could be determined, in most cases, with high resolution, and the fragments assigned to specific molecular structures.

At the same time, we found that NAMI-A highly facilitates progressive reduction of ferric cyt *c* to the corresponding ferrous form. This finding was quite unexpected as NAMI-A is a ruthenium(III) species. Mechanistic details of this redox process are still unclear, but it is reasonable to assume that reduction is mediated by ruthenium binding to a specific protein-binding site. Gourion-Arsiquaud et al. [39] recently described a high-affinity binding site for either zinc(II) or cadmium(II) in horse heart cyt *c*; on the basis of NMR data this site was assigned to His33. It was observed that occupancy of this site by metals may affect importantly the redox behavior of cyt *c* and stabilize its ferrous form although His33 is quite distant from the heme center. Notably, Yocom et al. [40, 41] had previously reported on the formation of a stable pentaammineruthenium(III)–His33 complex as the main product resulting from the reaction of aquopentaammineruthenium(II) with horse heart ferricytochrome *c*. In view of the known affinity of ruthenium(III) for histidine residues it is tempting to propose His33 as the most probable binding site for NAMI-A on cyt *c*.

An overall analysis of the results obtained so far for the interaction of NAMI-A with cyt *c* prompted us to formulate the following interpretation for its mechanism of action. We propose that NAMI-A, in its reaction with cyt *c*, somehow behaves as a "multistage missile." Indeed we have shown that the final species that remains bound to cyt *c* just corresponds to a small metallic fragment essentially containing the ruthenium center, while all the other "pieces" of the starting molecule (i.e., the various ligands) have been progressively lost. Thus, the ruthenium center seems to play the role of the "orbiter" capable of reaching its final target, while the ligands would correspond to the various stages assisting the "orbiter" on its way to the "target." This concept, originally proposed by Enzo Alessio (personal communication), finds here some further experimental support. It is likely that the actual functioning of NAMI-A may rely on such a characteristic behavior, which just corresponds to a new and more elaborate version of the "prodrug" theory. In this respect, it is worthwhile mentioning that a previous study by Temperini et al. [42] revealed that the final product of the reaction of NAMI-A with a short DNA fragment consisted of the bare ruthenium center linked to the DNA oligo, whereas all the other ligands of the ruthenium(III) center had been lost in the course of the reaction.

In conclusion, on the basis of the above-described results, we can state that proteins may interact differently with NAMI-A and affect in different ways its intrinsic degradation/activation processes under physiological-like conditions. While HEWL seems to protect the integrity of NAMI-A, cyt *c* favors, in contrast, its degradation. Thus, we can state that the overall effect of proteins on NAMI-A evolution in biological fluids critically and strictly depends on the *nature of the protein itself* and of the resulting metallodrug–protein interactions. Obvious consequences may be expected for ruthenium speciation and bioavailability following NAMI-A administration as well as for the main pharmacodynamic and pharmacokinetic aspects of this promising drug. A detailed understanding of these effects at the molecular level is, in our opinion, very important for a full understanding of the actual mode of action of these novel anticancer metallodrugs. In view of the intrinsic complexity of this matter, it is evident that much work and also much caution are needed in order to predict reactions of metallodrugs with proteins actually occurring inside cells. In any case, it is evident that

generalizations based on a limited number of data should be carefully avoided as we have shown here that two rather similar proteins (both small, globular, water soluble and strongly basic) affect NAMI-A reactivity in nearly opposite ways.

Acknowledgements CIRCMSB, MIUR, and Ente Cassa di Risparmio di Firenze are gratefully acknowledged for financial support. We thank AIRC for a grant to A.C. Scientific discussion with Enzo Alessio on the main aspects of this study turned out to be very illuminating.

References

1. Alessio E, Mestroni G, Bergamo A, Sava G (2004) Curr Top Med Chem 4(15):1525–1535
2. Siegel A, Siegel H (2004) Metal ions in biological systems, vol 42. Dekker, New York
3. Sava G, Gagliardi R, Bergamo A, Alessio E, Mestroni G (1999) Anticancer Res 19(2A):969–972
4. Rademaker-Lakhai JM, van den Bongard D, Pluim D, Beijnen JH, Schellens JH (2004) Clin Cancer Res 10(11):3717–3727
5. Hartinger CG, Zorbas-Seifried S, Jakupec MA, Kynast B, Zorbas H, Keppler BK (2006) J Inorg Biochem 100:891–904
6. Dittrich C, Scheulen ME, Jaehde U, Kynast B, Gneist M, Richly H, Schaad S, Arion VB, Keppler BK (2005) Proc Am Assoc Cancer Res 46:P472
7. Dyson PJ Sava G (2006) Dalton Trans 1929–1933
8. Frausin F, Scarcia V, Cocchietto M, Furlani A, Serli B, Alessio E, Sava G (2005) J Pharmacol Exp Ther 3(1):227–233
9. Lippert B (1999) Cisplatin, chemistry and biochemistry of a leading anticancer drug. Wiley, Weinheim
10. Reedijk J (1996) Chem Commun 801–806
11. Roberts JD, Peroutka J, Farrell N (1999) J Inorg Biochem 77:51–57
12. Zorzet S, Bergamo A, Cocchietto M, Sorc A, Gava B, Alessio E, Iengo E, Sava G (2000) J Pharmacol Exp Ther 295(3):927–933
13. Bergamo A, Sava G (2007) Dalton Trans 13:1267–1272
14. Pintus G, Tadolini B, Posadino AM, Sanna B, Debidda M, Bennardini F, Sava G, Ventura C (2002) Eur J Biochem 269(23):5861–5870
15. Sanna B, Debidda M, Pintus G, Tadolini B, Posadino AM, Bennardini F, Sava G, Ventura C (2002) Arch Biochem Biophys 403(2):209–218
16. Bergamo A, Messori L, Piccioli F, Cocchietto M, Sava G (2003) Invest New Drugs 21(4):401–411
17. Messori L, Orioli P, Vullo D, Alessio E, Iengo E (2000) Eur J Biochem 267(4):1206–1213
18. Jiang X, Wang X (2004) Annu Rev Biochem 73:87–106
19. McKenzie HA, White FH (1991) Adv Protein Chem 41:173–315
20. Casini A, Mastrobuoni G, Temperini C, Gabbiani C, Francese S, Moneti G, Supuran CT, Scozzafava A, Messori L (2007) Chem Commun 2:156–158
21. Casini A, Gabbiani C, Mastrobuoni G, Messori L, Moneti G, Pieraccini G (2006) Chem Med Chem 1(4):413–417
22. Banci L, Bertini I, Gray HB, Luchinat C, Reddig T, Rosato A, Turano P (1997) Biochemistry 36(32):9867–9877
23. Mestroni G, Alessio E, Sava G (1998) Int Patent WO 98/00431
24. Bacac M, Hotze AC, van der Schilden K, Haasnoot JG, Pacor S, Alessio E, Sava G, Reedijk J (2004) J Inorg Biochem 98(2):402–412
25. Bouma M, Nuijen B, Jansen MT, Sava G, Flaibani A, Bult A, Beijnen JH (2002) Int J Pharm 248(1–2):239–246
26. Mestroni G, Alessio E, Sava G, Pacor S, Coluccia M, Boccarelli A (1994) Metal Based Drugs 1:41–63
27. Ravera M, Baracco S, Cassino C, Zanello P, Osella D (2004) Dalton Trans 15:2347–2351
28. Groessl M, Reisner E, Hartinger CG, Eichinger R, Semenova O, Timerbaev AR, Jakupec MA, Arion VB, Keppler BK (2007) J Med Chem 50:2185–2193
29. Brindell M, Piotrowska D, Shoukry AA, Stochel G, van Eldik R (2007) J Biol Inorg Chem (in press)
30. Chen J, Chen L, Liao S, Zheng K, Ji L (2007) J Phys Chem B 111:7862–7869
31. Retailleau P, Ducruix A, Ries-Kautt M (2002) Acta Crystallogr Sect D 58:1576–1581
32. Norne JE, Lilja H, Lindman B, Einarsson R, Zeppezauer M (1975) Eur J Biochem 59(2):463–473
33. Adar F (1978) In: The porphyrins, vol 3. Physical chemistry A. Academic, New York, pp 167–209
34. Satterlee JD, Moench S (1987) Biophys J 52:101–107
35. Casini A, Mastrobuoni G, Ang WH, Gabbiani C, Pieraccini G, Moneti G, Dyson PJ, Messori L (2007) Chem Med Chem 2(5):631–635
36. Calderone V, Casini A, Mangani S, Messori L, Orioli PL (2006) Angew Chem Int Ed Engl 45(8):1267–1269
37. Timerbaev AR, Hartinger CG, Aleksenko SS, Keppler BK (2006) Chem Rev 106(6):2224–2248
38. Andersson T, Thulin E, Forsén S (1979) Biochemistry 18(12):2487–2493
39. Gourion-Arsiquaud S, Chevance S, Bouyer P, Garnier L, Montillet JL, Bondon A, Berthomieu C (2005) Biochemistry 44:8652–8663
40. Yocom KM, Shelton JB, Shelton JR, Schroeder WA, Worosila G, Isied SS, Bordignon E, Gray HB (1982) Proc Natl Acad Sci USA 79(22):7052–7055
41. Yocom KM, Winkler JR, Nocera DG, Bordignon E, Gray HB (1983) Chem Scr 21:29–33
42. Temperini C, Messori L, Orioli P, Ughetto G (2004) Crystal structure of the ruthenium complex NAMI-A and the oligonucleotide d(CGCGAATTCGCG) poster presentation at the 23rd Congresso AIC, Rome

Insights into the Molecular Mechanisms of Protein Platination from a Case Study: The Reaction of Anticancer Platinum(II) Iminoethers with Horse Heart Cytochrome *c*†

Angela Casini,‡ Chiara Gabbiani,‡ Guido Mastrobuoni,§ Raffaella Zoe Pellicani,⊥ Francesco Paolo Intini,⊥ Fabio Arnesano,⊥ Giovanni Natile,*,⊥ Gloriano Moneti,§ Simona Francese,§ and Luigi Messori*,‡

Laboratory of Metals in Medicine, Department of Chemistry, University of Florence, Via della Lastruccia 3-50019 Sesto Fiorentino, Italy, Mass Spectrometry Center, University of Florence, Via U. Schiff 6-50019 Sesto Fiorentino, Italy, and Dipartimento Farmaco−Chimico, Università di Bari, Via E. Orabona 4-70125 Bari, Italy

Received July 30, 2007; Revised Manuscript Received August 29, 2007

ABSTRACT: The interactions of anticancer metallodrugs with proteins are attracting a growing interest in the current literature because of their relevant pharmacological and toxicological consequences. To understand in more depth the nature of those interactions, we have investigated the reactions of four anticancer platinum(II) iminoether complexes, namely, *trans*- and *cis*-*EE* (*trans*- and *cis*-[$PtCl_2${(*E*)-HN═C(OCH_3)CH_3}$_2$], respectively) and *trans*- and *cis*-*Z* (*trans*- and *cis*-[$PtCl_2(NH_3)${(*Z*)-HN═C(OCH_3)CH_3}], respectively), with horse heart cytochrome *c* (cyt *c*). Our investigation was performed using mainly electrospray ionization mass spectrometry (ESI MS) but was also supported by NMR, inductively coupled plasma optical emission spectroscopy (ICP OES), and absorption electronic spectroscopy. ESI MS spectra clearly revealed the formation of a variety of platinum−protein adducts predominantly corresponding to monoplatinated cyt *c* species. From a careful analysis of the major ESI MS peaks, specific information on the nature of the protein-bound metallic fragments and on the underlying metallodrug−cyt *c* reactions was gained for the various cases. We found that *trans*-*EE* produces a major cyt *c* adduct (12 667 Da) that is different from that produced by either *cis*-*EE* or by *trans*-*Z* and *cis*-*Z* (12 626 Da). In particular, occurrence of extensive hydrolysis/aminolysis (the latter fostered by ammonium carbonate buffer) of the iminoether ligands and formation of the corresponding amides/amidines has been unambiguously documented. The reactivity of the iminoether ligands is greatly enhanced by the presence of cyt *c* as inferred from comparative NMR solution studies. Additional ESI MS measurements recorded on enzymatically cleaved samples of platinated cyt *c* adducts, together with NMR investigation of the cyt *c*/*trans*-*EE* adduct, strongly suggest that protein platination primarily occurs at Met 65. The biological and pharmacological implications of the described protein platination processes are discussed.

Metallodrugs are known to behave, in most cases, as "prodrugs". In other words, an activation step, usually consisting of a ligand-exchange and/or a redox process is required before they can exert their pharmacological effects (*1*−*7*). The resulting "activated" metal-containing species are, thus, the "chemical entities" truly responsible for the observed biological actions. Remarkably, these latter species manifest a high propensity to react with biomolecules and to transfer them "metal-containing molecular fragments", commonly through simple ligand substitution reactions.

For instance, the mechanism of action of cisplatin is thought to rely on coordination to adjacent DNA guanine nucleobases of a bidentate $[Pt(NH_3)_2]^{2+}$ fragment that is formally obtained through release of two water molecules from the "activated" $[Pt(NH_3)_2(H_2O)_2]^{2+}$ cation (*8*−*10*). Notably, introduction of kinetic restrictions to the production of these metallic fragments and to their transfer to target biomolecules results into a substantial loss of biological activity for the metallodrug, as was clearly demonstrated in the case of some representative gold(III) and ruthenium(III) anticancer compounds (*11*, *12*).

During the last 20 years, the interest of the scientific community working on anticancer platinum compounds has mostly focused on platinum interactions with DNA, the putative "primary" target, that were described and analyzed in hundreds of papers (*8*−*10*). In contrast, rather surprisingly, the reactions of platinum drugs with proteins have received very scarce attention.

Just a few studies were devoted to the analysis of the *in vitro* interactions of platinum drugs with the main serum proteins albumin and transferrin. In particular, in 1998, Ivanov et al. reported a pioneering NMR investigation on

† This work was supported by the Ministero dell'Università e della Ricerca (MIUR, PRIN2005 No. 2005032730), by the EC (COST Chemistry Project D39/0004/06), and by Ente cassa di Risparmio di Firenze.

* To whom correspondence should be addressed. Phone: +39 055 4573284(L.M.).Fax: +39055 4573385(L.M.).E-mail: luigi.messori@unifi.it (L.M.); natile@farmchim.uniba.it (G.N.).

‡ Department of Chemistry, University of Florence.

§ Mass Spectrometry Center, University of Florence.

⊥ Università di Bari.

10.1021/bi701516q CCC: $37.00
Published on Web 10/09/2007 PAGE EST: 10.8

thereaction of cisplatin with serum albumin and on the characterization of the resulting adducts (*13*). Subsequently, Khalaila et al. described and modeled the binding of cisplatin to transferrins (*14*). More recently, Mandal et al. have analyzed the interactions of platinum drugs with hemoglobin (*15*). Some other studies have analyzed the reactivity of platinum drugs with small model proteins. For instance, Gibson's group produced a few fundamental studies on the platinum/ubiquitin system (*16*−*20*), and very recently, some of us have reported high-resolution crystal structures of the adducts of cisplatin with superoxide dismutase (*21*) and lysozyme (*22*). The most relevant achievements obtained in this field during the past 20 years have been summarized by Timerbaev et al. in a comprehensive review that appeared in 2006 (*23*).

Yet, we believe that this topic deserves more and more attention as it is increasingly evident that the interactions of platinum drugs with proteins may play crucial roles in their uptake and biodistribution processes as well as in determining their toxicity profile. In addition, reactions of platinum drugs with proteins might be also involved in some aspects of their overall mechanism of action through direct interactions with "secondary" protein targets.

Nowadays, the study of the interactions occurring between metallodrugs and proteins may take new and considerable advantage from the availability of very sophisticated analytical tools. For instance, a number of papers have highlighted the great potential of modern mass spectrometry methods to characterize metal−protein adducts at a molecular level (*24*−*33*). Conversely, the rapid development of proteomic technologies and the use of advanced protein separation techniques, coupled to very sensitive metal detection methods, hold promise for the successful analysis of complex mixtures of platinated proteins and for the identification of those proteins that act as "platinum receptors" and/or "platinum targets".

We have recently shown that ESI MS is able to provide valuable and detailed information on the reactivity of classical anticancer platinum(II) complexes with various model proteins (*24*, *25*). In particular, a well-known and intensely studied small protein, namely, the horse heart cytochrome *c* (cyt *c* hereafter),[1] has been selected as the "test protein" for this kind of investigation upon consideration of a number of favorable properties (*24*, *34*). Accordingly, we report here on the reactions of cyt *c* with a few representative platinum(II) iminoether complexes, a family of promising anticancer agents developed in the laboratory of Bari.

Pt(II) iminoethers are indeed very interesting metallodrugs that exhibit innovative and well-documented antitumor properties (*35*, *36*). These compounds may be straightforwardly prepared by alcoholysis of the parent platinum(II) nitrile complexes (*37*). The overall geometry around the platinum center is preserved during the alcoholysis reaction; however, the formed iminoether ligands can have either *Z* or *E* configuration, depending upon the relative positions of the alkoxide and platinum ions with respect to the C═N double bond (Chart 1). Within this family of platinum

Chart 1: Schematic Drawing of the Selected Platinum Iminoether Complexes

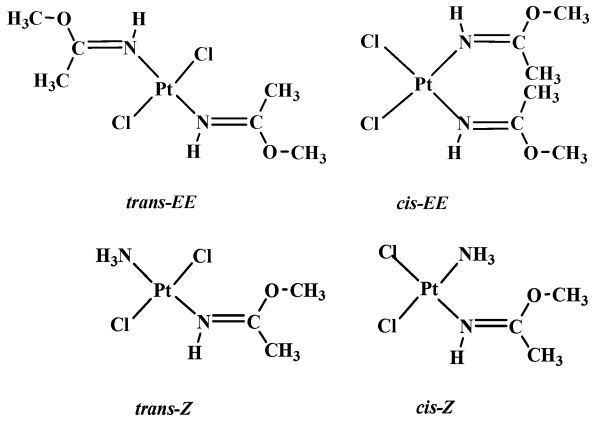

iminoethers, *trans*-[$PtCl_2${(*E*)-HN═C(OCH_3)CH_3}$_2$] (*trans-EE*) was found to be as active as cisplatin toward P388 leukemia and Lewis lung carcinoma in mice (*38*, *39*) through formation of stable DNA monofunctional adducts (*40*). Remarkably, the presence of only one iminoether ligand resulted to be sufficient for promoting the antitumor activation of the trans geometry. Accordingly, the complex *trans*-[$PtCl_2(NH_3)${(*Z*)-HN═C(OCH_3)CH_3}] (*trans-Z*), turned out to be highly active against murine P388 leukemia and SKOV-3 human cancer cell xenograft in nude mice (*41*).

Four representative platinum iminoether complexes, abbreviated as *trans-* and *cis-EE* (*trans-* and *cis*-[$PtCl_2${(*E*)-HN═C(OCH_3)CH_3}$_2$], respectively), and *trans-* and *cis-Z* (*trans-* and *cis*-[$PtCl_2(NH_3)${(*Z*)-HN═C(OCH_3)CH_3}], respectively) were selected for the present study. All these compounds were previously characterized, both chemically and pharmacologically (*37*, *38*, *41*), and their chemical structures are represented in Chart 1.

The main reason for the present investigation and also its primary goal is to describe the reactions that occur between selected platinum−iminoether compounds and cyt *c* and to elucidate the nature of the resulting adducts. Through the study of a specific case, we hoped to unravel representative and mechanistically relevant interactions that take place, within biological fluids, between reactive platinum species and the pool of soluble proteins.

MATERIALS AND METHODS

Sample Preparation for ESI Mass Spectrometry. The synthesis of the iminoether complexes has been carried out as already reported (*37*). Horse heart cytochrome *c* was purchased from Sigma (code C7752). Metal complexes/cyt *c* adducts were prepared in ammonium carbonate buffer (25 mM, pH 7.4), with a protein concentration of 5×10^{-4} M and platinum to protein ratio of 3:1. The reaction mixtures were incubated for different time intervals (3, 6, 24, 72, and 168 h) at 310 K. Samples were extensively ultrafiltered using Centricon YM-3 (Amicon Bioseparations, Millipore Corporation) in order to remove the unbound platinum complex.

After a 100-fold dilution with MilliQ water, ESI MS spectra were recorded by direct introduction, at 3 μL/min flow rate, in a LTQ linear ion trap (Thermo, San Jose, CA) equipped with a conventional ESI source. The specific conditions used for these experiments were as follows: spray voltage 3.5 kV, capillary voltage 40 V, and capillary

[1] Abbreviations: cyt *c*, cytochrome *c*; ESI MS, electrospray ionization mass spectrometry; *trans-EE*, *trans*-[$PtCl_2${(*E*)-HN═C(OCH_3)CH_3}$_2$]; *cis-EE*, *cis*-[$PtCl_2${(*E*)-HN═C(OCH_3)CH_3}$_2$]; ICP OES, inductively coupled plasma optical emission spectroscopy.

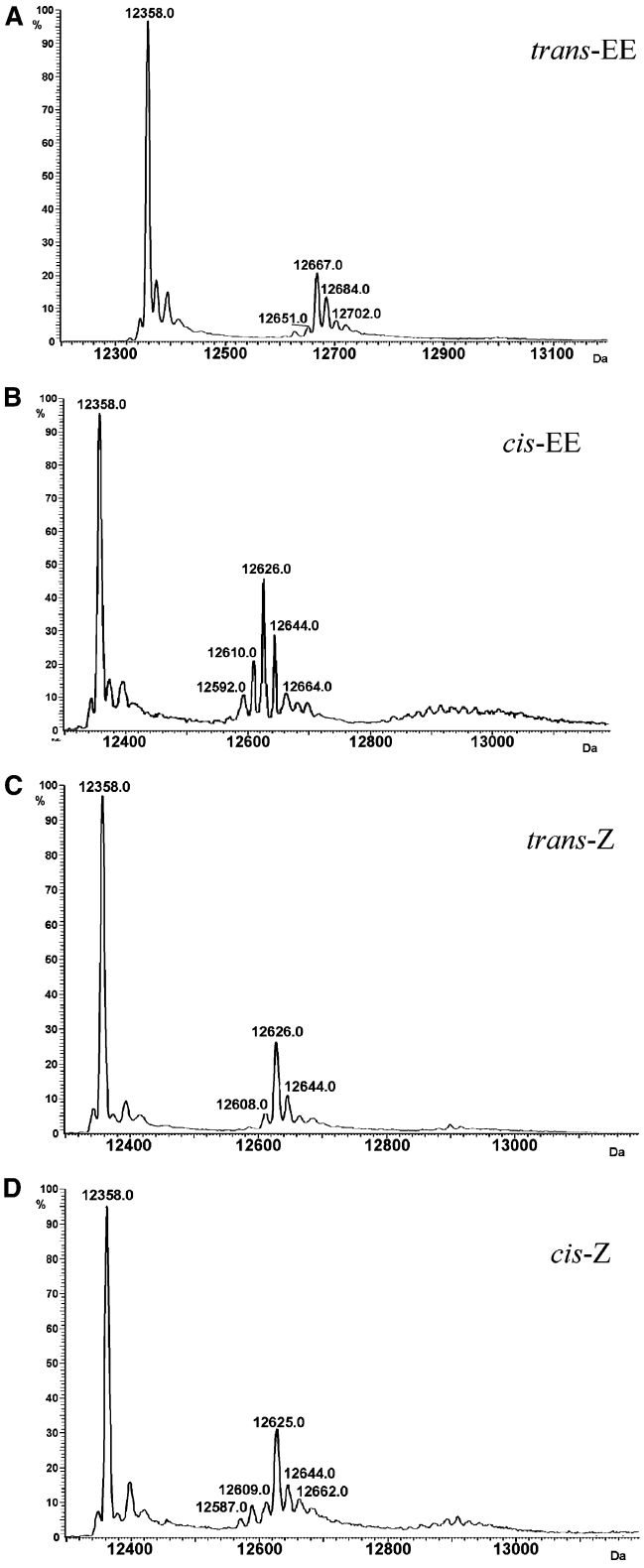

FIGURE 1: Deconvoluted ESI MS spectra of cyt *c* adducts with *trans-EE* (A), *cis-EE* (B), *trans-Z* (C), and *cis-Z* (D). The platinum/protein ratio is 3:1, and the incubation time at 310 K is 24 h.

temperature 353 K. Sheath gas was set at 18 a.u. (arbitrary units), whereas sweep gas was set at 5 a.u. and auxiliary gas was kept at 0 a.u. ESI spectra were acquired using Xcalibur software (Thermo), and deconvolution was obtained using Bioworks software (Thermo). The mass step size in deconvolution calculation was 1 Da, and the spectrum range considered was 1100−2000 *m*/*z*. The same experiments were repeated varying capillary temperature (363 to 453 K), but the peak patterns and relative abundances were not influenced (data not shown).

Spectra of the same samples were also recorded on an Orbitrap high-resolution mass spectrometer (Thermo, San Jose, CA), and the obtained results were fully consistent (data not shown). The instrument was equipped with a conventional ESI source. The working conditions were the following: spray voltage 2.3 kV, capillary voltage 20 V, and capillary temperature 403 K. Sheath gas was set at 12 a.u., the sweep gas and the auxiliary gas were kept at 0 a.u. For acquisition, Xcalibur 2.0 software (Thermo) was used, and monoisotopic and average deconvoluted masses were obtained by using integrated Xtract tool. For spectra acquisition a nominal resolution (at *m*/*z* 400) of 60 000 was used.

Determination of the Binding Site. For the enzyme-digestion analysis, 40 μL of cyt *c* (10^{-4} M), either free or reacted with *trans-EE* or *cis-EE*, was diluted at a concentration of 5 μM in 10 mM ammonium bicarbonate (pH 7.4), and endoproteinase Asp-N (Sigma, P3303) was added to a ratio of 1:50 (w/w). The mixture was incubated for 16 h at 310 K and after digestion was acidified with 0.05% formic acid before ESI MS analysis, using the LTQ Orbitrap mass spectrometer and the instrumental parameters mentioned before.

ICP OES Measurements. ICP OES analyses were recorded using an Optima 2000 instrument (Perkin-Elmer, Europe). The samples containing adducts of cyt *c* with the various platinum complexes were prepared as described above for the ESI MS studies.

NMR Studies. The complex *trans*-[$PtCl_2${(*E*)-$H^{15}N$=$C(OCH_3)CH_3$)}$_2$] was prepared as already reported (*37*) and then used in two types of experiments. In one case the complex (1 mg, 0.0024 mmol) was dissolved in 1 mL of ammonium carbonate buffer (25 mM) prepared by dissolving $(NH_4)_2CO_3$ (2.4 mg, 0.025 mmol) in H_2O/D_2O (9:1, 1 mL). In a second experiment the same complex was dissolved in ^{15}N-enriched ammonium carbonate buffer prepared by dissolving Ag_2CO_3 (6.7 mg, 0.024 mmol) and ($^{15}NH_4$)Cl (2.7 mg, 0.048 mmol) in 1 mL of H_2O/D_2O (9:1) and filtering the solution in order to remove the precipitated AgCl. The pH of both ammonium carbonate buffers was adjusted to 7.4 by addition of $HClO_4$ (1 M solution). The time-dependent transformations of the two samples were monitored by 1D and 2D NMR spectroscopy using Bruker Instruments Avance 300 UltraShield, equipped with a broad-band probe, and Avance 600 UltraShield Plus, equipped with a triple-resonance (TXI) probe with pulsed field gradients along the *z*-axis.

The complex *trans*-[$PtCl_2${(*E*)-HN=C($O^{13}CH_3$)CH_3)}$_2$] was prepared as reported in the Supporting Information. For monitoring the hydrolysis of this ^{13}C methoxide-enriched complex in the presence of cyt *c*, a solution of the complex in H_2O/D_2O (9:1 v/v, pH 6.9; 1.5 mM concentration) was treated with an equimolar amount of cyt *c*. For comparison purposes, a second complex solution similar to the previous one, but deprived of cyt *c*, was also investigated. The two solutions were incubated for 1 week at 310 K and monitored through 1D ^{13}C and 2D ^{1}H,^{13}C-edited HSQC (heteronuclear single quantum correlation) NMR spectra at 600 MHz.

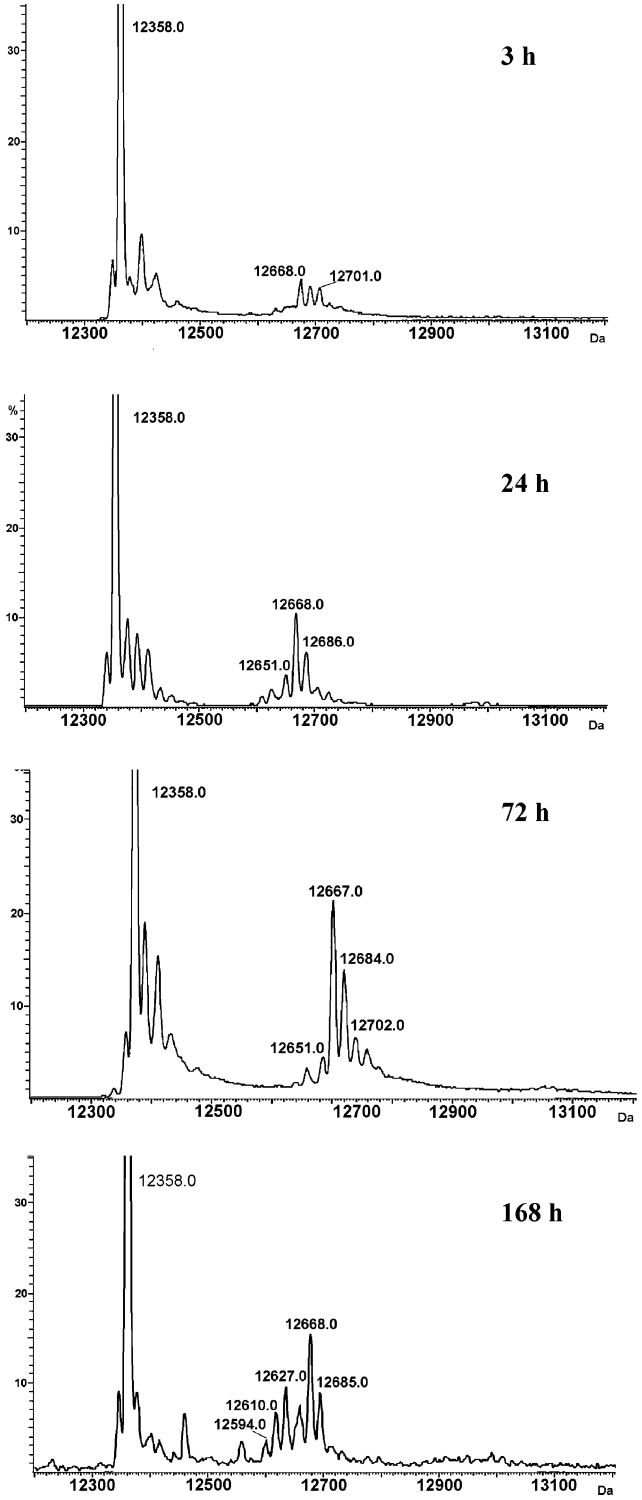

FIGURE 2: Time-dependent spectral profiles for the *trans-EE*/cyt *c* derivative. Spectra were recorded after 3, 24, 72, and 168 h of incubation of the sample at 310 K.

For the identification of the platinum coordination site of cyt *c*, natural abundance $^{1}H,^{13}C$-edited HSQC (*42*−*44*) spectra were recorded at 293 K for a sample of pure cyt *c* and for a sample containing a 1:1 mixture of cyt *c* and *trans-EE* incubated for 1 week at 310 K.

For HSQC experiments, 16 transients were acquired over an F2 (^{1}H) spectral width of 14 ppm into 1024 complex data points for each of 256 t_1 increments in TPPI mode (*45*) with an F1(^{13}C) spectral width of 70 ppm centered at 40 ppm. All 2D NMR data were acquired using a gradient-enhanced sequence in which coherence selection and water suppression are achieved via gradient pulses. The sequence was optimized with a delay $1/(4J_{CH})$ of 1.72 ms. Decoupling during the acquisition time was achieved using a GARP decoupling scheme (*46*). Data zero-filled in F1 were subjected to apodization using a squared cosine bell function in both dimensions prior to Fourier transformation and phase correction. The data were analyzed with the program CARA (The Computer Aided Resonance Assignment Tutorial, R. Keller, 2004, CANTINA Verlag). Resonance assignment was carried out by using available ^{1}H and ^{13}C chemical shifts data at 293 K (*47*, *48*), with the aid of 2D TOCSY (total correlation spectroscopy) and NOESY (nuclear Overhauser enhancement spectroscopy).

RESULTS

Preparation and Characterization of Metal−*Protein Adducts.* In order to investigate comparatively their interactions with the chosen test protein, all four platinum iminoether compounds were individually reacted with horse heart cyt *c* at a molar ratio of 3:1 (metal/protein) and at physiological pH. Samples of the individual reaction mixtures, taken at increasing time intervals after mixing, were subjected to extensive ultrafiltration and then analyzed for Pt content by ICP OES. Under the applied experimental conditions, the protein platination was found to be relatively fast and nearly comparable for the four samples. The Pt/cyt *c* ratio was ≥1.0 already after 1 h of incubation and increased only marginally for longer incubation times. Even after very long incubation times (168 h), the platination levels never exceeded a Pt/cyt *c* ratio of 1.5; in all cases a significant amount of Pt was recovered in the low molecular weight fraction. Remarkably, *cis-EE*, at variance with the other three tested compounds, was shown to cause some direct cyt *c* damage, possibly as a consequence of partial proteolysis, that could be directly monitored through spectrophotometric analysis (however, the total protein loss never exceeded 15%).

ESI MS Studies of the Adducts. Characteristic features were detected in the ESI MS profiles of platinated cyt *c* samples that are diagnostic of the formation of stable platinum−protein adducts. Representative deconvoluted ESI MS spectra of the protein adducts formed after 24 h of incubation with the four platinum(II) iminoether compounds, and subsequent extensive ultrafiltration, are shown in Figure 1. Beyond the peak characteristic of native cyt *c*, located at 12 358 Da, a number of intense additional peaks of higher molecular mass are also observed, which likely correspond to platinum−cyt *c* adducts.

Inspection of the ESI MS spectra provides straightforward insight into the stoichiometry of the resulting metallodrug−cyt *c* adducts. In full agreement with the ICP OES results, indicating that the monoplatinated adducts are the dominant species, also the majority of the ESI MS peaks correspond to *monoplatinated* cyt *c* with peaks falling in the 12 550−12 700 range. In a few cases, some weak features with masses higher than 12 800 Da (notably in the 12 800−13 100 Da range) were also observed, which are indicative of *doubly platinated* species.

To identify the precise nature of the protein-bound Pt fragments, a detailed analysis of the major ESI MS peaks belonging to the various platinated species was carried out.

Scheme 1: Proposed Reaction Scheme for *trans-EE* in Ammonium Carbonate Buffer, pH 7.4, and 310 K

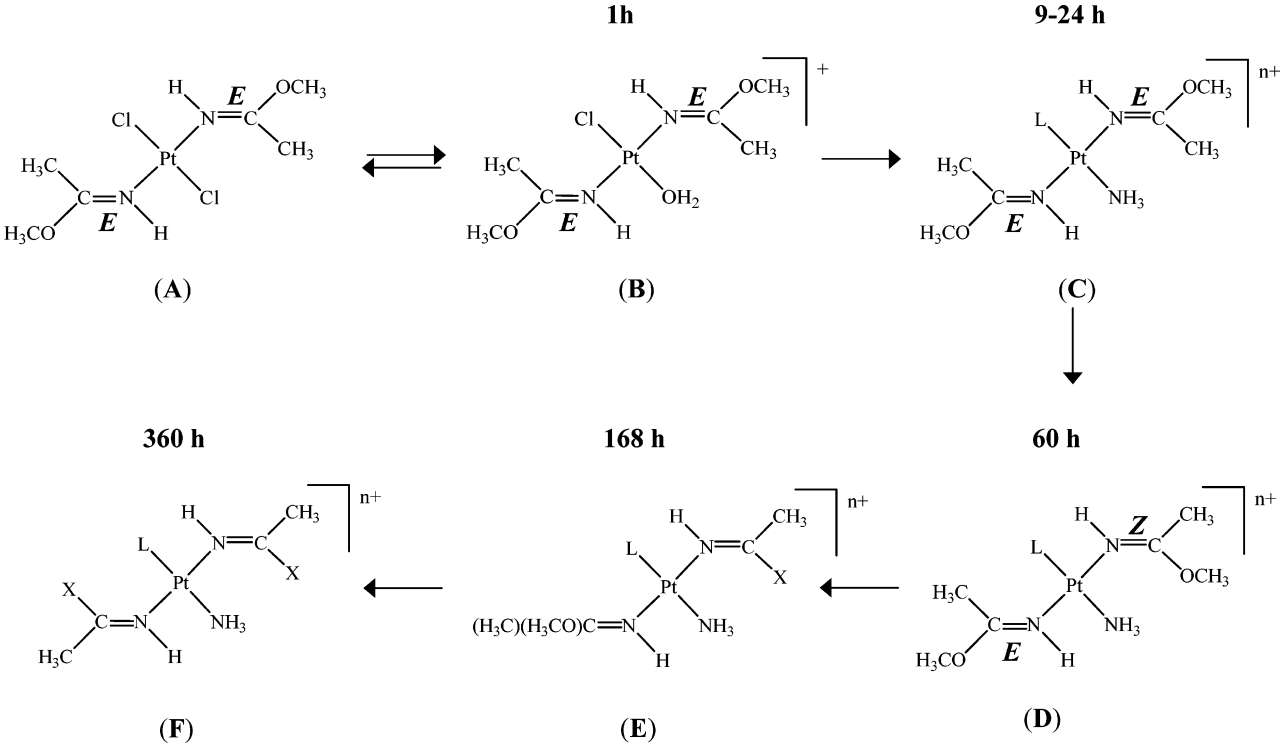

X = OH (**E**) or NH_2 (**F**); L= OH_2 or NH_3

Notably, the ESI MS spectrum of the *trans-EE*/cyt *c* derivative is dominated by a peak at 12 667 Da, which corresponds to addition to the protein of a molecular fragment of mass 309 Da. Rather surprisingly, this mass does not correspond to retention of the two intact iminoether ligands on the platinum center (expected mass of ∼340 Da) but to protein binding of a molecular fragment containing the platinum ion and two acetamide/acetamidine ligands (expected mass of ∼311 Da). These latter ligands are thought to originate from hydrolysis/aminolysis of the iminoether ligands (the aminolysis being fostered by the presence of a high concentration of ammonium carbonate buffer; it is to be noted that the mass of acetamide is only 1 Da greater than that of acetamidine). So far the hydrolysis/aminolysis of the iminoether ligand was only observed at high pH.

Conversely, in the case of *cis-EE*, *cis-Z*, and *trans-Z*, the ESI MS spectra of the Pt/cyt *c* adducts are dominated by a peak corresponding to a mass increase of 268 Da (peak at ∼12 626 Da in the deconvoluted spectra). This latter mass value corresponds well to a platinum(II) ion coordinated to both an acetamide/acetamidine and an aqua/amine ligand.

In all cases, the ESI MS results point out that, under the solution conditions used in our experiments, the platinum-bound iminoether ligands are not lost but undergo important chemical transformations (hydrolysis/aminolysis). Only in the case of *cis-EE* there was release of one iminoether ligand probably due to trans labilization induced by the coordinated cyt *c*.

Our interpretation of the ESI MS results was further supported by additional experiments in which cyt *c* was reacted with either *trans-EE* or *cis-EE* bearing deuterated C-methyl groups. A mass increase of 6 units was observed in the case of *trans-EE*, whereas in the case of *cis-EE*, the measured mass increase was of only 3 units. A complete assignment of the peaks detected in the ESI MS spectra is given in the reaction Schemes 2 and 3 reported later on in the discussion.

Time-Dependent ESI MS Studies. A number of additional ESI MS measurements were carried out, at different intervals over 1 week time, to monitor the time-dependent behavior of the various adducts. A representative example is reported in Figure 2, where the evolution of the ESI MS spectra of *trans-EE*/cyt *c* over 168 h is shown. After 3 h of incubation, there is already a weak multiplet centered at ∼12 668 Da corresponding to addition to the protein of the mentioned 311 Da platinum fragment. For longer incubation times (24, 72, and 168 h) at 310 K, similar spectral features are observed (the peak at 12 668 Da is always the most intense) implying that the nature of the main protein-bound platinum fragment does not change. However, some significant variations in peak intensities are observed between 72 and 168 h, implying that the system is still subject to slow changes. A similar behavior was found for the ESI MS peaks of cyt *c* adducts with *cis-EE*, *cis-Z*, and *trans-Z*, when expanding the observation period to 168 h.

NMR Studies on the Solution Behavior of trans-EE. The hydrolysis/aminolysis reactions documented by ESI MS for platinum-coordinated iminoether ligands were rather unexpected. Thus, additional experiments were carried out to better elucidate this critical point and to gain independent information on this controversial issue. Specifically, high-resolution NMR studies were performed on *trans-EE* in the same medium (ammonium carbonate buffer, pH 7.4) at 310 K.

After dissolution of *trans*-[$PtCl_2${(*E*)-HN═C(OCH_3)-CH_3)}$_2$] in ammonium carbonate buffer, the first observed transformation (1 h reaction time) is a solvolytic process in which one of the two trans chlorido ligands is replaced

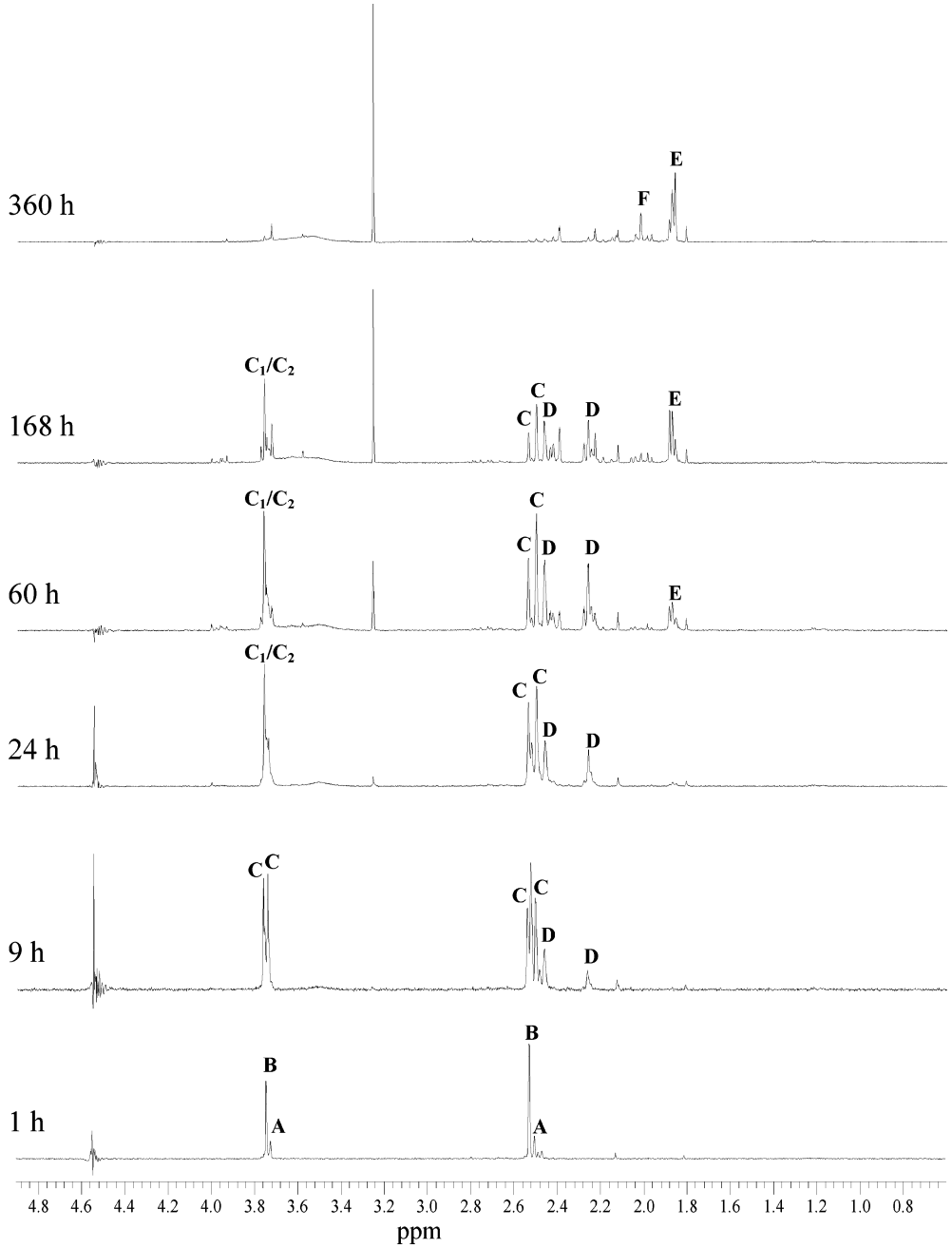

FIGURE 3: ^{1}H NMR spectra (600 MHz) in H_2O/D_2O (9:1) of *trans*-[$PtCl_2${(*E*)-$H^{15}N{=}C(OCH_3)CH_3$}$_2$] (2.4 mM) in ammonium carbonate buffer (25 mM, pH 7.4) at 310 K.

by a molecule of solvent (H_2O). The starting complex (**A** in Scheme 1) has ^{1}H signals at 2.50 (CH_3,^{13}C ~21.0 ppm), 3.72 (OCH_3,^{13}C ~55.0 ppm), and 7.35 ppm (NH, ^{15}N ~90.5 ppm), whereas the new species (**B**) has signals at 2.54 (CH_3, ^{13}C 21.5 ppm), 3.75 (OCH_3, ^{13}C 55.0 ppm), and 7.50 ppm (NH, ^{15}N 91.5 ppm) and is assigned to the monosolvated species. One hour after dissolution the ratio between **A** and **B** is ca. 1:9 (Figure 3).

For longer reaction times (9−24 h) a further transformation leads to the formation of complex species bearing coordinated amine (broad signals around 3.5 ppm). Two new species (**C_1** and **C_2** in Figure 3) have proton signals at 2.55 and 2.51 ppm (CH_3, ^{13}C ~21.0 ppm) and at 3.77 and 3.74 ppm (OCH_3, ^{13}C ~55.5 ppm), which are in accordance with the new compounds **C_1** and **C_2** having the iminoether ligands in the original *E* configuration. Another newly formed species (labeled **D** in Figure 3) has signals at 2.46 (CH_3, ^{13}C ~21.0 ppm), 2.30 (CH_3, ^{13}C ~19.0 ppm), and 4.00 ppm (OCH_3, the intensity of this signal is comparable to those of the other two signals if the spectrum is acquired without suppression of the solvent signal; ^{13}C ~58.0 ppm), which can be ascribed to a complex having one iminoether ligand in *E* and the other in *Z* configurations (an upfield shift of the methyl protons and a downfield shift of the methoxy protons are common features in the switch from *E* to *Z* configuration of an iminoether ligand coordinated to platinum; an analogous trend is also observed for the chemical shifts of the ^{13}C nuclei).

Iminoether ligands are also characterized by imino protons in the 7.0−8.0 ppm region. Signals for all compounds (**A**−**D**) were observed in this region (Figure 1S in the Supporting Information).

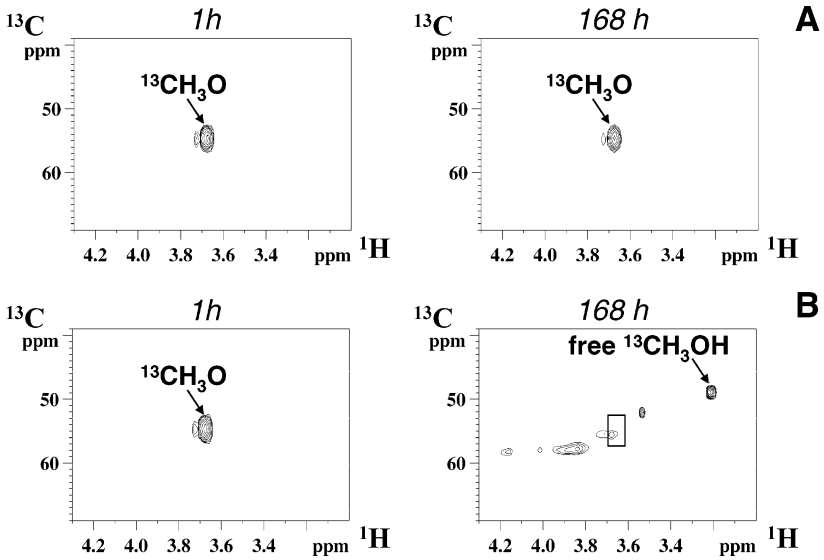

FIGURE 4: 2D ^{1}H,^{13}C-edited HSQC spectra of ^{13}C methoxide-enriched *trans-EE* alone (A) and with 1 equiv of cyt *c* (B), recorded after 1 h (left panels) and after 1 week (right panels) at 310 K. The peak positions of ^{13}C methoxide in the complex and of free ^{13}C methanol are indicated.

The coordination to platinum of ammonia was investigated in more detail by performing the reaction in ^{15}N-enriched ammonium carbonate buffer. The presence in the [^{1}H,^{15}N] HMQC (Figure 2S in the Supporting Information) of at least four signals (^{15}N chemical shift between −80.0 and −60.0 ppm, ^{1}H chemical shift between 3.5 and 4.1 ppm) coupled with platinum ($^{1}J_{Pt,N}$ ranging between 260 and 280 Hz and $^{2}J_{Pt,H} \sim 57$ Hz), strongly supports the formation of platinum complexes bearing coordinated amine ligand(s).

For still longer reaction times (60 h) a significant amount of free methanol (^{1}H signal at 3.26 ppm and ^{13}C signal at 49.2 ppm) is formed. Simultaneously, new methyl signals (**E** in Figure 3) around 1.85 ppm (^{13}C ∼24.5 ppm) and new iminic signals around 5.50 ppm (^{15}N 68.0 ppm) appear. The chemical shifts of the latter set of signals are characteristic of a platinum-coordinated amide. Therefore a hydrolysis of the iminoether ligand with formation of an amide and of free methanol takes place. At still longer times (168 h) the amounts of free methanol and of species containing amide ligands increase at the expenses of species containing imnoether ligands.

After 15 days the iminoether signals disappear almost completely while signals **E** further increase and new signals (**F**) at 2.09 (CH_3, ^{13}C 20.5 ppm) and 6.00 ppm (NH) appear. We can assign the **F** signals to amidine complexes by comparison with the chemical shifts of authenticated platinum−amidine compounds. The formation of the different species as inferred from NMR results is shown in Scheme 1.

Thus, the NMR experiments have confirmed the occurrence (*but only over a time intervals of 1−2 weeks*) of extensive hydrolysis/aminolysis with release of methanol and conversion of the iminoether into amide/amidine (see Figure 3).

In the light of the NMR results obtained on the *trans-EE* complex, it is evident that the presence of cyt *c* leads to a great and generalized enhancement of the reactions taking place at the level of the platinum-coordinated iminoether ligands. Such transformations could take place before platinum coordination to cyt *c* or soon after coordination of the platinum iminoether complex to cyt *c*. In any case the presence of cyt *c* would have a great effect on the rate of hydrolysis. In order to further prove the catalytic role of cyt *c* on the hydrolysis of iminoether ligands, a ^{13}C methoxide-enriched *trans-EE* complex was prepared and its hydrolysis in buffered water solution (1.5 mM concentration, pH 6.9) was monitored in the presence or absence of a stoichiometric amount of cyt *c*. The extent of hydrolysis after 1 week at 310 K (easily monitored by the appearance of ^{13}C-enriched methanol) was negligible in the absence of cyt *c*, whereas it was quantitative in the presence of cyt *c* (Figure 4 and Figure 3S in the Supporting Information). It is to be noted that under these experimental conditions the amount of platinum coordinated to cyt *c* is in the range of 20−25% while the iminoether hydrolysis is almost complete; therefore, it is also possible to conclude from this experiment that cyt *c* catalyzes hydrolysis of the iminoether ligands also on the free complex. It can be hypothesized that electrostatic interaction between cyt *c* and *trans-EE* taking place at basic protein surface can foster such a hydrolysis.

Assignment of the Primary Platinum Binding Site. The above-reported results, but in particular the strong tendency to form monoplatinated derivatives, strongly favor the idea that cyt *c* possesses a primary binding site for platinum drugs. As platinum(II) compounds are known to manifest relatively high affinity only for a few amino acid side chains, namely, Cys, Met, and His, we analyzed the primary sequence of the protein and its crystal structure in order to identify which potential platinum(II) binding sites were characterized by a good solvent accessibility. The protein exhibits seven candidate binding sites: two Cys (14 and 17), two Met (65 and 80), and three His (18, 26, and 33). Among them the two cysteine residues are involved in the covalent binding of the heme group to the polypeptide chain, while Met 80 and His 18 are recruited in the axial coordination of the iron in the heme pocket. Therefore, only Met 65 and His 26 and 33 can be predicted to form adducts with platinum(II) compounds. Moreover, previous studies have supported the view that Met 65 might indeed represent the primary binding site for platinum drugs on horse heart cyt *c* (*49*). The latter hypothesis can be probed with a simple experiment of cyt *c*

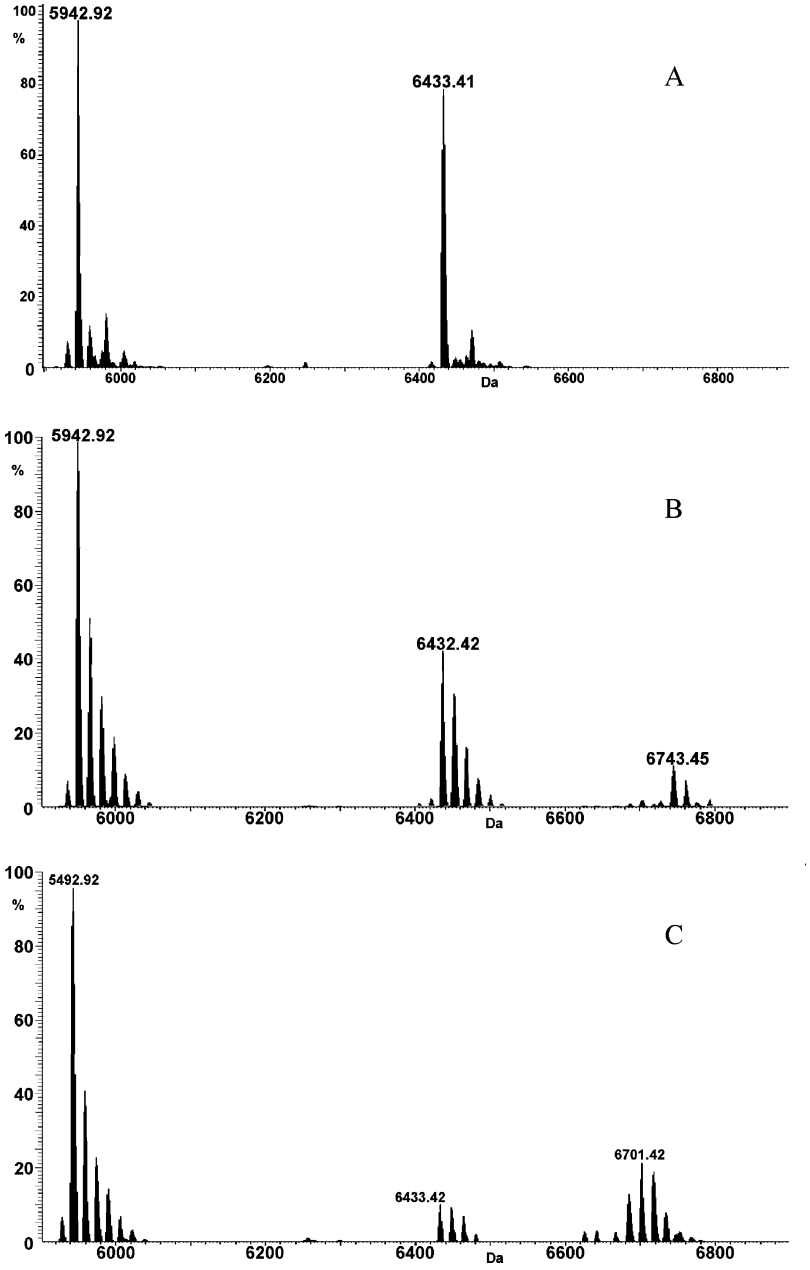

FIGURE 5: Deconvoluted ESI MS spectra of Asp-N treated samples of cyt *c* alone (A) or after incubation with an excess of *trans-EE* (B) or *cis-EE* (C). Data were recorded with an Orbitrap high-resolution mass spectrometer (Thermo, San Jose, CA).

Scheme 2: Proposed Reaction Scheme for *trans-EE* with Cytochrome *c*

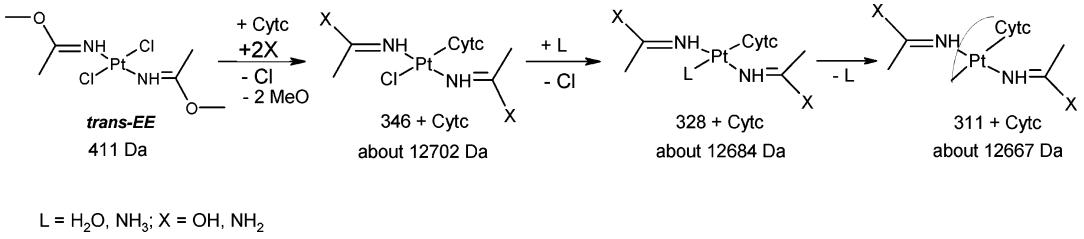

proteolysis using the endoproteinase Asp-N. This enzyme is known to hydrolyze peptide bonds on the N-terminal side of aspartic and cysteic acid residues. In the case of horse heart cyt *c*, Asp-N causes selective cleavage only at the N-terminal site of an aspartic residue, and this single cleavage results into the separation of Met 65 from all the other potential binding sites (His 26 and 33). Therefore, a protein sample was treated with either *trans-EE* or *cis-EE*, incubated with Asp-N, and then analyzed by ESI MS in comparison to a control. The obtained results are shown in Figure 5. The deconvoluted ESI MS spectrum of Asp-N treated nonplatinated cyt *c* reveals two main fragments that correspond to the expected products: the peptide 1−49 (including the heme) and the peptide 50−104 (molecular weights of ∼5944 and 6433 Da, respectively; Figure 5A). In contrast, the ESI MS analysis of the platinated species produced the

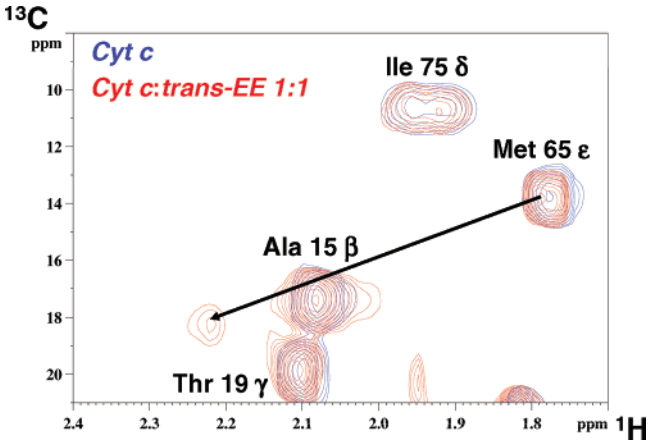

FIGURE 6: Overlay of 2D $^{1}H,^{13}C$-edited HSQC spectra, recorded at 20 °C, of cyt *c* alone (blue contours) and after 1 week of incubation at 310 K with 1 equiv of *trans-EE* (red contours). Resonance assignments of this spectral region are reported. The spectral change induced by Pt^{II} complexation to Met 65 is indicated with an arrow.

spectra shown in Figure 5B and 5C. It is evident that, in addition to peaks of the two main fragments, a third group of peaks having molecular masses greater than those of the larger fragment is observed. In the case of *trans-EE*, the third multiplet exhibits a mass increase of ∼311 Da that nicely corresponds to the mass of the larger protein fragment plus a platinum fragment carrying two acetamide/acetamidine ligands. Conversely, in the case of *cis-EE*, the third multiplet exhibits a mass increase of ∼268 Da corresponding to a platinum fragment carrying an acetamide/acetamidine and an aqua/amine ligand. No signs of platination of the smaller fragment were detected.

The latter result provides clear evidence that metalation occurs selectively on the larger fragment (peptide 50−104), i.e., in the peptide containing Met 65. In the light of these data it is rather straightforward to propose that Met 65 represents the primary binding site for platinum(II) iminoethers in horse heart cyt *c*.

NMR experiments were also set to further confirm the involvement of Met 65 in coordination to platinum residues. Therefore, equimolar amounts of cyt *c* and *trans-EE* were allowed to react in water solution (1.5 mM concentration, pH 6.9) and the $^{1}H,^{13}C$ HSQC spectrum monitored as a function of time. Although under these experimental conditions only a fraction of cyt *c* reacts with platinum (ca. 20−25%), the newly formed species could be characterized. In particular a new cross-peak (belonging to Met 65 ϵ-CH_3) appears downfield of the corresponding peak in native cyt *c* (shift of ^{1}H and ^{13}C resonances from 1.78 to 2.22 ppm and from 13.8 to 18.2 ppm, respectively, Figure 6) (*50*, *51*). Very similar shifts were already observed for platinum coordination to methionine in some model polypeptides. Therefore, it is possible to conclude that, behind any reasonable doubt, platinum coordination occurs at Met 65 of cyt *c*.

DISCUSSION

The present study has highlighted the effectiveness of an ESI MS-based approach for the characterization of platinum−protein adducts at a molecular level. Indeed, relying primarily on ESI MS results, it has been possible to achieve a rather detailed description of the metallodrug/protein adducts, comprising the identification of the protein-bound metallic fragments and the assignment of the primary metal binding site for cyt *c*.

Preferential formation of monoplatinated adducts was observed for all investigated platinum compounds supporting the view that cyt *c* bears a single, high-affinity, binding site for these platinum(II) species. Upon careful analysis of the various ESI MS peaks, a comprehensive identification of the various platinated species and of the underlying reactions was achieved (see Schemes 2 and 3).

trans-EE is proposed to release a chloride ligand and bind cyt *c*. Concomitantly, replacement of the OCH_3 groups by water/ammonia takes place leading to the formation of acetamide/acetamidine ligands (amination is fostered by the presence of ammonium carbonate buffer). In turn, protein binding promotes replacement of the trans chlorido ligand by a water/ammonia molecule, whereas the imine ligands remain coordinated to the platinum center. The postulated sequence of events and peak assignments (specifically at ca. 12 667 and 12 684 Da) are given in Scheme 2.

In the case of *cis-EE*, after the release of the first chlorido ligand and binding of cyt *c*, the iminoether ligand that is trans to the protein is lost, while the iminoether ligand which is cis to the protein is retained (hydrolysis/aminolysis converts the iminoether into the corresponding amide/amidine). The reaction pattern and peak assignment are described in Scheme 3 (specifically at ca. 12 626 and 12 644 Da).

Finally, for *cis-Z* and *trans-Z* it is found that both of them maintain the platinum-coordinated iminoether ligand which, as always, undergoes hydrolysis/aminolysis with transformation into the corresponding amide/amidine.

Remarkably, the above-reported interpretation of the ESI MS data reveals a peculiar and largely unexpected behavior for these iminoether ligands, i.e., occurrence of extensive hydrolysis/aminolysis and formation of the corresponding amide/amidine. It is evident that such a reactivity is greatly enhanced by a direct interaction of the metal complexes with the protein as it emerges from independent NMR measurements performed on *trans-EE* either alone or in the presence of a stoichiometric amount of cyt *c*. Under identical experimental conditions, pure *trans-EE* remains stable, whereas 1:1 mixtures of *trans-EE* and cyt *c* undergo extensive ligand hydrolysis. Overall, these results imply that platinum drugs dissolved in biological media—and thus in the presence of many chemical components, including macromolecules—may manifest a chemical reactivity that is profoundly distinct from that observed when they are just dissolved in simple buffered solutions. These observations pose important "caveats" to extrapolating the behavior observed in solution for metallodrug to that believed to occur inside cells. It is proposed that the hydrolysis of iminoethers is fostered by electrostatic interactions between the metal complex and basic surface areas of the protein.

In addition, important differences have emerged in the reactivities of the various tested compounds with cyt *c*. At variance with *trans-EE*, *cis-EE* was shown to release one of its iminoether ligands, most likely the one which is trans to the bound protein. Thus, the same type of molecular fragments was found in the adducts of cyt *c* with *cis-EE*, *cis-Z*, and *trans-Z*. Remarkably, the time-dependent evolution of the various platinated adducts was found to manifest a

Scheme 3: Proposed Reaction Scheme for *cis-EE* with Cytochrome *c*

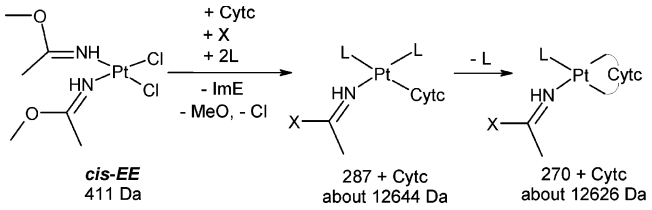

L = H_2O, NH_3; X = OH, NH_2; ImE = iminoether

significant stability even over relatively long time periods (168 h); only in the case of *cis-EE* some relevant protein degradation was observed already within 24 h.

A final comment concerns the specific localization of the platinum binding sites on cyt *c*. On the grounds of the above results (mainly formation of monoadducts), it is evident that cyt *c* has a primary binding site significantly stronger than any other. Previous studies have reported that Met 65 represents a high-affinity binding site for platinum drugs (*49*). This hypothesis is now strongly supported by additional ESI MS studies performed on cyt *c* proteolytic fragments showing that platination occurs selectively on the larger fragment (i.e., the fragment containing Met 65). The latter conclusion is also fully supported by NMR investigations showing a characteristic downfield shift of the Met 65 methyl signal upon reaction with the metallic substrate.

Concluding Remarks and Perspectives. Overall, the strategy here illustrated has turned out to be particularly successful in monitoring the reactivity of platinum metallodrugs with the model protein cyt *c* and in elucidating, at the molecular level, the formation, nature, and evolution of the resulting platinum−protein adducts. It has emerged very clearly that *interactions with this specific protein do profoundly alter the intrinsic reactivity of platinum compounds*, leading to the observation of rather unexpected chemical transformations at the level of the platinum ligands. The comparative analysis of the present results with those previously obtained on classical platinum(II) anticancer drugs, the results of a specific partial proteolysis experiment, and the NMR monitoring of methionine chemical shifts make us confident that Met 65 is the major binding site for platinum(II) iminoethers on cyt *c*.

The mechanistic implications of the present work also deserve a final comment. The results obtained here for cyt *c* are attractive since they might be of general significance and could help in understanding what is occurring inside cells during treatment with platinum drugs. Of course, some specificities in the metal/protein interactions can be expected depending upon nature and surface exposure of different amino acids and their affinity for platinum (consider for instance the case of cysteine-rich metallothioneins, a group of proteins displaying high affinity for platinum and other soft metals). Some literature is indeed available on this issue. However, since it is now firmly established that a large number of proteins (and not only a few ones) are platinated *in vitro*, we can reasonably assume that reactions similar to those described here for platinum iminoethers toward cyt *c* may actually occur inside cells. These arguments reinforce the importance of the present strategy based on the use of specific model proteins.

ACKNOWLEDGMENT

The authors are grateful to Professor Dan Gibson for valuable discussion. Dr. Angela Casini thanks AIRC for a Grant.

SUPPORTING INFORMATION AVAILABLE

Experimental section including information on the synthesis of complex *trans*-[$PtCl_2${(*E*)-HN═C($O^{13}CH_3$)CH_3}$_2$] and ^{13}C NMR data. This material is available free of charge via the Internet at http://pubs.acs.org.

REFERENCES

1. Special Issue on Medicinal Inorganic Chemistry. (1999) *Chem. Rev. 99*, 2201−2842.
2. Keppler, B. K. (1993) *Metal Complexes in Cancer Chemotherapy*, VCH, Weinheim, Germany.
3. Sigel, A., and Sigel, H. (2004) *Metal Ions in Biological Systems*, Vol. 42, Marcel Dekker, Inc., New York, Basel, The Netherlands.
4. Gielen, M., and Tiekink, E. R. T. (2005) *Metallotherapeutic Drugs and Metal-Based Diagnostic Agents: The Use of Metals in Medicine*, Wiley, Weinheim, Germany.
5. Zhang, C. X., and Lippard, S. J. (2003) New metal complexes as potential therapeutics, *Curr. Opin. Chem. Biol. 7*, 481−489.
6. Guo, Z., and Sadler, P. J. (1999) Medicinal inorganic chemistry, *Adv. Inorg. Chem. 49*, 183−306.
7. Farrell, N. (2004) Polynuclear platinum drugs, *Met. Ions Biol. Syst. 42*, 251−296.
8. Lippert, B. (1999) *Cisplatin: Chemistry and Biochemistry of a Leading Anticancer Drug*, John Wiley & Sons, Inc., New York.
9. Wang, D., and Lippard, S. J. (2005) Cellular processing of platinum anticancer drugs, *Nat. Rev. Drug Discovery 4*, 307−320.
10. Reedijk, J. (2003) New clues for platinum antitumor chemistry: kinetically controlled metal binding to DNA, *Proc. Natl. Acad. Sci. U.S.A. 100*, 3611−3616.
11. Messori, L., Marcon, G., Orioli, P., Fontani, M., Zanello, P., Bergamo, A., Sava, G., and Mura, P. (2003) Molecular structure, solution chemistry and biological properties of the novel [ImH]-[*trans*-IrCl(4)(Im)(DMSO)], (I) and of the orange form of [$(DMSO)_2$H][*trans*-$IrCl_4(DMSO)_2$], (II), complexes, *J. Inorg. Biochem. 95* (1), 37−46.
12. Messori, L., Abbate, F., Marcon, G., Orioli, P., Fontani, M., Mini, E., Mazzei, T., Carotti, S., O'Connell, T., and Zanello, P. (2000) Gold(III) complexes as potential antitumor agents: solution chemistry and cytotoxic properties of some selected gold(III) compounds, *J. Med. Chem. 43* (19), 3541−3548.
13. Ivanov, A. I., Christodoulou, J., Parkinson, J. A., Barnham, K. J., Tucker, A., Woodrow, J., and Sadler, P. J. (1998) Cisplatin binding sites on human albumin, *J. Biol. Chem. 273* (24), 14721−14730.
14. Khalaila, I., Allardyce, C. S., Verma. C. S., and Dyson, P. J. (2005) A mass spectrometric and molecular modelling study of cisplatin binding to transferrin, *ChemBioChem 6* (10), 1788−1795.
15. Mandal, R., Kalke, R., and Li, X. F. (2004) Interaction of oxaliplatin, cisplatin, and carboplatin with hemoglobin and the resulting release of a heme group, *Chem. Res. Toxicol. 17* (10), 1391−1397.
16. Gibson, D., and Costello, C. E. (1999) A mass spectral study of the binding of the anticancer drug cisplatin to ubiquitin, *Eur. Mass Spectrom. 5*, 501−510.
17. Balter, L., and Gibson, D. (2005) Mass spectrometric studies of the formation and reactivity of *trans*-[$PtCl_2$(Am)-(piperidinopiperidine)] × HCl complexes with ubiquitin, *Rapid Commun. Mass Spectrom. 19* (24), 3666−3672.
18. Najajreh, Y., Ardeli-Tzaraf, Y., Kasparkova, J., Heringova, P., Prilutski, D., Balter, L., Jawbry, S., Khazanov, E., Perez, J. M., Barenholz, Y., Brabec, V., and Gibson, D. (2006) Interactions of platinum complexes containing cationic, bicyclic, nonplanar piperidinopiperidine ligands with biological nucleophiles, *J. Med. Chem. 49* (15), 4674−4683.
19. Peleg-Shulman, T., Najajreh, Y., and Gibson, D. (2002) Interactions of cisplatin and transplatin with proteins: Comparison of binding kinetics, binding sites and reactivity of the Pt−protein adducts of cisplatin and transplatin towards biological nucleophiles, *J. Inorg. Biochem. 91*, 306−311.

20. Najajreh, Y., Peleg-Shulman, T., Moshel, O., Farrell, N., and Gibson, D. (2003) Ligand effects on the binding of *cis*- and *trans*-[$PtCl_{(2)}$Am(1)Am(2)] to proteins, *J. Biol. Inorg. Chem. 8* (1−2), 167−175.
21. Calderone, V., Casini, A., Mangani, S., Messori, L., and Orioli, P. L. (2006) Structural investigation of cisplatin−protein interactions: selective platination of His19 in a cuprozinc superoxide dismutase, *Angew. Chem., Int. Ed. 45* (8), 1267−1269.
22. Casini, A., Mastrobuoni, G., Temperini, C., Gabbiani, C., Francese, S., Moneti, G., Supuran, C. T., Scozzafava, A., and Messori, L. (2007) *Chem. Commun. 14* (2), 156−158.
23. Timerbaev, A. R., Hartinger, C. G., Aleksenko, S. S., and Keppler, B. K. (2006) *Chem. Rev. 106* (6), 2224−2248.
24. Casini. A., Gabbiani, C., Mastrobuoni, G., Messori, L., Moneti, G., and Pieraccini, G. (2006) Exploring metallodrug−protein interactions by ESI mass spectrometry: the reaction of anticancer platinum drugs with horse heart cytochrome *c*, *ChemMedChem 1* (4), 413−417.
25. Hartinger, C. G., Ang, W. H., Casini, A., Messori, L., Keppler, B. K., and Dyson P. J. (2007) Mass spectrometric analysis of ubiquitin platinum interactions of leading anticancer drugs: MALDI versus ESI, *J. Anal. At. Spectrom.*, in press.
26. Cristoni, S., and Bernardi, L. R. (2003) Development of new methodologies for the mass spectrometry study of bioorganic macromolecules, *Mass Spectrom. 22*, 369−406.
27. Loo, J. A. (1997) Studying noncovalent protein complexes by electrospray ionization mass spectrometry, *Mass Spectrom. Rev. 16*, 1−23.
28. Hu, P., Ye, Q. Z., and Loo, J. A. (1994) Calcium stoichiometry determination for calcium binding proteins by electrospray ionization mass spectrometry, *Anal. Chem. 66*, 4190−4194.
29. Mann, M., Hendrickson, R. C., and Pandey, A. (2001) Analysis of proteins and proteomes by mass spectrometry, *Annu. Rev. Biochem. 70*, 437−473.
30. Jonsson, A. P. (2001) Mass spectrometry for protein and peptide characterisation, *Cell. Mol. Life Sci. 58*, 868−884.
31. Hartinger, C. G., Alexenko, S., Timerbaev, A. R., and Keppler, B. K. (2005) The binding of platinum complexes to human serum albumin studied by electrospray ionization-ion trap-mass spectrometry (ESI-IT-MS) *Novel Approaches for the Discovery and the Development of Anticancer Agents*, CESAR, Vienna, P16.
32. Yang, G., Miao, R., Jin, C., Mei, Y., Tang, H., Hong, J., Guo, Z., and Zhu, L. (2005) Determination of binding sites in carboplatin-bound cytochrome *c* using electrospray ionization mass spectrometry and tandem mass spectrometry, *J. Mass Spectrom. 40* (8), 1005−16.
33. Mandal, R., and Li, X. F. (2006) Top-down characterization of proteins and drug−protein complexes using nanoelectrospray tandem mass spectrometry, *Rapid Commun. Mass Spectrom. 20* (1), 48−52.
34. Casini, A., Mastrobuoni, G., Ang, W. H., Gabbiani, C., Pieraccini, G., Moneti, G., Dyson, P. J., and Messori, L. (2007) Exploring metallodrug−protein interactions by ESI mass spectrometry: ESI MS characterization of protein adducts of anticancer ruthenium(II)−arene PTA (RAPTA) complexes, *ChemMedChem 2* (5), 631−635.
35. Natile, G., and Coluccia, M. (2001) Current status of trans-platinum compounds in cancer therapy, *Coord. Chem. Rev., 216/217*, 383−410.
36. Coluccia, M., and Natile, G. (2007) Trans-platinum complexes in cancer therapy, *Anticancer Agents Med. Chem. 7* (1), 111−123.
37. Cini, R., Caputo, P. A., Intini, F. P., and Natile, G. (1995) Mechanistic and stereochemical investigation of imino ethers formed by alcoholysis of coordinated nitriles: X-ray crystal structures of *cis*- and *trans*-bis(1-imino-1-methoxyethane)dichloroplatinum(II), *Inorg. Chem. 34*, 1130−1137.
38. Coluccia, M., Nassi, A., Roseto, F., Boccarelli, A., Mariggiò, M. A., Giordano, D., Intini, F. P., Caputo, P., and Natile, G. (1993) A trans-platinum complex showing higher antitumor activity than the cis congeners, *J. Med. Chem. 36*, 510−512.
39. Coluccia, M., Boccarelli, A., Mariggiò, M. A., Cardellicchio, N., Caputo, P., Intini, F. P., and Natile, G. (1995) Platinum(II) complexes containing iminoethers: a trans platinum antitumour agent, *Chem.−Biol. Interact. 98*, 251−266.
40. Brabec, V., Vrana, O., Novakova, O., Kleinwachter, V., Intini, F. P., Coluccia, M., and Natile, G. (1996) DNA adducts of antitumor *trans*-[$PtCl_2$ (E-imino ether)$_2$], *Nucleic Acids Res. 24*, 336−341.
41. Leng, M., Locker, D., Giraud-Panis, M. J., Schwartz, A., Intini, F. P., Natile, G., Pisano, C., Boccarelli, A., Giordano, D., and Coluccia, M. (2000) Replacement of an NH_3 by an iminoether in transplatin makes an antitumor drug from an inactive compound, *Mol. Pharmacol. 58*, 1525−1535.
42. Palmer, A. G., III, Cavanagh, J., Wright, P. E., and Rance, M. (1991) Sensitivity improvement in proton-detected 2-dimensional heteronuclear correlation NMR spectroscopy, *J. Magn. Reson. 93*, 151−170.
43. Kay, L. E., Keifer, P., and Saarinen, T. (1992) Pure absorption gradient enhanced heteronuclear single quantum correlation spectroscopy with improved sensitivity, *J. Am. Chem. Soc. 114*, 10663−10665.
44. Schleucher, J., Schwendinger, M., Sattler, M., Schmidt, P., Schedletzky, O., Glaser, S. J., Sørensen, O. W., and Griesinger, C. (1994) A general enhancement scheme in heteronuclear multidimensional NMR employing pulsed field gradients, *J. Biomol. NMR 4*, 301−306.
45. Marion, D., and Wüthrich, K. (1983) Application of phase sensitive two-dimensional correlated spectroscopy (COSY) for measurements of $^1H-^1H$ spin-spin coupling constants in proteins, *Biochem. Biophys. Res. Commun. 113*, 967−974.
46. Shaka, A. J., Barker, P. B., and Freeman, R. (1985) Computer optimized decoupling scheme for wideband applications and low-level operation, *J. Magn. Reson. 64*, 547−552.
47. Banci, L., Bertini, I., Gray, H. B., Luchinat, C., Reddig, T., Rosato, A., and Turano, P. (1997) Solution structure of oxidized horse heart cytochrome *c*, *Biochemistry 36*, 9867−9877.
48. Liu, W., Rumbley, J., Englander, S. W., and Wand, A. J. (2003) Backbone and side-chain heteronuclear resonance assignments and hyperfine NMR shifts in horse cytochrome *c*, *Protein Sci. 12*, 2104−2108.
49. Cox, M. C., Barnham, K. J., Frenkiel, T. A., Hoeschele, J. D., Mason, A. B., He, Q. Y., Woodworth, R. C., and Sadler, P. J. (1999) Identification of platination sites on human serum transferrin using (13)C and (15)N NMR spectroscopy, *J. Biol. Inorg. Chem. 4* (5), 621−631.
50. Arnesano, F., Scintilla, S., and Natile, G. (2007) Interaction between platinum complexes and a methionine motif found in copper transport proteins, *Angew. Chem., Int. Ed.*, in press.
51. Lijuan, J., Yu, C., Guozi, T., and Wenxia, T. (1997) Studies on the interaction between cytochrome *c* and *cis*-$PtCl_2(NH_3)_2$, *J. Inorg. Biochem. 65*, 73−77.

BI701516Q

3.5. Conclusions

The complementation of X-ray diffraction and NMR with ESI MS technique for the characterisation of metallodrug-protein adducts has undoubtedly allowed a significant progress in this specific research area. Indeed, thanks to the results provided by these methods, the molecular mechanisms of the reactions of metallodrugs with protein targets could be described at least in elected cases with a high accuracy.

The considered approaches are independent but highly complementary, X-ray crystallography providing a full description of the structure of the metallodrug-protein adducts while ESI MS offering valuable information on the temporal evolution of these adducts. Putting together these two pieces of information usually results in an exhaustive structural and functional picture of the analysed systems and of the underneath reactions. Notably, one major limitation arises from the intrinsic difficulty in obtaining good quality crystals for X-ray diffraction analysis. Indeed, crystal structures of metallodrug-protein have been solved until now only in a very limited number of cases. In these cases, ESI MS may be complemented by independent information achieved by application of other physicochemical techniques.

In any case, on the ground of the representative examples reported above, a rather satisfactory and comprehensive description of the reactivity of metallodrugs with protein targets can be inferred that might be of broader validity.

Metallodrugs behave very frequently as pro-drugs. This means that they must necessarily undergo an activation step, in most cases a simple aquation reaction, before they can react with protein targets. Generally, this activation step represents the rate limiting step; however we have shown how the kinetics of this activation step may be greatly influenced by a direct interaction of the metallodrug with the proteins. This is the reason for the unexpectedly similar reactivity profiles of the reactions of carboplatin and cisplatin with cytochrome c, earlier mentioned.

The resulting “activated metallodrugs” usually contain a weakly coordinated water molecule that is easily removed and replaced by a stronger ligand provided by the protein itself. Only a few protein residues perform this function with the “soft” metal ion here considered, mainly histidines, methionines, cysteines, through a nitrogen or a sulphur donor. This second ligand substitution reaction leads to the formation of the so called metallodrug/protein complex or adduct, the main object of present investigations. Notably, both X-ray diffraction and ESI MS studies converge in showing that, in spite of the large

number of potential donors on the protein surface, adduct formation takes place preferentially only in a few positions, implying a rather high selectivity in metal binding.

The functional characterisation of the newly formed entities -i.e the metallodrug protein adducts- is of extreme importance in relation to their possible biological roles. Indeed, if the adduct is shown to be devoid of any further reactivity we can assess quite safely that the reaction has led to inactivation of the metallodrug (provided that the protein itself is not an important biological target). Conversely, if the adduct conserves the capacity of further reacting with other biomolecules and/or transferring the metallic fragment to other species, one can state that the formed adduct is still a biologically active species and that it may also serve as a reservoir of the metallodrug itself.

Overall, the studies we have carried out on metallodrugs and model proteins permit a rather accurate characterisation of their interaction modes at a molecular level. Of course, when carrying out this type of investigations, one must never forget that just very simplified systems were analysed. Nonetheless, the reactivity patterns here formulated for the simplified systems may be a good reference in the study of cellular systems.

4. CHARACTERIZATION AND LOCALIZATION OF ALLERGENIC PROTEINS IN ROSACEAE FRUITS BY HIGH RESOLUTION MASS SPECTROMETRY (HRMS) AND MASS SPECTROMETRY IMAGING (MSI)

4.1. Introduction

4.1.1. Non- specific Lipid Transfer Proteins

Non-specific lipid transfer proteins (ns-LTPs) are relevant allergens of non-pollen-related allergies to Rosaceae fruits in the Mediterranean area.[80] The family of ns-LTPs generally includes 9-kD monomeric proteins, having a total number of amino acids varying from 91 to 95 residues[81] with eight cysteine residues, located at conserved positions, which are linked in four disulfide bridges, responsible for the LTP compact folding and for the hydrophobic tunnel in their central cavity.

Common structural features between LTPs from different fruits are the basis of their allergenic clinical cross-reactivity.[82,83] LTPs were found to be secreted and located in the cell wall and usually accumulate in the outer epidermal layers of plant organs,[84] thus explaining the stronger allergenicity of peels compared with pulps of Rosaceae fruits.[85]

Characterization of LTPs is usually done on extracted protein, purified through a combination of gel filtration, ion exchange and/or reverse-phase HPLC and their molecular mass is determined either by gel filtration or by SDS-gel electrophoresis, seldom by mass spectrometric analysis.[86]

---

[80] Sanchez-Monge, R., Lombardero, M., Garcia-Selles FJ, Barber D, Salcedo G. *J. All. Clin. Immunol.* **1999**, *103*, 514-9.

[81] Kader JC. *Annu. Rev. Plant Physiol. Plant Mol. Biol.* **1996**, *47*, 627–54

[82] Aalberse RC. *Clin. Molec. Allergy*. **2007**, *5*, 2

[83] Fernandez Rivas M. *Allergol Immunopathol (Madr).* **2003**, *31*(3), 141-6.

[84] Borges J.-P., JauneauA., Brulé C., Culerrier R., Barre A., Didier A., Rougé P. *Plant Phys. & Bioch.* **2006**, *44*, 535–542

[85] Fernandez Rivas M., Cuevas M. *Clin. Exper. Allergy,* **1999**, *29*, 1239-1247

[86] Pastorello E.A., Farioli L., Pravettoni V., Robino A.M., Scibilia J., Fortunato D., Conti A., Borgonovo L., Bengtsson A., Ortolani C. *J. Allergy Clin. Immunol.,* **2004**, *114* (4), 908-914

Usually primary sequence of extracted protein can be obtained by N-terminal amino acid sequencer, sequencing the first 20-30 N-terminal amino acids. The purification of LTP from their native sources is often a quite difficult task; this is an obstacle for obtainment of sufficient (and sufficiently pure) quantities of protein for successive conventional analyses.[87] A powerful and commonly used method to assign the sequence of these allergens also consists in recombinant techniques: total RNA is extracted, retrotranscripted on DNA, which is then amplified and sequenced. In this case, the most probable complete amino acid sequence of the protein is deduced by software analysis.[88] The complete amino acid sequences determined up to now for purified LTPs usually correspond to those deduced from the nucleotide sequences of LTP genes, but quite often more than one cDNA sequence is present and in many cases a direct comparison of the recombinant and natural forms has not been carried out. Thus, many sequences of allergens remain only cDNA-obtained, and still need the confirmation with the extracted protein.

Between MS techniques which are used for the molecular characterization of the protein, traditional mass spectrometers can easily give the protein MW, together with those of tryptic peptides, whereas advanced mass spectrometry techniques are able to obtain at the same time the accurate mass of a protein and sequence information by the so called *Top Down* MS approach.[89] Recent developments in mass spectrometric technologies, as Mass Spectrometry Imaging (MSI), made this technique a powerful alternative to classical techniques commonly used to localize biomolecules in biological tissues.[90] Although MSI has several limitations in comparison to other techniques as immunohistochemistry (lower resolution achievable, 15 μm against < 1 μm), it has the great advantage to localize in a fast way more than one protein at time, avoiding the need of a specific antibody for each protein under analysis. Moreover in immunohistochemistry analysis, there is the risk of cross-reactivity leading to false positives, whilst MSI localizes a given molecule by mean of one of its intrinsic property, i.e. its molecular mass.[91]

---

[87] Vassilopoulou V. E., Zuidmeer L., Akkerdaas J. , Rigby N. , Moreno F.J., Papadopoulos N. J., Saxoni-Papageorgiou P., Mills C., van Ree R. *Mol Nutr Food Res.* **2007,** *51,* 360- 366

[88] Díaz-Perales A.., Sanz M.L., García-Casado G., Sánchez-Monge R., García-Selles F.J., Lombardero M., Polo F., Gamboa P.M., Barber D., SalcedoG. *J Allergy Clin. Immunol.,* **2003**, *111* (3), 628-633

[89] Kjelden F., Zubarev R.A. *The Encyclopedia of Mass Spectrometry,* Elsevier, 2005, vol 2-Part A, 190-197

[90] Caprioli R.M., Farmer T.B., Gile J. *Anal. Chem*. **1997**, *69*, 4751-4760

[91] Chaurand, P., Sanders, M.E., Jensen, R.A., Caprioli, R.M. *Am. J. Pathol*., **2004**, *165*, 1057-1068

Among LTPs, the most important allergen is peach LTP, Pru p 3,[92] which is responsible for almost all allergic reactions to peaches observed in the Mediterranean area.[93] As other LTPs, Pru p 3 has been found to accumulate in exocarp in almost all of the peach varieties.[94,95] Since 1992 when an IgE-binding component of peach with a 8-10kD MW was immunologically characterized and named Pru p 1,[96] many efforts have been undertaken to characterize the protein sequence of this allergen and several different sequences are present in the literature. In this work we developed a new extraction-purification method for peach LTP Pru p 3.We extracted the protein from three different varieties and, working on the purified protein, we exploited traditional (ESI-LIT) and innovative (LTQ-Orbitrap and MALDI–ToF) mass spectrometry techniques in order to easily and unambiguously assess the exact sequence. Moreover, we used MSI to easily and rapidly localize the protein in the fruit.

4.2. Methods

4.2.1. Mass spectrometry

As its name suggests, Orbitrap is a device that is able to store and trap ions. However it is not a conventional ion trap as three-dimensional or linear ion trap[97,98], because there is neither RF nor a magnet to hold ions inside, but an electrostatic field that traps ions.[99,100] The electrostatic attraction towards the central electrode is compensated by a centrifugal force that arises from the initial tangential velocity of ions, which makes ion moving like a satellite on orbit.

---

[92] Pastorello E.A., Farioli L., Pravettoni V., Ortolani C., Ispano M., Monza M. *J Allergy Clin Immunol*, **1999**, 103, 520-6.

[93] Fernandez-Rivas M., Gonzalez-Mancebo E., Rodriguez-Perez R., Benito C., Sanchez-Monge R., Salcedo G., Alonso D., Rosado A., Tejedor M.A., Vila C., Casas M.L *J. Allergy Clin. Immunol.,* **2003**, *112* (4), 789-795

[94] Botton A., Vegro M., De Franceschi F., Ramina A., Gemignani C., Marcer G., Pasini G., Tonutti P. *Plant Science*. **2006,** *171* (1), 106-113

[95] Borges JP., Jauneau A., Brule C., Culerrier R., Barre A., Didier A., Rouge P. *Plant Physiology And Biochemistry,* **2006,** *44* (10), 535-542

[96] Llconart R., Cistero A., Carreira J., Batista A., Moscoso del Prado J. *Annals Of Allergy*, **1992**, *69*, 128-130

[97] John F. J. Todd Mass Spectrometry Reviews Volume 10, Issue 1, Date: January 1991, Pages: 3-52

[98] Douglas DJ, Frank AJ., Mao D. *Mass Spectrometry Reviews*, **2005**, *24*, 1-29

[99]Makarov, A., *Anal. Chem*. **2000**, *72*, 1156–1162.

[100] Hardman, M., Makarov, A., *Anal. Chem*. **2003**, *75*, 1699–1705.

The electrostatic field forces ions to move in complex spiral patterns. The axial component of these oscillations can be detected as an image current on the two halves of an electrode encapsulating the Orbitrap (figure 12). A Fourier transform is employed to obtain oscillation frequencies for ions with different m/z values, which can be determined from these values. Since ions can be trapped for long times, the frequency of their image current can be registered with high accuracy, allowing the obtainment of a high resolution mass spectrum. The resolution and mass accuracy are very competitive with those obtainable in other instruments as FT-ICR mass spectrometers and better than in ToF ones.

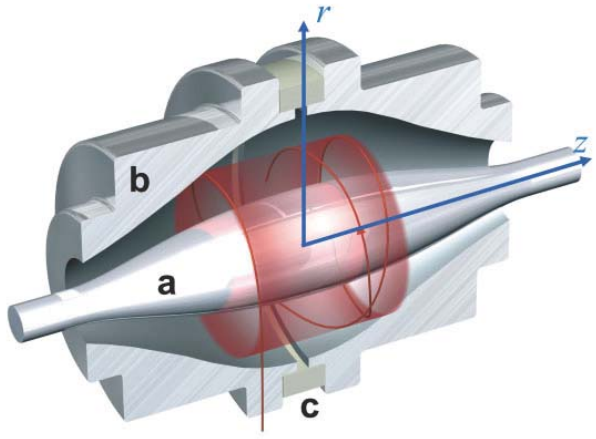

Figure 12. schematic representation of Orbitrap mass analyzer.

A perfect combination of this mass analyzer is with conventional linear ion traps, because the first allows high resolution measurements, whilst the second allows to perform MS^n experiment. Thus also product ions of these experiments can be registered with high resolution and high mass accuracy, opening new perspectives in a wide range of applications.

In addition to that advantages, Orbitrap mass spectrometer opens the door to that was the exclusive realm of FT-ICR, i.e. the "*Top Down*" approach[101]. In fact, so far, the use of instrumentation other than FT-ICR allowed only the classical "*bottom up*" approach; in proteome analysis this strategy involves cleaving the protein into peptide fragments that are smaller but still sufficiently distinctive to allow protein identification; however complete sequence coverage of proteins is rarely achieved, thus limiting the ability to examine site-specific mutations and post-translational modifications of individual proteins, which may be important in biological function. "*Top down*" approach, where intact proteins are ionized and fragmented in mass spectrometer, allows an exhaustive characterization of intact proteins, without the need for prior chemical or enzymatic proteolysis, but requires high resolution mass spectrometers in order to determine charge states of multiple charged protein ions.

[101] Kjelden F., Zubarev R.A. *The Encyclopedia of Mass Spectrometry*, Elsevier, **2005**, *vol. 2-Part A*, 190-197

The Orbitrap is an analyzer with a sufficiently high resolving power to encourage attempts for analyzing intact proteins. The mode of operation is measuring the intact protein mass in the Orbitrap, selecting one of the charge states of the protein and dissociating it in the ion trap, and then measure the fragments in the Orbitrap. This allow an unambiguous charge state determination of fragment ions and identification of most of the unmodified and modified proteins by database searching.

MALDI (matrix-assisted laser desorption ionization) mass spectrometry imaging (MALDI MSI) is a new technology able to generate molecular profiles and two-dimensional ion density maps of biomolecules directly from the surface of tissue sections.[102] This allows specific information to be obtained on the relative abundance and spatial distribution of a wide range of molecules both endogenous and xenobiotics.

An outline of the technique is as follows; typically, a thin tissue slice (10-20μm) is covered with matrix which co-crystallizes with the molecules present in the tissue. Most commonly a 337 nm N_2 laser is fired in a defined raster over the section; absorption of the UV radiation from the laser pulse by the crystals, subsequently causes matrix and analyte molecules to desorb from the sample surface, and a mass spectrum, containing all the mass signals of the compounds desorbed, is acquired for each point of the raster. A data set consisting of an ordered array of mass spectra is created, where each spectrum represents the local molecular composition at known *x*,*y* coordinates. Ultimately, an image can be generated for each of the mass signals detected throughout the section. In particular, the intensities of individual *m/z* values in each spectrum, corresponding to the molecular weights of specific compounds, can be extracted to produce images of the areas, within the tissue, in which that particular molecule was located, similarly to the digital imaging in photography where each image is composed of an ordered array of thousands of pixels.[103] Since molecular maps can be obtained for one or more molecules simultaneously without the use of chemical probes, IMS is highly complementary to immunohistochemistry and *in vivo* imaging techniques such as Magnetic Resonance Imaging, Positron Emission Tomography, near IR-fluorescence Imaging, and Whole Body Autoradiography (WBA).

[102] Kumar A., Agarwal S., Heyman J.A., Matson S., Heidtman M., Piccirillo S., Umansky L., Drawid A., Jansen R., Liu Y., Cheung KH., Miller P., Gerstein M., Roeder GS., Snyder M., *Genes Dev.*, **2002**, *16*, 707.
[103] Caprioli RM., Farmer TB. and Gile J. *Anal. Chem*. **1997,** 69, 4751.

4.2.3. Sample preparation and MS analysis

Peach LTP was purified from three different varieties of peach: "Italia K2" (white flesh), "Toscana" (yellow flesh) and "Rita star" (Nectarine yellow flesh). Skins were obtained cutting 2 to 3 mm from the external part of peaches. Ground skins or pulp of peaches were homogenized in phosphate-buffered saline (PBS) buffer; after centrifugation, the supernatants were filtered, dialyzed and concentrated on centrifugal filter devices (cut-off 5 kDa). The retentate, containing the protein fraction, was recovered and filtered through 0.45µm filters.

The total protein extract was purified on a reverse phase C8column in a preparative HPLC system coupled to UV detector (240 nm). 150µl of total protein extract were injected each time. The fraction eluting from 20 to 45 minutes was collected, dried, redissolved in water and definitively purified on a reverse phase C18 column coupled to an ESI-MS detector. Purification was efficiently achieved by using a T-split before the MS analyzer. LTP sequence characterization was achieved by previously digesting the purified protein for 24 hours with trypsin, followed by disulfide bridge reduction by means of dithiotreitol (DTT) for 1h and alkylation of free thiols with iodoacetamide for 1 h.

Peptide analysis was performed on a RP-HPLC system coupled to ESI-MS analyzer using in source fragmentation. Protein exact mass determination was performed on a high resolution FT Orbitrap mass spectrometer.

The same LTP sample used for accurate mass determination was reduced by adding 5 mM tributylphosphine and incubating for 30 min at 37 °C before performing *Top Down* MS/MS experiments. The multicharged ions 6^+, 7^+ and 8^+ and ions were fragmented in order to obtain sequence information.

Few thin slices (about 250 µm) were cut from frozen peach and mounted on conductive ITO (Indium tin oxide) microscope slides, then sprayed with a MALDI a matrix (sinapinic acid) solution. Multiple spraying cycles were performed, allowing solvent evaporation between cycles, until complete matrix coverage of the tissue.

MALDI-ToF spectra were acquired from tissue slices with a 400 µm spatial resolution, both on x- and y-axis and collected data were analyzed with FlexImaging 2.0™ software.

4.3. Results

At present in literature five Pru p3 sequences exist, but only one has been determined by direct protein sequencing (table 1). As it is highlighted, there are still some differences among the sequences, probably due to protein isoforms or to sequencing errors. It is interesting to consider that Q4VUZ0_PRUPE and Q8H2B2_PRUPE sequences were obtained by the same group using cDNA and the same clone but they differ not only in the length, but also for two amino acids, in position 6 and 76. This can be possible because the varieties used in each work are different (Sentry in 2002 and Early Giant in 2006), but it can be also due to DNA sequencing errors.

Protein ID	Pru p3 sequence (variable positions highlighted)
NLTP1_PRUPE	ITCGQVSSAL APCIPYVRGG GAVPPACCNG IRNVNNLART TPDRQAACNC LKQLSASVPG VNPNNAAALP GKCGVHIPYK ISASTNCATV K
Q9LED1_PRUPE	ITCGQVSSSL APCIPYVRGG GAVPPACCNG IRNVNNLART TPDRQAACNC LKQLSASVPG VNPNNAAALP GKCGVSIPYK ISASTNCATV K
Q8H2B2_PRUPE	ITCGQVSSNL APCIPYVRVG GAVPPACCNG IRNVNNLART TPDRQAACNC LKQLSASVPG VNPNNAAALP GKCGVHIPYK ISASTNCATV
Q5RZZ3_PRUPE	ITCGQVSSSL APCIPYVRGG GAVPPACCNG IRNVNNLART TPDRQAACNC LKQLSASVPG VNPNNAAALP GKCGVSIPYK ISASTNCATV K
Q4VUZ0_PRUPE	ITCGQASSSL APCIPYVRGG GAVPPACCNG IRNVNNLART TPDRQAACNC LKQLSASVPG VNPNNAAALP GKCGVSIPYK ISASTNCATV K
protein sequencing	nucleotide sequencing (from Swissprot database)

Table 1. Peach LTP sequenze present in Swissprot database.

It has to be remarked that two different works,[104,105] done by two different groups actually agreed on the sequence, also confirming the molecular weight by MALDI-ToF analysis and directly sequencing the N-terminal aminoacids of the immunoreactive protein extracted from peach.

For each considered peach variety the content was investigated both in pulps and skins. The HPLC-UV chromatograms clearly show the almost exclusive presence of LTP in the outer part of the peaches.

The ESI-MS spectrum of purified LTP showed the presence of only one isoform of the protein; furthermore, MW of the purified protein perfectly matches the sequences Q5RZZ3_PRUPE and Q9LED1_PRUPE. It should be further underlined that all varieties showed the presence of the same protein with the same molecular weight, indicating that always the same LTP was present in the three peach varieties.

[104] Diaz-Perales A., Garcia-Casado G., Sanchez-Monge R., Barber D., Salcedo G., Submitted (OCT- **2001**) to EMBL/GenBank/DDBJ databases.

[105] Zuidmeer L., van Leeuwen AW., Kleine Budde I., Cornelissen J., Bulder I., Rafalska I., Tellez Besoli N., Akkerdaas JH., Asero R., Fernandez Rivas M., Sancho A., Rigby N., van Ree R. Lipid transfer proteins from fruit: cloning, expression and measurement. Submitted (OCT-**2004**) to EMBL/GenBank/DDBJ databases.

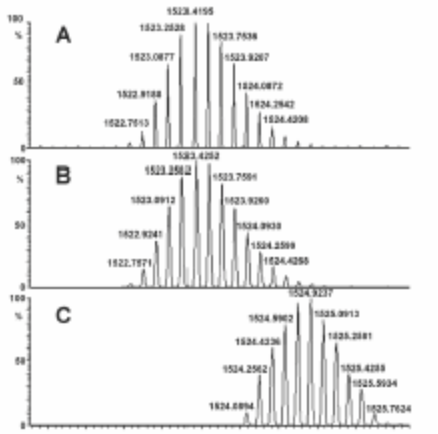

Figure 13. Isotopic pattern of purified LTP 6+ ion (B) theoretical isotopic pattern of 6+ ion from Q9LED1 sequence (oxidized form), (C) isotopic pattern of purified LTP 6+ ion (reduced form).

The peptides generated after tryptic digestion allowed the identification according to their MW and to fragments generated by the in source fragmentation. The found tryptic peptides covered the 88% of the entire sequence, thus providing a reliable indication on the protein identity. Again, these data strongly suggest that the extracted protein corresponds unequivocally to the sequences Q5RZZ3_PRUPE and Q9LED1_PRUPE.

This observation was further confirmed by measurement in high resolution FT mass spectrometer. In this case measured monoisotopic mass of intact protein was 9129.46, in perfect agreement with the theoretical mass from the sequence Q9LED1_PRUPE and with the presence of 4 disulphide bridges. Figure 13 shows the theoretical and the measured isotopic pattern of 6^+ on. The presence of disulphide bridges was confirmed after reduction with 5 mM tributylphosphine, as shown by a mass increment of 8.064 Da.

Top Down approach was attempted directly on oxidized LTP but the MS/MS spectrum was very poor, probably due to the presence of disulphide bridges that make the protein structure very compact and resistant to fragmentation under the selected experimental conditions. On the other hand, the MS/MS spectrum of reduced protein gave enough information to elucidate the identity of aminoacids in position 6, 9, 19, and 76, which differ among the various sequences reported in the database. In fact, ions observed in MS/MS experiment can be generated only by Q9LED1_PRUPE and Q5RZZ3_PRUPE sequences.

Thus the *Top Down* approach confirmed in a very fast and clear-cut way its full sequence with 100% of protein sequence coverage.

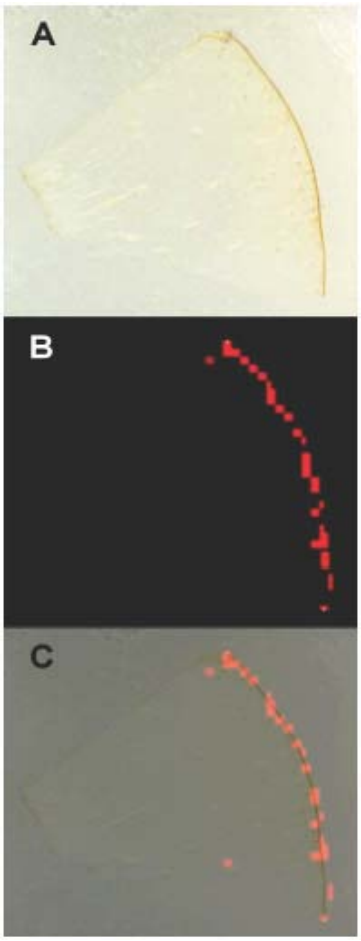

Figure 14. (A) Optical image of peach slice. (B) Molecular image of Pru p 3 signals registered from the slice. (C) Overlapping of optical and molecular images showing Prup 3 localization in the fruit skin.

In order to monitor Pru p 3 distribution in peach pulp IMS analysis was performed on 250 µm slices cut from frozen fruit. The analysis of acquired data showed that the Pru p 3 signal was present almost exclusively in the more external layer of the fruit, corresponding to the skin (figure 14). On the other hand, in the pulp no signal belonging to peach LTP was observed, in perfect agreement with literature.

4.4. Conclusions

In conclusion, a new method for LTP purification has been developed essentially based on two subsequent purification by preparative and analytical HPLC of the extracted peach fraction. In one-two days of work, this method easily allows to obtain enough amounts of relatively pure LTP for full structural characterization, avoiding also the use of low-resolution gel permeation chromatography. The purification technique here presented, although including two steps of purification, was appreciably faster than all the others methods present in the literature, yielding a highly pure protein. The most innovative part of the work concerns the use of a mass spectrometer in the purification step: this allows the accurate, immediate purification of the target protein. Following this method, peach LTP was purified from three different peach varieties.

The application of advanced mass spectrometry techniques definitely confirmed the true sequence of peach LTP found in our sample; most importantly, this study demonstrated the enormous potential of high resolution MS and Imaging MS techniques for rapidly obtaining high quality structural and functional data on food-relevant proteins.

At the moment this study is continuing with the characterization of other LTP from plum and pomegranate; however, despite a protocol for the whole study is already established, a rapid obtainment of results is hampered by the presence of different LTP isoforms in the same fruit and in different varieties. This will force to refine LTP purification, in order to separate, at least partially, the different isoforms.

4.5. Publications

Traditional and advanced mass spectrometry techniques combined with MALDI imaging for complete characterization of peach LTP allergen
(in preparation)

5. GENERAL CONCLUSIONS

In this PhD thesis applications of mass spectrometry to different biological problems were presented, highlighting potentialities and limits of this technique.

At present mass spectrometry field is in rapid expansion, owing to the technological advancements in instrumentation, and its role in structural biology research is growing.

In fact, the high sensitivity and the ability to analyze inhomogeneous and complex mixtures without previous purification allow to cover the study of those systems, where classical techniques, as NMR and X-ray crystallography, fail in providing useful information.

In the study of wasps venom, mass spectrometry turned out to be an invaluable tool, because allowed the analysis of samples taken from single specimens, practically avoiding any sample preparation. Moreover, in the same analysis, made possible the characterization of venom component and the *de novo* sequencing of several peptidic species.

The study for the characterization of protein/metallodrug interactions showed clearly how critical the integration between classical and novel techniques is in the understanding this kind of experimental systems. In some cases "structural" technique provided very accurate information on the nature of metallodrug/protein complexes, but failed in many other. Instead mass spectrometry did not provide so detailed information, but covered this lack supplying rich information also when the other techniques were not able to. Merging the data coming from different angles made possible a deep understanding of these interaction, their stoichiometry and kinetics and the structure of resulting adducts.

Finally, the study for the characterization of non-specific LTP from Rosaceae fruits demonstrated the potentialities that nowadays advanced mass spectrometry techniques, as high resolution Fourier transform and Imaging mass spectrometry, are offering to the scientific community. The possibility to characterize an entire protein in the mass spectrometer and the possibility to analyze drugs, peptides and proteins directly from biological tissue sections open the door to a variety of studies that just some years ago were simply inconceivable.

Concluding, it has to be underlined that MS cannot answer to all the question and often the information provided is not sufficient as it is to completely understand complex biological systems. It is only the integration between different technique, able to provide complementary, and sometimes overlapping, information, to be the key to achieve this

result, as the biological problem can be tackled from different point of view, obtaining the maximum information.